JOURNAL ON

COMMUNICATIONS

VOLUME XLII JULY 1991

NONLINEAR CIRCUITS

JOURNAL ON COMMUNICATIONS

A PUBLICATION OF THE SCIENTIFIC SOCIETY FOR TELECOMMUNICATIONS, HUNGARY

SPONSORED BY

HUNGARIAN TELECOMMUNICATIONS COMPANY

HUNGARIAN BOARDCASTING COMPANY

TERTA

BHG BUDAPEST

TKI

FOUNDATION FOR THE "DEVELOPMENT OF CONSTRUCTION"

Editorial office
Gábor Áron u. 65.
Budapest, O.O.Box 15.
Hungary, H—1525

phone (361) 135-1097
(361) 115-2247
fax (361) 135-5560

Subscription rates
Hungarian subscribers
1 year, 12 issues 2900 HUF, single copies 360 HUF
Individual members of Sci. Soc. for Telecomm.
1 year, 12 issues 480 HUF, single copies 60 HUF
Foreign subscribers
12 issues 90 USD, 6 English issues 60 USD, single copies 15 USD
Transfer should be made to the Hungarian Foreign Trade Bank, Budapest, H—1821, A/C No. MKKB 203-21411

JOURNAL ON COMMUNICATIONS is published monthly, alternately in English and Hungarian by TYPOTEX Ltd. H—1015 Bp. Batthyány u. 14., phone: (361) 201-3317, fax: (361) 162-1804. Publisher: Zsuzsa Votisky. Type-setting by DIAMANT Ltd. Printed by HUNGAPRINT, Budapest, Hungary
HUISSN 0866-5583

EDITORIAL

Most characteristics of analog systems are nonlinear, thus it is expedient to review occassionally the progress in the field of nonlinear circuits. This area was previously reviewed by L. O. Chua in 1984 [1]. At that time, the main problems were circuit analysis, stability, existence and uniqueness of the solution, classification of nonlinear circuits, etc. However, bifurcations were also mentioned as a possible direction of further research.

Since then, to put it simply, the progress can be characterized by two major steps. In addition to some results in the above mentioned classical problems, valuable research has been carried out in the area of chaotic oscillations. Subsequently, the attention partially shifted to neural networks.

In the theory of chaos, the goal was to obtain exact conditions for the existence of chaos. Moreover, several simple circuits exhibiting chaotic oscillations have been investigated, and simplified geometrical models for chaotic attractors have been constructed. The theory culminated in the classification of chaotic attractors. The achievements in this field were reviewed in 1988 [2], and a new journal entitled "Bifurcation and Chaos" was launched in March 1991.

In the field of neural networks, the emphasis was on the analysis of various neural structures such as Hopfield nets, perceptrons and cellular neural networks, and on the investigation of some useful properties of neural networks such as their information storing capability, robustness, stability, signal to noise ratio etc. These properties were utilized in solving practical problems as speech processing, picture transformation, character recognition and several other problems in the field of artificial intelligence, where parallel computing is essential.

Following a rapid increase in the number of papers dealing with neural networks (marked by the appearance of the new journal "Neural Networks" in 1988) the topic has recently been getting less attention. A possible reason for this is that technological progress, like results in quantum-effect devices research [4], enables conventional digital computers to become still strong competitors of neural network based analog computers during the forthcoming decade. Nevertheless, for certain practical problems such as character recognition, neural computing algorithms implemented on digital computers have already proved their relevance. The area of neural networks was reviewed almost annually in several periodicals (see for example [3]).

This issue of the Journal on Communications is intended to illustrate, within our possibilities, that the topic of nonlinear circuits lives on in spite of the smaller interest towards classical circuit theory. In the selection of the papers, we were looking for a proper balance between traditional and new areas, theory and practice, and, besides selecting papers of widely recognized specialists in nonlinear circuits, our purpose was to introduce some results by talented young researchers. In order to meet these requirements four areas have been chosen:

- investigation of existence and uniqueness of the solution of nonlinear resistive circuits,
- dynamics of nonlinear circuits, including chaotic oscillations,
- computer simulation of nonlinear circuits, and
- some practical problems in the application of neural networks.

The guest editor hopes that the readers will find this issue useful and wishes to express his gratitude to the contributing authors for their cooperation.

J. LADVÁNSZKY

REFERENCES

[1] L. O. Chua, "Nonlinear Circuits", *IEEE Trans. on CAS*, January 1984, pp. 69—87

[2] "Chaos and Bifurcations of Circuits and Systems", special issue, edited by T. Matsumoto and F. M. A. Salam, *IEEE Trans. on CAS*, July 1988

[3] "Neural Networks", special issue, edited by N. El-Leithy and R. W. Newcomb, *IEEE Trans. on CAS*, May 1989

[4] Capasso, F., S. Sen, L. M. Lunardi, and A. Y. Cho, "Quantum Transistors and Circuits Break Through the Barriers", *IEEE Circuits and Devices*, May 1991, pp. 18—25.

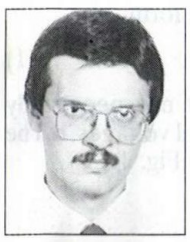

János Ladvánszky received the Electrical Engineer, the Candidate of Technical Science and the Dr. Univ. degrees from the Technical University of Budapest and the Hungarian Academy of Sciences in 1978, 1988, and 1990, respectively. He has been with the Research Institute for Telecommunications since 1978, where he is now a senior researcher. His main interests are microwave measurements, transistor modelling, nonlinear circuit theory and neural networks.

Dr. Ladvánszky is the author or co-author of more than 50 papers and research reports. He is an associate editor of the Journal on Communications and a member of the Telecommunication Systems Commitee of the Hungarian Academy of Sciences. For his scientific achievements he received the Pollák—Virág award from the Scientific Association for Telecommunications, Hungary, and several other awards and distinctions.

ON THE SOLUTION OF NONLINEAR RESISTIVE NETWORKS

MARTIN HASLER

DEPARTMENT OF ELECTRICAL ENGINEERING
SWISS FEDERAL INSTITUTE OF TECHNOLOGY LAUSANNE
1015 LAUSANNE, SWITZERLAND

The existence and uniqueness of the solution of a nonlinear resistive circuit does not depend on the precise parameter values and on the precise form of the characteristic of the nonlinear resistors if certain topological conditions are satisfied. It is shown how these conditions are expressed in terms of signs of voltages and currents, thereby giving them an intuitive meaning. The relation to our previous approach which is slightly less intuitive but algorithmically more efficient is established. Other applications of the same criteria are mentioned.

1. INTRODUCTION

Electronics courses teach the students which circuits perform what functions. However, no profound explanation is given. There is a wide gap between basic circuit theory and electronics. Filling this gap remains an important theoretical task. Indeed, if this gap were filled, circuit theory would be more far-reaching and electronics more systematic. This paper gives an account of research efforts directed to this goal. They represent only one step in this direction and most of the work remains to be done.

The notion of *circuit* has many facets. It may designate on the one hand a physical object and on the other hand a model of that same object. On the model side all parameters, such as resistances, semiconductor parameters, etc. may be specified, or the circuit may be described by the kind of constituents it is composed of and by their connections. This last characterization is often referred to as *circuit topology,* or *circuit structure.* Studying a circuit at this level means looking for circuit properties that do not depend on element values and other circuit parameters. Such properties are usually referred to as *topological properties.* Stating that a ciruit can perform a given function (e.g. amplification) is a topological property, because varying the circuit parameters will not alter the qualitative nature of the function, at least if the parameter variations are not too large.

Probably the most basic question is how many equilibrium points, called *DC-operation points,* a circuit has. Many signal processing functions require a unique DC-operation point. Among them are: amplification, amplitude limiting, memoryless logic operations such as OR, AND, etc. Others rely on many DC-operation points, e.g. flip-flops and static memories in general.

Experience with electronic circuits over the years has convinced the engineers that certain circuit topologies always have a single DC-operation point, without ever having seen a proof of this fact. The efforts of Sandberg, Willson, Nielsen [1], [2] and later of Nishi, Chua [3], [4] have led to existence and uniqueness theorems for DC-operation points. Even though they constitute remarkable achievements, they still do not belong to engineering curricula. The reason might be that the matter is too complex for a basic circuit theory course. In this paper, we present our own approach to the same problem [5], [6], with special emphasis on the concrete meaning of the different graph-theoretical constructs. By this we hope to convince the reader that the subject is not as involved as it might seem, and that insight can be gained into the properties of nonlinear circuits, not only through the theorems themselves but also through their proofs.

The graph-theoretical criteria for the existence and the uniqueness of the DC-operation point that will be introduced can be checked for small circuits by inspection. For larger circuits, combinatorial algorithms have been developed. This leads to a new kind of software, namely computer programs that determine qualitative properties. To be honest, it must be admitted that our algorithms have exponential complexity in the number of resistors and therefore are not able to cope with very large circuits. It may well be, however, that special algorithms can be developed for a restricted class of circuits, e.g. all-transistor circuits, which have lower complexity.

2. STANDARD EQUATIONS

In this Section, we introduce the circuits we consider and the system of equations that describe them. Since we are only interested in static properties of dynamic circuits, namely the number of DC-operation points, we can restrict our attention to resistive circuits. To a DC-operation point of the dynamic circuit corresponds a solution of the resistive circuit obtained by removing the capacitors and short-circuiting the inductors. This solution is composed of constant voltages and currents. Therefore, in the sequel all voltages and currents will be constants rather than functions of time.

A circuit is a connection of circuit elements. We admit the following elements which are all 1-ports.

a) *V-resistors*

They obey a constitutive relation of the form

$$i = g(v) \tag{1}$$

where g is continuous, increasing but not necessarily strictly increasing, and defined for all real voltages v. The symbol of a V-resistor is represented in Fig. 1.

b) *I-resistors*

They obey a constitutive relation of the form

$$v = h(i) \tag{2}$$

where h is continuous, increasing but not necessarily strictly increasing, and defined for all real currents i. The symbol of an I-resistor is represented in Fig. 2.

c) *Voltage sources*

As usual, a voltage source is described by the constitutive relation

$$v = E \tag{3}$$

where E is a constant. The symbol is given in Fig. 3.

d) *Current sources*

As usual, a current source is described by the constitutive relation

$$i = I \tag{4}$$

where I is a constant. The symbol is given in Fig. 4.

e) *Nullator*

A nullator is described by the two constitutive relations

$$v = 0 \tag{5}$$

$$i = 0 \tag{6}$$

and represented by the symbol Fig. 5.

f) *Norator*

A norator has no constitutive relation. It is represented by the symbol of Fig. 6.

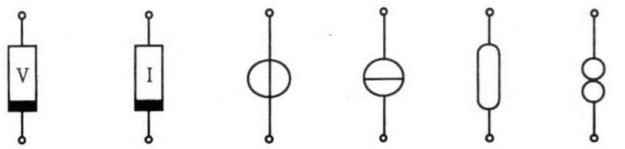

Fig. 1. *Fig. 2.* *Fig. 3.* *Fig. 4.* *Fig. 5.* *Fig. 6.*

Remark 1 :

a) These 6 basic elements are sufficient for resistive circuits in the sense that all static devices that can be described by lumped constants can sufficiently well be modeled by a connection of the 6 elements. To illustrate this, we give the circuit models of a voltage amplifier with a nonlinear characteristic (Fig. 7) and the Ebers-Moll model of a bipolar npn transistor (Fig. 8).

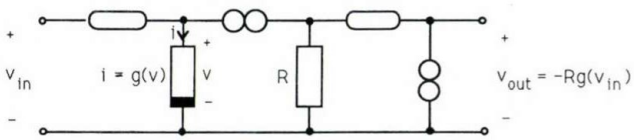

Fig. 7.

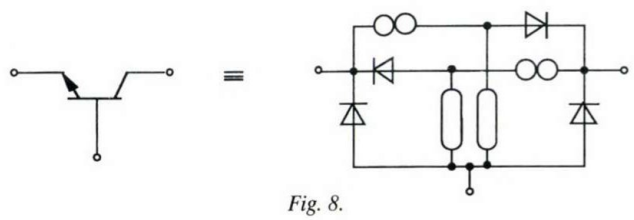

Fig. 8.

In Fig. 7 the nonlinear resistor is a V-resistor, whereas the linear resistor can be classified as a V- or an I-resistor. In Fig. 8, the nonlinear resistors are diodes which are V-resistors.

b) The voltage source is a special V-resistor, namely with a constant function g. Nevertheless, it is advantageous to introduce a special category for this element. The same remark applies to the current source.

Definition 1

A *nonlinear resistive circuit* is a connection of elements that belong to the above introduced six types. The *circuit parameters* are the functions g and h that describe the nonlinear resistors and the values of the voltage and current sources. A *nonlinear resistive circuit structure* is a nonlinear resistive circuit where the circuit parameters are not specified. More precisely, a nonlinear resistive circuit structure is a graph whose branches are labelled by the six element types.

Definition 2

The *standard equations* of a nonlinear resistive circuit are the Kirchhoff voltage and current equations together with the constitutive relations (1)—(6) of the circuit elements. A *solution* of the circuit is a set of branch voltages and currents that satisfy the standard equations.

Remark 2

a) If there are as many nullators as norators, there are 2b standard equations where b is the number of branches of the circuit graph, or, equivalently, the number of circuit elements. There are also 2b unknowns, the branch voltages and currents. If the number of nullators and norators is not equal then the number of equations and unknowns does not match. Therefore, we assume throughout this paper an equal number of nullators and norators.

b) Given a circuit, its solution is computed by some numerical algorithm, either by a Newton—Raphson or a homotopy method [7]. There remains, however, the question how many solutions there are. Usually, this question cannot be answered reliably by numerical computations. Furthermore, such a computation deals only with a specific set of parameters. The criteria we discuss in this paper are of a quite different nature. They allow to establish the existence and the uniqueness of the solution for a whole class of circuits. In the end, they lead to combinatorial algorithms. The idea is that the combinatorial algorithm should precede the numerical algorithm in the analysis of a circuit. Together, they give reliable information on the behavior of the circuit.

3. ORIENTATIONS

Suppose we are not interested in the precise solution of a circuit but only in the sign of the circuit variables. As we shall see, this rudimentary information about the solution is what we need for qualitative analysis. From a more practical point of view, it might be useful for circuit testing.

For each voltage v_k, we introduce the variable

$$\hat{v}_k = \text{sign}(v_k) \tag{7}$$

and for each current i_k the variable

$$\hat{i}_k = \text{sign}(i_k) \tag{8}$$

where

$$\text{sign}(x) = \begin{cases} +1 \text{ for } x > 0 \\ 0 \text{ for } x = 0 \\ -1 \text{ for } x < 0 \end{cases} \tag{9}$$

Thus, $\hat{v}_k$ and $\hat{i}_k$ can take the values $+1, -1$ and 0. Note that the sign of a voltage or current is always defined with respect to an arbitrarily chosen reference direction on the

corresponding branch of the circuit graph. Hence, $\hat{v}_k$ can be identified with an orientation as follows : If $\hat{v}_k = 1$, the branch is orientated as its reference direction, if $\hat{v}_k = -1$, the branch is orientated against its reference direction and if $\hat{v}_k = 0$, the branch is not orientated. Proceeding in this way, a set of branch voltages $\{v_k\}$ leads to a partial orientation of the branches, defined by $\{\hat{v}_k\}$. If this orientation had been chosen as the reference direction, all voltages v_k would be nonnegative. The same procedure can be applied to a set of currents as well.

If we start from a circuit solution, the voltages and the currents in general lead to different partial orientations of the branches. Similarly, the voltages of different solutions lead in general to different partial orientations and the same is true for the currents.

Definition 3

Consider a graph G.

a) A partial orientation of the branches of G is a *voltage orientation,* if there is a set of branch voltages $\{v_k\}$ that satisfies Kirchhoff's voltage laws such that $\{\hat{v}_k\}$ is precisely this partial orientation.

b) A partial orientation of the branches of *G* is a *current orientation,* if there is a set of branch currents $\{i_k\}$ that satisfies Kirchhoff's current laws such that $\{\hat{i}_k\}$ is precisely this partial orientation.

In Figs. 9 and 10, a current and a voltage distribution are represented that satisfy Kirchhoff's laws. The corresponding orientations are marked by arrows. Note that the two orientations differ on two branches. One branch is not orientated in the current orientation and two branches in the voltage orientation.

The next definition refers to circuits rather than graphs because the constitutive relations of the elements play a role. Actually, it is tied to circuit structures rather than circuits because the existence of a circuit is required, but no constraint is imposed on the circuit parameters.

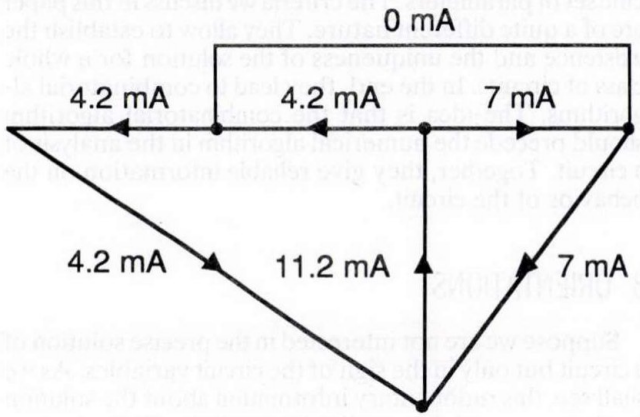

Fig. 9.

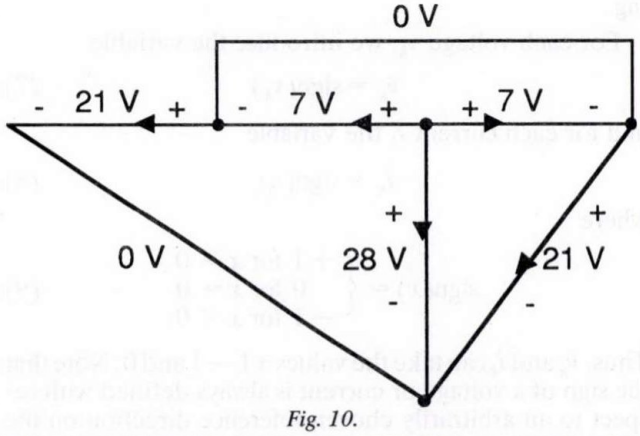

Fig. 10.

Definition 4

Consider a nonlinear resistive circuit structure S. A voltage orientation and a current orientation of the graph of S are *incrementally compatible* if there is a circuit C with structure S and two solutions $\{v_k^{(1)}, i_k^{(1)}\}$ and $\{v_k^{(2)}, i_k^{(2)}\}$ of C such that $\Delta\hat{v}_k$ and $\Delta\hat{i}_k$ are the corresponding partial orientations, as defined by (7) and (8), where $\Delta v_k = v_k^{(1)} - v_k^{(2)}$ and $\Delta i_k = i_k^{(1)} - i_k^{(2)}$.

In Fig. 11, a nonlinear resistive circuit structure is represented whose graph is the same as in Figs. 9 and 10. In Fig. 12, a nonlinear resistive circuit is represented whose only nonlinear resistor has the piecewise linear characteristic of Fig. 13. This circuit has the structure of Fig. 11.Two solutions are indicated in Fig. 13, one below the other. Subtracting the lower solution from the upper yields the voltage and current increments given in Figs.9 and 10. Therefore, the voltage and current orientation marked in Figs. 9 and 10 by arrows are incrementally compatible with respect to the nonlinear resistive circuit structure of Fig. 11.

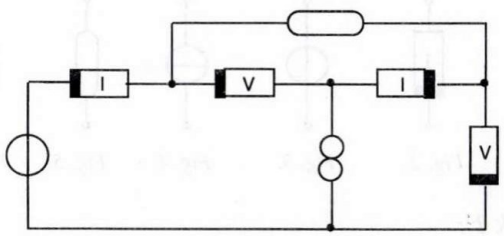

Fig. 11.

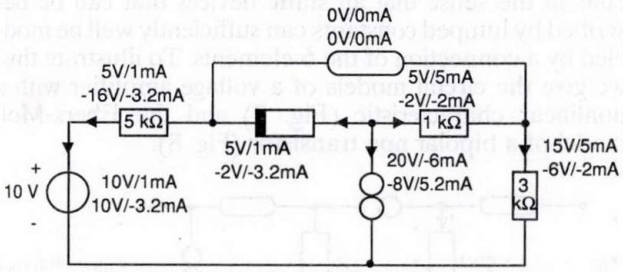

Fig. 12.

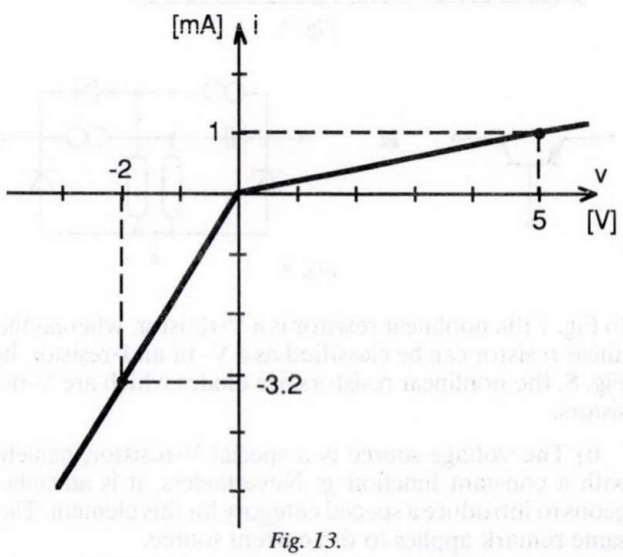

Fig. 13.

Remark 3

a) If $v_k^{(1)}$ and $v_k^{(2)}$ satisfy Kirchhoff's voltage laws then so do Δv_k and thus $\hat{\Delta} v_k$ is a voltage orientation. Similarly for the currents.

b) The *trivial partial orientation,* where no branch is orientated, is both a voltage and a current orientation. Furthermore, the trivial voltage and the trivial current orientation are incrementally compatible for any nonlinear resistive circuit structure. Indeed, take any solution **(v,i)** of any circuit with structure S and set $\mathbf{v}^{(1)} = \mathbf{v}^{(2)} = \mathbf{v}$, $\mathbf{i}^{(1)} = \mathbf{i}^{(2)} = \mathbf{i}$ which implies $\Delta\mathbf{v} = \Delta\mathbf{i} = 0$.

The question now arises whether it is possible to characterize the voltage and current orientations without reference to actual voltages and currents and whether it is possible to express incremental compatibility without introducing circuit parameters and corresponding solutions. Are there analogs off Kirchhoff voltage and current laws and constitutive relations for the $\hat{\Delta} v_k$'s and the $\hat{\Delta} i_k$'s ? Surprisingly, the answer is negative for Kirchhoff's laws and affirmative for the constitutive relations. This will be discussed in sections 4 and 5. In particular, we shall see that the characterization of voltage and current orientations are of basic graph theoretical nature rather than of arithmetic form, as is the case for Kirchhoff's laws.

4. VOLTAGE AND CURRENT ORIENTATIONS

Definition 5

Consider a partially orientated graph. A *loop (cutset)* is *uniform* if all of its orientated branches are similarly directed around the loop (within the cutset).

We now give two equivalent characterizations of voltage and current orientation. The first requires the absence of certain uniform loops and cutsets, the "bad" loops and cutsets, and the second the presence of certain other uniform loops and cutsets, the "good" ones.

Theorem 1

Consider a graph G.

a) A partial orientation of G is a voltage orientation if and only if there is no uniform loop that contains at least one orientated branch.

b) A partial orientation of G is a current orientation if and only if there is no uniform cutset that contains at least one orientated branch.

Theorem 2

Consider a graph G.

a) A partial orientation of G is a voltage orientation if and only if each orientated branch is part of a uniform cutset composed exclusively of orientated branches.

b) A partial orientation of G is a current orientation if and only if each orientated branch is part of a uniform loop composed exclusively of orientated branches.

Theorem 2 is illustrated in Figs. 14 and 15 for the current and the voltage orientation of Figs. 9 and 10. The required uniform loops and cutsets are indicated by distinet lines.

Proof of theorems 1 and 2

1. "Only if" part of theorem 1

Suppose $\{\hat{v}_k\}$ is a voltage orientation of G. Take it as a reference direction of the orientated branches and take any reference direction for the remaining branches. By definition, there is a set of voltages $\{v_k\}$ such that (7) holds.

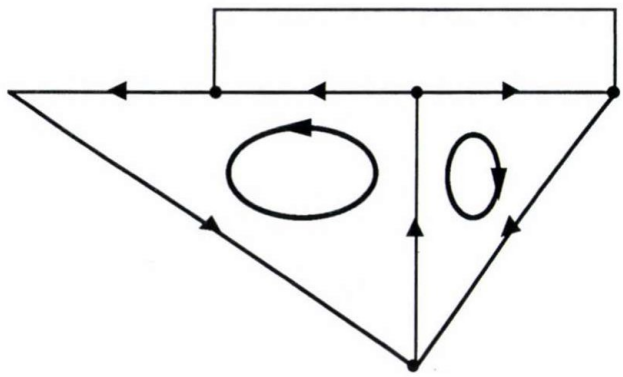

Fig. 14.

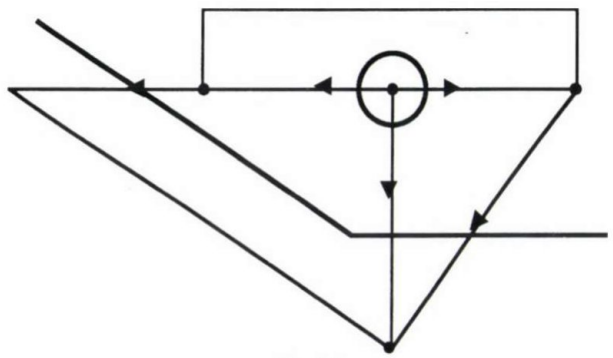

Fig. 15.

Hence, $v_k = 0$ whenever branch k is not orientated and, due to the choice of reference direction, $v_k > 0$ whenever branch k is orientated. Suppose there is a uniform loop with at least one orientated branch. Kirchhoff's voltage law for this loop is

$$\sum_{\text{loop}} v_k = 0 \tag{10}$$

But since all $v_k \geq 0$ and at least one $v_k > 0$, the LHS of (10) is positive and thus (10) cannot hold. We conclude that there is no uniform loop with at least one orientated branch.

The proof for the current orientations is dual.

QED.

2. "If" part of theorem 2

Consider a partial orientation of G such that all orientated branches take part in a cutset composed only of orientated branches. Take this orientation as a reference direction for the orientated branches and choose any reference direction for the other branches. Let C be the set of all uniform cutsets composed exclusively of orientated branches. For each $c \in C$ consider the set of voltages defined by

$$v_k^{(c)}(E) = \begin{cases} E & \text{if branch } k \text{ is part of } c \\ 0 & \text{otherwise} \end{cases} \tag{11}$$

where E is any positive constant voltage. The cutset c divides the set of nodes into two subsets. The branch voltages $v_k^{(c)}(E)$ derive from the node potential where one subset is at potential E and the other at potential zero. Hence, they satisfy Kirchhoff's voltage laws. Finally, we define

$$\mathrm{v}_k(E) = \sum_{c \in C} v_k^{(c)}(E) \tag{12}$$

Then $\{v_k(E)\}$ also satisfy Kirchhoff's voltage laws. Furthermore, $v_k(E)$ is a positive multiple of E for each orientated branch, and thus positive, and 0 for all non orientated branches. Hence, $\{\hat{v}_k(E)\}$ coincides with the original partial orientation which implies that this orientation is a voltage orientation.

The dual proof applies to the partial orientation with the „good" uniform loops. Here, we define

$$i_k(I) = \sum_{l \in L} i_k^{(l)}(I) \tag{13}$$

where L is the set of all uniform loops composed only of orientated branches and

$$i_k^{(l)}(I) = \begin{cases} I & \text{if branch } k \text{ is part of } l \\ 0 & \text{otherwise} \end{cases} \tag{14}$$

Then $i_k(I)$ satisfies Kirchhoff's current law, it is a positive multiple of the positive constant I if the branch k is orientated and 0 otherwise, and $\{\hat{i}_k(I)\}$ is the original partial orientation.

QED.

3. Equivalence of theorems 1 and 2

The proof is based on the colored branch theorem [8], [9]. Consider any partial orientation of the branches of G and color the orientated branches green and the other branches red. Then, according to the colored branch theorem, each green branch either belongs to a uniform cutset composed of green branches, or a uniform loop composed of green and red branches. Therefore, the condition that there is no uniform loop with at least one orientated branch (theorem 1a)) is equivalent to the condition that each orientated branch belongs to a uniform green-only cutset (theorem 2a)).

Coloring the non orientated branches blue instead of red leads to the equivalence of theorems 1b) and 2b).

QED.

The next theorem is not needed in the sequel. Nevertheless, we think it is instructive in the present context.

It is a well-known fact in circuit theory that any set of currents that satisfy Kirchhoff's current laws can be decomposed into a sum of loop currents. Indeed, it is sufficient to choose a maximal set of independent loops. The sums of all possible loop currents then coincide with the set of all current distributions that satisfy Kirchhoff's current laws. The dual statement is true for voltage distributions that satisfy Kirchhoff's voltage laws. A maximal set of independent loops can e.g. be obtained by considering a complete tree. Its links generate such a maximal set.

The current distributions obtained in the proof of the "if" part of theorem 2 are of a special nature. They are sums of positive loop currents of uniform loops. The question now arises whether any set of currents that satisfy Kirchhoff's current laws can be decomposed in this way. The answer is affirmative. However, the partial orientation and thus the set of uniform loops has to be adapted to the set of currents. The dual properties hold for voltage distributions too.

Theorem 3

Consider a graph G.

a) Let $\{v_k\}$ be a set of branch voltages that satisfy Kirchhoff's voltage law. Then there is a partial orientation of the branches of G, a set C of uniform cutsets composed exclusively of orientated branches and a set of $|C|$ positive voltages E_c such that

$$v_k = \sum_{c \in C} v_k^{(c)}(E_c) \tag{15a}$$

where $v_k^{(c)}(E_c)$ is given by (11).

b) Let $\{i_k\}$ be a set of branch currents that satisfy Kirchhoff's current law. Then there is a partial orientation of the branches of G, a set L of uniform loops composed exclusively of orientated branches and a set of $|L|$ positive current I_l such that

$$i_k = \sum_{l \in L} i_k^{(l)}(I_l) \tag{15b}$$

where $i_k^{(l)}(I_l)$ is given by (14).

Proof

We prove b) because a) can be obtained by a simple reasoning about the node potentials. A perfectly dual proof can also be given for a).

Let $\{i_k\}$ be a set of branch currents that satisfy Kirchhoff's current law and orientate the branches of G according to $\{\hat{i}_k\}$. Take this partial orientation as the reference direction for the branches. With respect to this orientation we have $i_k \geq 0$ for all branches. Let j be the branch with smallest positive current. Since this branch is orientated, it belongs to a uniform loop L_j of orientated branches. Define a new set of branch currents

$$\check{i}_k = \begin{cases} i_k - i_j & \text{if } k \text{ belongs to } L_j \\ i_k & \text{otherwise} \end{cases} \tag{16}$$

Then $i_k \geq \check{i}_k \geq 0$. It follows that $\check{i}_k$ satisfies again Kirchhoff's current law and that whenever $i_k = 0$ we have $\check{i}_k = 0$. Actually, in the new current distribution at least one more branch has zero current, namely branch j. Another way expressing $\check{i}_k$ is

$$\check{i}_k = i_k - i_k^{(L_j)}(i_j) \tag{17}$$

where $i_k^{(L_j)}(i_j)$ is given by (14).

Now we can repeat the above construction. We first remove the orientation from the branches where $i_k > 0$ but $\check{i}_k = 0$, in particular from branch j. Then we identify the branch $\check{j}$ with the smallest current $i_{\check{j}}$, define a new current distribution by (16), etc.

At each step in the iteration, at least one more branch has zero current. Thus, the iteration stops after a finite number of steps when all currents are zero. Since by (17) at each step we have subtracted a positive loop current, the original current distribution $\{i_k\}$ is a sum of positive loop currents. The loops are uniform and composed of orientated branches with respect to the orientation of the corresponding iteration. But since subsequent iterations simply have less orientated branches, but otherwise coincide with previous orientations, the loops are uniform and composed of orientated branches in the original orientation $\{\hat{i}_k\}$ as well.

QED.

For the current distribution of Fig. 9, the partial orientation of the branches, the uniform loops and the positive loop currents are represented in Fig. 16. For the voltage distribution of Fig. 10, the partial orientation of the resistors, the uniform cutsets and the positive cutset voltages are represented in Fig. 17.

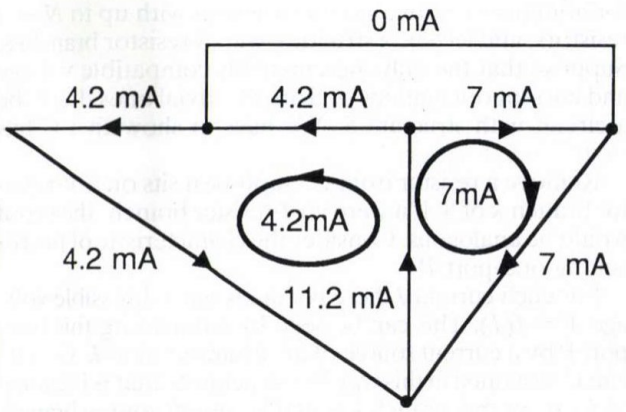

Fig. 16.

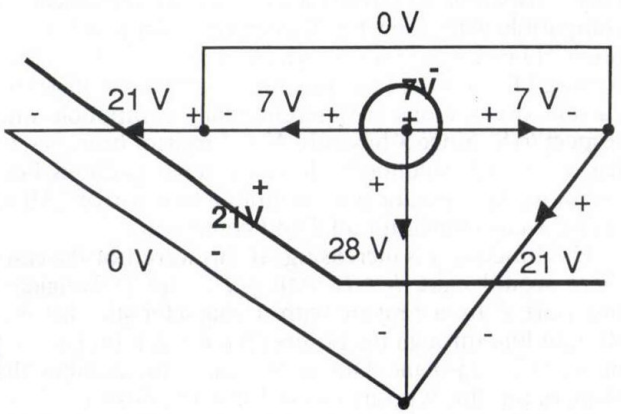

Fig. 17.

5. COMPATIBLE VOLTAGE AND CURRENT ORIENTATIONS

The compatibility condition for voltage and current orientations can be expressed by a set of equations that correspond directly to the constitutive relations of the circuit elements.

Theorem 4

Suppose a nonlinear resistive circuit structure S is given. A voltage orientation $\{\hat{\Delta}v_k\}$ and a current orientation $\{\hat{\Delta}i_k\}$ are incrementally compatible if and only if for each branch k that does not carry a norator one of the following conditions is satisfied :

a) If k carries a V-resistor

$$\hat{\Delta}v_k = \hat{\Delta}i_k \text{ or } \hat{\Delta}i_k = 0 \tag{18}$$

b) If k carries an I-resistor

$$\hat{\Delta}v_k = \hat{\Delta}i_k \text{ or } \hat{\Delta}v_k = 0 \tag{19}$$

b) If k carries a voltage source

$$\hat{\Delta}v_k = 0 \tag{20}$$

c) If k carries a current source

$$\hat{\Delta}i_k = 0 \tag{21}$$

d) If k carries a nullator

$$\hat{\Delta}v_k = \hat{\Delta}i_k = 0 \tag{22}$$

Proof

"Only if" part

Consider a circuit C with structure S, two solutions of C and their increments. Since the current in a V-resistor is an increasing function of the voltage, the current increment is either zero or it has the same sign as the voltage increment. This fact is expressed by (18). Similarly for I-resistors. Relations (20)—(22) are evident.

QED.

"If" part

Let a voltage and a current orientation of the graph G of S be given and denoted by $\{\hat{\Delta}v_k\}$ and $\{\hat{\Delta}i_k\}$, respectively. Hence there are voltages Δv_k and currents Δi_k that satisfy the respective Kirchhoff laws such that

$$\hat{\Delta}v_k = \text{sign}\,(\Delta v_k) \tag{23a}$$

$$\hat{\Delta}i_k = \text{sign}\,(\Delta i_k) \tag{23b}$$

Suppose that for each branch, the corresponding condition out of (18)—(22) is satisfied, except for the norator branches where no condition is imposed. Then define the circuit C as follows. Take the graph G and introduce the nullators and norators where required for the structure S.

Furthermore,

a) on a V-resistor branch of S introduce a linear resistor with admittance $G_k = \Delta i_k / \Delta v_k$ if $\Delta v_k \neq 0$ and any positive value if $\Delta v_k = 0$. It follows from (18) that $G_k \geq 0$ and thus the linear resistor is a V-resistor.

b) on an I-resistor branch introduce a linear resistor with resistance $R_k = \Delta v_k / \Delta i_k$ if $\Delta i_k \neq 0$ and any positive value if $\Delta i_k = 0$. It follows from (19) that $R_k \geq 0$ and thus the linear resistor is an I-resistor.

c) on a source branch of S introduce the corresponding source and set its value to zero. It follows that circuit C has structure S and that $(\Delta \mathbf{v}, \Delta \mathbf{i})$ and $(\mathbf{v} = \mathbf{0}, \mathbf{i} = \mathbf{0})$ are two solutions of C. The resulting increments are $(\Delta \mathbf{v}, \Delta \mathbf{i})$ themselves. Hence, $\{\hat{\Delta}v_k\}$ and $\{\hat{\Delta}i_k\}$ are incrementally compatible.

QED.

The compatibility conditions of the current orientation in Fig. 9 and the voltage orientation in Fig. 10 with respect to the nonlinear resistive circuit structure in Fig. 11 are readily checked.

It is easy to generalize our approach to include controlled sources. The different definitions have to be modified to accomodate the new elements in an obvious way. Theorem 4 then has to be supplemented with the appropriate conditions.

A voltage controlled voltage source with a positive coefficient α whose ports are the branches j and k obeys the constitutive relations

$$v_k = \alpha v_j \tag{24}$$

$$i_j = 0 \tag{25}$$

and leads to the incremental compatibility conditions

$$\hat{\Delta}v_k = \hat{\Delta}v_j \tag{26}$$

$$\hat{\Delta}i_j = 0 \tag{27}$$

The other three types of controlled sources can be discussed similarly.

It could be suspected that the ideal transformers and gyrators can also be embedded into this framework. It turns out, however, that this is not the case, because the transformation and gyration ratios appear simultaneaously in two constitutive relations and therefore the proof of the "if" part of theorem 4 does not go through [6].

6. EXISTENCE AND UNIQUENESS OF THE SOLUTION

In this Section we answer the following question:

When do all circuits with a given nonlinear resistive structure S have exactly one solution?

A necessary condition follows immediately from definition 4: The only incrementally compatible voltage and current orientations of S are the trivial ones where no branch is orientated. Indeed, if one of them were nontrivial, there would be a circuit C with structure S and two solutions of C such that the signs of the voltage and current increments coincided with the corresponding orientations. Hence, not all increments could vanish und thus the two solutions would have to be distinct.

We shall prove that this condition is not only necessary, but also sufficient. First, we treat the very special case where there are no resistors.

Lemma 1

Consider a resistive circuit structure S without resistor branches. All circuits with structure S have exactly one solution if and only if the only incrementally compatible voltage and current orientations are the trivial ones. In this case, the solution is a continuous function of any source value.

Proof:

By the above arguments, we only have to prove the "if" part and the continuity. Suppose that the only incrementally compatible voltage and current orientations are the trivial ones.

Assume there is a circuit C with structure S which has no solution or more than one solution. Since C is a linear circuit, it is described by a system of linear equations whose determinant is zero. Set the source values to zero. The resulting system becomes homogeneous and since its determinant is zero, it has an infinity of solutions. This cannot be the case, however, because the voltage and current increments between any two different solutions would lead to nontrivial incrementally compatible voltage and current orientations. Thus, any circuit with structure S has exactly one solution. Furthermore, the solution is an affine function of any source value and therefore continuous.

QED.

Theorem 5

Consider a nonlinear resistive circuit structure S. All circuits with structure S have exactly one solution if and only if the only incrementally compatible voltage and current orientations are the trivial ones. In this case, the solution is a continuous function of any source value.

Proof

Again, we only have to prove the "if" part of the theorem. The proof goes by induction on the number N of resistors. It is illustrated in Fig. 18. For $N = 0$, theorem 5 reduces to lemma 1. Let us suppose that the theorem holds for nonlinear resistive circuit structures with up to $N-1$ resistors, and let S be a structure with N resistor branches. Suppose that the only incrementally compatible voltage and current orientations of S are the trivial ones. Let C be a circuit with structure S. We have to show that C has exactly one solution.

Remove a resistor from C. Suppose it sits on a V-resistor branch k of S. If it were an I-resistor branch, the proof would be analogous. Consider the characteristic of the resulting one-port P.

For each current I there is exactly one admissible voltage $V = f(I)$. This can be seen by terminating this one-port P by a current source of an arbitrary value I. The circuit C′ obtained in this way has structure S′ that is identical to S except that branch k is now a current source branch. Any voltage and current orientations that are incrementally compatible with respect to S′ are also incrementally compatible with respect to S, because on branch k condition (21) is required for S′, which implies condition (18) required for S. Consequently, only the trivial voltage and current orientations are incrementally compatible with respect to S′. Since S′ has only $N-1$ resistor branches, C′ has exactly one solution by the induction hypothesis. Furthermore, this solution is a continuous function of I. Thus, $f(I)$ is well-defined for all I and continuous.

The function f is increasing. If this were not the case, there would exist $I_1 < I_2$ with $f(I_1) > f(I_2)$. Terminate one-port P by a resistor with a characteristic that is a straight line through the points $(f(I_1), -I_1)$, $(f(I_2), -I_2)$ in the $(V, -I)$-plane. Due to the above inequalities, the slope of this line is positive and thus the resistor is a V-resistor. Therefore, the resulting circuit C″ has structure S. However, the solutions of C′ with source values I_1 and I_2 constitute two distinct solutions of C″. The corresponding increments generate a nontrivial incrementally compatible voltage and current orientation which is in contradiction with the hypothesis.

Now let us return to the original circuit C. It can be considered as the one-port P terminated by the original V-resistor whose constitutive relation is, say, $i_k = g(v_k)$. By expressing a solution of C by the port variables (V, I), we have

$$-I = g(V) \tag{28}$$

$$V = f(I) \tag{29}$$

or

$$g(f(I)) + I = 0 \tag{30}$$

Since the LHS of (30) is a strictly increasing continuous function of I, with limit $\pm\infty$ as $I \to \pm\infty$, equation (30), and thus C, has exactly one solution.

Finally, we have to show the continuity of the solution as a function of any source value E. Let us denote the unique solution of (30) by $I(E)$. Hence

$$g(f(I(E))) + I(E) = 0 \tag{30a}$$

Let us further denote the characteristic of the one-port P, *taking account of the parameter* E, by

$$V = f(I, E) \tag{31}$$

By the induction hypothesis, $f(I, E)$ is continuous both in I and E. Let E_1 and E_2 be any two values for E and suppose that $I(E_1) < I(E_2)$. Then

$$0 \le I(E_2) - I(E_1) = g(f(I(E_1), E_1)) -$$

$$- g(f(I(E_2), E_1)) + g(f(I(E_2), E_1)) - g(f(I(E_2), E_2)) \le$$

$$\le g(f(I(E_2), E_1)) - g(f(I(E_2), E_2)) \tag{32}$$

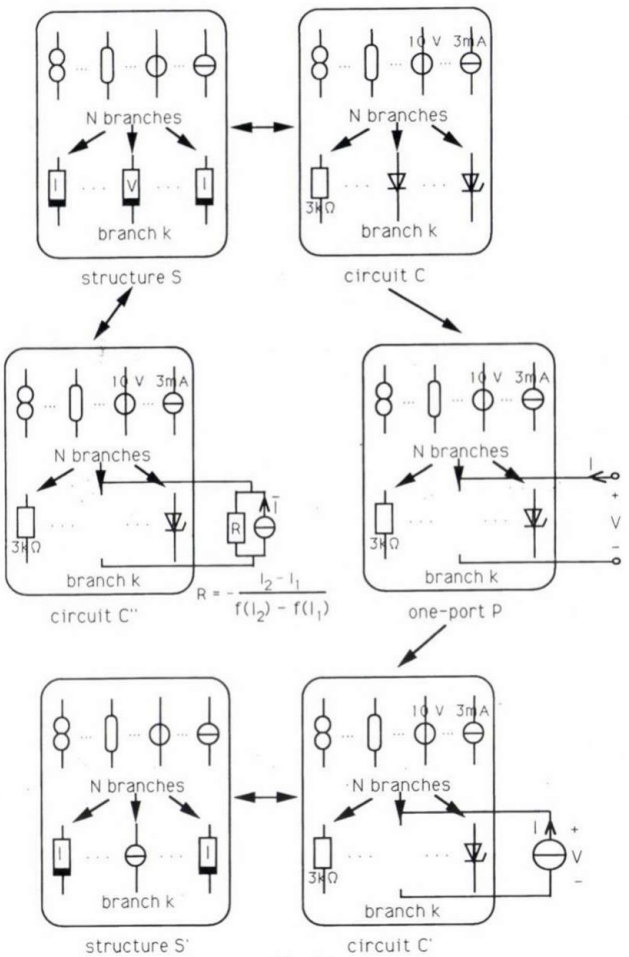

Fig.18.

The last inequality holds because $g(f(.))$ is an increasing function. The continuity of $f(I,E)$ on E then implies the continuity of $I(E)$.

QED.

Remark 4

a) In [6], theorem 5 has been proved by relating first the nonlinear problem to the corresponding linear problem and then by proving the theorem for linear circuits. While this intermediate step is of interest by its own, the above approach represents a shortcut.

b) Again in [6], theorem 5 has been generalized to resistors that are neither voltage nor current controlled, to resistors with decreasing characteristics and to linear and nonlinear controlled sources.

c) Finally, we refer to [6] for examples that illustrate theorem 5. They are discussed in terms of another topological criterion, but the two approaches will be related in the next section.

7. VARIANTS OF THE TOPOLOGICAL CRITERIA

To determine whether or not a given nonlinear resistive circuit structure has nontrivial incrementally compatible voltage and current orientations is a task that is in principle of exponential complexity in the number of branches. Indeed, there are 3^b possible partial orientations of the graph, where b is the number of branches, and thus 3^{2b} possible pairs of partial orientations. For each pair one has to check whether

- the first is a voltage orientation
- the second is a current orientation
- the two partial orientations are incrementally compatible.

Evidently, this is not a clever way to proceed and it is worthwile to spend some effort in trying to improve the method. Actually, the original criterion used in [5] is based on single partial orientations of the resistor branches. Using this criterion, we only have to consider 3^N orientations, where N is the number of resistors. The complexity is still exponential, but with a much smaller exponent. Theorem 6 below relates the two approaches.

Definition 6

Let S be a nonlinear resistive circuit structure. A partial orientation of the resistor branches is *uniform,* if every orientated resistor

a) belongs to a uniform loop composed exclusively of orientated resistor, voltage source and norator branches, and

b) belongs to a uniform cutset composed exclusively of orientated resistor, current source and norator branches.

Note that this definition does not distinguish between V-resistors and I-resistors.

Definition 7

Let S be a nonlinear resistive circuit structure. Consider a voltage orientation $\{\hat{\Delta}v_k\}$ and a current orientation $\{\hat{\Delta}i_k\}$ that are incrementally compatible on S. The corresponding *reduced nonlinear resistive circuit structure* S′ and the *associated partial orientation* $\{\hat{\Delta}r_k\}$ *of the resistors* of S′ are obtained as follows. Set $\hat{\Delta}r_k=0$ for the norator, nullator and source branches of S. For a resistor branch k of S proceed as follows:

- If $\hat{\Delta}v_k=\hat{\Delta}i_k$, set $\hat{\Delta}r_k=\hat{\Delta}v_k$.
- If $\hat{\Delta}v_k=0$, but $\hat{\Delta}i_k\neq 0$, set $\hat{\Delta}r_k=0$ and transform the resistor branch into a voltage source branch.
- If $\hat{\Delta}i_k=0$, but $\hat{\Delta}v_k\neq 0$, set $\hat{\Delta}r_k=0$ and transform the resistor branch into a current source branch.

We say also that $\{\hat{\Delta}v_k\}$, $\{\hat{\Delta}i_k\}$ *extend* $\{\hat{\Delta}r_k\}$.

Theorem 6

a) Let S be a nonlinear resistive circuit structure and suppose we have a voltage and a current orientation that are incrementally compatible on S. Consider the reduced nonlinear resistive circuit structure S′ and the associated partial orientation of the resistors of S′. This partial orientation is uniform.

b) Let S′ be a nonlinear resistive circuit structure and suppose we have a uniform partial orientation of the resistors of S′. Consider any nonlinear resistive circuit structure S that is identical to S′, except that certain voltage source and current source branches of S′ are, respectively, I-resistor and V-resistor branches in S. Then there is an incrementally compatible voltage and current orientation on S which extends the given partial orientation of S′.

Proof

Let $\{\hat{\Delta}v_k\}$, $\{\hat{\Delta}i_k\}$ denote the voltage and current orientation of S and $\{\hat{\Delta}r_k\}$ the partial orientation of the resistors of S′.

a) We first prove that every orientated resistor branch of S′ is part of a uniform cutset composed exclusively of orientated resistors, norators and current sources.

Take an orientated resistor branch j of S′. Then $\hat{\Delta}r_j=\hat{\Delta}v_j=\hat{\Delta}i_j\neq 0$. Due to theorem 2a), branch j is part of

a uniform cutset composed branches with nonvanishing voltage orientation in S. In $\{\hat{\Delta}r_k\}$ the cutset remains uniform, but some branches have lost their orientation. These are the norator and the current source branches. In addition, the V-resistor branches with $\hat{\Delta}i_k=0$ and $\hat{\Delta}v_k \neq 0$ have also lost their orientation, but at the same time, they have become current source branches. Hence, the cutset is uniform in S′ and is composed only of orientated resistors, norators and current sources.

In a dual fashion, we prove that every orientated resistor branch of S′ is part of a uniform loop composed exclusively of orientated resistors, norators and voltage sources.

b) Starting from the orientation $\{\hat{\Delta}r_k\}$, we construct $\{\hat{\Delta}i_k\}$ stepwise as follows. At each step we shall call the actual orientation O. At the beginning, O coincides with $\{\hat{\Delta}r_k\}$.

Let j be an orientated resistor branch of S′. Then there is a uniform loop L'_j through j composed of orientated resistor, norator and voltage source branches of S′. Orientate its norator and voltage source branches such that the loop remains uniform. We shall denote L'_j also by L_j.

Next consider an orientated resistor branch m of S′ that does not belong to L'_j. Consider the loop L'_m through m that is uniform in $\{\hat{\Delta}r_k\}$. Orientate the norator and voltage source branches that belong to L'_m, but not to L'_j, in the sense of L'_m. Note that L'_m might not be uniform in O, because of the branches in $L'_j \cap L'_m$. However, $L'_m \setminus L'_j$ can be completed to a uniform loop L_m with respect to O by taking other branches of L'_j because from any node in L'_j there is a directed path leading to any other node of L'_j.

Then take an orientated resistor branch of S′ that does not belong to $L'_j \cup L'_m$ and repeat the process. We can continue in this way until there is no orientated resistor branch left. Now we have to show that O is a voltage orientation on S. By construction, any branch that belongs to a uniform loop L'_α with respect to $\{\hat{\Delta}r_k\}$ is orientated and belongs to a uniform loop L_α with respect to O. There is no other orientated branch of O because such a branch would also have to be orientated in $\{\hat{\Delta}r_k\}$, but all orientated branches of $\{\hat{\Delta}r_k\}$ are resistors and are part of one of these loops. Thus, by theorem 2b O is a current orientation which we denote now by $\{\hat{\Delta}i_k\}$.

Starting again from $\{\hat{\Delta}r_k\}$, we construct the voltage orientation $\{\hat{\Delta}v_k\}$ in the dual way, using the uniform cutsets C'_α with respect to $\{\hat{\Delta}r_k\}$ and transforming them into the uniform cutsets C_α with respect to $\{\hat{\Delta}v_k\}$.

Finally, we have to show that $\{\hat{\Delta}v_k\}$ and $\{\hat{\Delta}i_k\}$ are incrementally compatible on S. For this purpose we have to distinguish the different kinds of branches.

- If j is a norator branch, there is no condition to check.
- If j is a nullator branch, it does not belong to any loop L'_α or cutset C'_α. Thus, it does not belong to any loop L_α or cutset C_α either, and $\hat{\Delta}v_j=\hat{\Delta}i_j=0$.
- If j is a voltage source branch, it does not belong to any cutset C'_α. Thus, it does not belong to any cutset C_α either, and $\hat{\Delta}v_j=0$.
- If j is a current source branch, it does not belong to any loop L'_α. Thus, it does not belong to any loop L_α either, and $\hat{\Delta}i_j=0$.
- If j is a V-resistor branch on S, three different cases have to be distinguished. If j is a current source branch on S′, the above reasoning for current source branches applies, with the conclusion that $\hat{\Delta}i_j=0$. If j is a resistor branch on S′ with a nonvanishing orientation $\hat{\Delta}r_j$, then this orientation is maintained through the extension process and thus $\hat{\Delta}v_j=\hat{\Delta}i_j \neq 0$. Finally, if j is a resistor branch on S′ with a $\hat{\Delta}r_j=0$, then the above reasoning for a nullator applies, with the conclusion that $\hat{\Delta}v_j=\hat{\Delta}i_j=0$.
- If j is an I-resistor branch, we apply the arguments that are dual to the V-resistor case.

QED.

Let us now try to use the partial orientations of the resistors to prove that all circuits with a given nonlinear resistive circuit structure S have exactly one solution. According to theorem 5, we have to prove that there are no nontrivial voltage and current orientations that are incrementally compatible on S.

In view of theorem 6, we look for uniform partial orientations of the resistors on S. Suppose we have found a nontrivial one. Then by theorem 6b), we can extend it to a nontrivial voltage and current orientation that are incrementally compatible on S, and by theorem 5, we conclude that there are circuits with structure S that have either more than one or no solution.

However, if there is no nontrivial uniform partial orientation of the resistors in S, we cannot yet conclude that all circuits with structure S have exactly one solution, and this for two reasons:

1. There might still be a structure S′ in which certain resistor branches of S are replaced be the appropriate source branches, that has a nontrivial uniform partial orientation of the resistors.
2. There might be incrementally compatible voltage and current orientations on S where both orientations of all resistors are zero, but some other branches have nonzero orientation. The associated partial orientation of the resistors would be trivial.

Both cases can be excluded if an additional condition is satisfied.

Definition 8

A pair of conjugate trees of a nonlinear resistive circuit structure is defined by the following conditions:

a) The first tree is composed of all norator, all voltage source and some resistor branches.

b) The second tree is composed of all nullator, all voltage source and the same resistor branches as the first tree.

Note that the set of tree resistor branches identifies the pair of conjugate trees. Given a set of resistor branches, it may or it may not determine a pair of conjugate trees.

Theorem 7

Suppose S is a nonlinear resistive circuit structure which satisfies the following two conditions:

a) The I-resistor branches determine a pair of conjugate trees.

b) There is no nontrivial uniform partial orientation of the resistors.

Proof: cf. [5].

Using theorem 7, we only have to consider 3^N orientations, where N is the number of resistors, but in addition we have to check whether there is a pair of conjugate trees. Fortunately, there is an algorithm of polynomial complexity that solves this problem [6], [10]. Thus, the main computational burden remains the search for orientations.

There is another reason for considering pairs of conjugate trees. It has been shown in [11] that the circuits that have more than one, but a finite number of solutions have a nonlinear resistive circuit structure that

- has a pair of conjugate trees as required by condition a) of theorem 7, and

• has a nontrivial uniform partial orientation of the resistors.

Hence, the circuit structures that can be used for static memories must belong to this class.

8. CONCLUSION

We have shown how the existence and uniqueness problem for the solution of nonlinear resistive circuits is linked to the signs of voltage and current increments. The material presented has been published before, mainly in [5] and [6], but a few additional results are included, in particular, a result that establishes more precisely the criteria based on a single partial orientation of the resistor branches, as intorduced in [5], and two partial orientations of all branches, as used in [6].

From a fundamental point of view, we show how to do circuit theory only with the signs of voltages and currents and what kinds of conclusions can be drawn from this analysis. We are convinced that many other applications along the same lines can be found. Some have already been described [12,13].

ACKNOWLEDGEMENTS

Thanks are due to A. Premoli and the University of Trieste, Italy, for their hospitality when this paper was written. This work has been supported financially by the Swiss National Science Foundation, grant no. 2.25.290.

REFERENCES

[1] Willson, A.N. (ed.), *Nonlinear networks: Theory and analysis,* IEEE Press Book, New York, 1974.

[2] Nielsen, R.O. and A.N. Willson, "A fundamental result concerning the topology of transistor circuits with multiple equilibria", *Proc. IEEE,* vol. 68, pp. 196-208, 1980.

[3] Nishi, T. and L.O. Chua, "Topological criteria for nonlinear resistive circuits containing controlled sources to have a unique solution", *IEEE Trans. Circuits and Systems,* vol. 31, pp. 722-741, August 1984.

[4] Nishi, T. and L.O. Chua, "Nonlinear op-amp circuits: Existence and uniqueness of solution by inspection", *Int. J. Circuit Theory Appl.,* vol. 12, pp. 145-173, 1984.

[5] Hasler, M., "Non-linear non-reciprocal resistive circuits with a structurally unique solution", *Int. J. Cir. Theor. Appl.,* vol. 14, pp. 237-262, 1986.

[6] Fosséprez, M., "Topologie et comportement des circuits non linéaires non réciproques", *Presses Polytechniques Romandes,* 1989.

[7] Ortega, J.M. and W.C. Rheinboldt, *Iterative solution of nonlinear equations in several variables,* Academic Press, San Diego, 1970.

[8] Vandewalle, J. and L.O. Chua, "The colored branch theorem and its applications in circuit theory", *IEEE Trans. on Circuits and Syst.,* vol, CAS-27, pp. 816-825, 1980.

[9] Hasler, M. and J. Neirynck, "Nonlinear circuits", *Artech House,* Boston, 1986.

[10] Fosseprez, M. and M. Hasler, "Algorithms for the Qualitative Analysis of Nonlinear Resistive Circuits", *IEEE ISCAS Proceedings,* pp. 2165-2168, May 1989, Portland, Or.

[11] Fosséprez, M. and M. Hasler, "Resistive Circuits with Several Solutions", *Int. J. Cir. Theor. Appl.,* vol. 18, pp. 625-638, 1990.

[12] Chauffoureaux, P. and M. Hasler, "Monotonicity in nonlinear resistive circuits", *Proc. ISCAS'90,* pp. 395-398, New Orleans, 1990.

[13] Hasler, M. "Stability of parasitic dynamics at a DC-operating point: Topological analysis", to appear in *Proc. ISCAS'91,* Singapore, 1991.

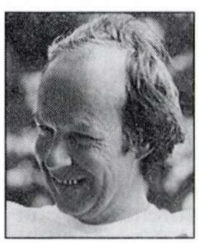

Martin Hasler received the Diploma in 1969 and the Ph. D degree in 1973 from the Swiss Federal Institute of Technology, Zurich, both in physics.

He continued research in mathematical physics at Bedford College, University of London, from 1973 to 1974. At the end of 1974 he joined the Circuits and Systems Group of the Swiss Federal Institute of Technology, Lausanne, where he was given the title of a Professor in 1984. His research interests are in the field of nonlinear circuits and systems. He is the coauthor, with J. Neirynck of the books *Electrical Filters and Nonlinear Circuits* (Artech House, Boston, MA) and, with Y. Kamp, of the book *Recursive Neural Networks for Associative Memory* (J. Wiley & Sons).

COMPLEX DYNAMICS IN SIMPLE ELECTRONIC CIRCUITS

MACIEJ J. OGORZALEK

IMISUE
DEPARTMENT OF ELECTRICAL ENGINEERING
ACADEMY OF MINING AND METALLURGY
KRAKÓW, POLAND

In this review paper we present an engineer's view on complex dynamical properties encountered in simple electronic circuits. We discuss the properties of circuit behaviour that indicate complex behaviour and chaotic motion: sensitive dependence on initial conditions, fractal structure of limit sets, basin boundaries and bifurcation parameter space. Brief overview of mathematical concepts and methods of analysis is included. Several examples of circuits exhibiting complex behaviour are presented. These include: chaotic autonomous RC circuit; digital filter exhibiting fractal structures of trajectories and fractal properties of the parameter space; digital phase locked loop displaying chaos; neural-type oscillator showing transition to chaos under external excitation.

1. INTRODUCTION

Most of existing electrical and electronic equipment consists of devices, circuits and systems which in nature are nonlinear. Electrical and electronic engineers are used to dealing with complicated systems although they usually extract only simple features such as steady solutions or periodic behaviour, perhaps most interesting from the point of view of practical applications. As pointed out by T. Matsumoto in his review paper [45], evidence shows that there is no reason why oscillations in circuits should be periodic or noise should be an unpredictable feature.

It is a natural way to explain system behaviour with the aid of simple mathematical models. It was something of a surprise for researchers to find out that such simple models could also display extremely complex (We use here the adjective complex to describe behaviour of simple systems which involves some hard to describe and not just random structures. This should not be confused with the notion of complex systems ie. systems consisting of a very large number of components whose behaviour arises from the combined effect.), exotic, seemingly random behaviour, as appeares to have been first observed by Yoshisuke Ueda in his early experiments with the Duffing oscillator [68, 69]. During the last decade, there has been an enormous increase in quantity of publications concerning complex phenomena. The research has been concentrated in two directions: development of theory and applications. Mathematical studies provide a unifying framework for understanding the complex phenomena.

Why is chaos important for an electrical engineer?

Firstly, a wide variety of examples (real circuits, not analog computer models) show that, because of the inherent nonlinearity of decives used to build a circuit, chaos is likely to occur, if not in normal modes of operation than under small deviations from the desired conditions. Secondly, if one accepted that chaos is possible in electric systems then it becomes important to understand the underlying mechanisms and predict what features might cause malfunctioning of the circuit, and on the other hand, what features could be useful in applications and whether chaotic phenomena could be controlled (turned on and off) by tuning some appropriety chosen parameters.

Chaotic mathematical models are necessarily nonlinear but may take many different forms. To make this paper self-contained, let us briefly review some basic notions. Throughout this paper, we will consider deterministic dynamical systems i.e. systems whose dynamical behaviour is governed by a set of equations giving the time evolution of the state of the system from a knowledge of its previous history. Of particular interest in electrical applications are the following types of systems:

- autonomous differential equation of the form:

$$\frac{dx(t)}{dt} = f(x(t)) \tag{1}$$

with an initial condition $x(t_0) = x_0$,

- nonautonomous, periodically forced differential equation of the form:

$$\frac{dx(t)}{dt} = f(x(t),t) \tag{2}$$

where $x(t_0) = x_0$, and $f(.,t) = f(.,t+T)$ is periodic with period T.

In the above mentioned two cases, $x(t) \in R^n$ is called the state of the system, and function $f: R^n \to R^n$ ($f: R^n \times R \to R^n$) is called the vector field. Solution $\Phi_t(x_0)$ of equation (1) or (2) with initial condition x_0 is called a trajectory (or an orbit).

- difference equation of the form:

$$x(k+1) = g[x(k)] \tag{3}$$

where $x(k) \in R^n (k \in Z^+$ is called the state of the system function $g: R^n \to R^n$ is called the vector field. Sequence of points x_i, $x_i = g[x_{i-1}] i = 1,2,\ldots \infty$ is called a trajectory (orbit).

Asymptotic behaviours of solutions of dynamical systems as $t \to \infty$ will be of our primary interest. (In practice such behaviours are called the steady state.) Asymptotic behaviours could be extremely rich and complicated ([9], [10], [11], [38], [59]). There is a necessity to find the features that differentiate one kind of solutions from another.

Throughout this paper for characterisation of system's behaviour, we shall use the following mathematical concepts [34]:

- Invariant set

A subset $S \subset R^n$ such that: $\Phi_t(x) \in S \; \forall \; x \in S \forall t \in R$ is called the invariant set.

• Limit set

The set of all points p satisfying : $\exists \{t_i\} : \Phi_{t_i}(x)_{t_i \to \infty} \to p$, where p is called the ω-limit set of point x.

The set of all points p satisfying : $\exists \{t_i\} : \Phi_{t_i}(x)_{t_i \to -\infty} \to p$ is called the α- limit set of point x.

Typical examples of limit sets are: equilibrium points, limit cycles etc.

• Attractor (attracting set)

The set- $A \subset R^n$ is called an attractor if there exists its neighbourhood U such that : $\forall x \in U : \Phi_t(x) \in U$ for $t \geq 0$ and $\Phi_t(x)_{t \to \infty} \to A$

• Domain (basin) of attraction

The set $A_\Omega = U_{t \leq 0} \Phi_t(U)$ is called the domain of attraction of attractor A

Having the above considerations in mind, let us look at typical types of behaviour encountered in nonlinear electrical circuits. [9]—[10], [36], [38], [59]:

• Here are some examples of nonlinear autonomous circuits:

— All solutions tend to the unique equilibrium point. Typical amplifiers, filters etc. should behave in this manner.
— All solutions tend to one of several equilibria. This is the normal regime for memory cells, flip-flops etc.
— All solutions tend to the unique periodic state. Electronic oscillators belong to this class.
— Some solutions tend towards a periodic state, some converge to one of equilibrium points. This is usually a simple but abnormal mode of operation of oscillators (latch-up).
— Some of the solutions or all of them do not converge to an equilibrium, periodic orbit or a quasi-periodic one. All solutions are bounded, System behaves in a random way — it is chaotic.
— There exists a possibility of coexistence of many solutions mentioned above. The actual solution depends then on the choice of initial conditions and could be constant, periodic, quasi-periodic or chaotic.
— There exists as well the possibility of divergence of solutions.

• Typical types of behaviour encountered in nonautonomous nonlinear circuits driven by a periodic signal of period T are:

— All solutions converge towards a unique periodic solution of period T. Signal processing circuits, power systems normally behave in this manner.
— All solutions converge towards a unique periodic solution of period $\frac{n}{m} T$. (e.g. frequency dividers and multipliers, rectifiers, PLLs etc.)
— All solutions tend towards one of many periodic solutions of period $\frac{n}{m} T$ (higher harmonics or sub-harmonics)
— Solutions are chaotic — there is no synchronising effect of the external signal whatsoever.

General methods for designing nonlinear circuits with prescribed type of behaviour do not exist. Usually it is a matter of experience of the engineer/designer to give the correct answer. But in many cases, even a simple signal processing system is designed by trial-and-error. Existence of chaotic solution from the engineer's point of view is just another nuisance, causing malfunctioning of circuits. Thus the efforts in research should be concentrated on developing methods of recognizing, anticipating and avoiding chaotic behaviour. There were several attempts made in this direction (see e.g. [37]). In the next Section, we shall discuss the problem of recognizing chaos among other types of motions on the basis of observations and measurements.

2. RECOGNIZING COMPLEXITY AND CHAOS

Already Poincaré in his works concerning the qualitative theory of differential equations noticed that even simple physical systems whose dynamics are described by such equations can exhibit extremely complex behaviour which is neither periodic nor quasi-periodic. Solutions of these systems behave in an apparently random manner. It should be stressed, however, that being solutions of differential equations, they are uniquely determined by initial conditions.

There is no commonly accepted definition of a chaotic solution. Classification of orbits proposed by Birkhoff [7] enables us to place the chaotic orbits among other types of trajectories. Classification of trajectories is the following:

• constant trajectories (limit set — point)
• periodic orbits (limit set — closed curve)
• quasi-periodic orbits (limit set — torus)
• recurrent trajectories (Cantor-like limit set — strange attractor; (Cantor set is a nonempty set having neither internal nor isolate points)).

Following such a classification, chaotic orbits belong to the last group — they are bounded, unstable and possess a limit set having a Cantor-like structure often called a strange attractor.

In a more colloquial meaning, we call chaotic all trajectories that are not divergent, are highly irregular and do not possess any periodicity in time.

Many authors accept the intuitively simplest definition of chaos — a solution which is not a fixed point or periodic or quasi-periodic orbit. Unfortunatelly such a definition does not specify any properties of chaotic oscillations. Thus we do know what it is not but the answer to the question what it is remains open.

The adjective complex is often used to describe not only chaotic behaviour but also the structure of the parameter or initial condition spaces which even in the case of non-chaotic attractors could have an extremely complicated structure characterised by fractal dimension. (The notion of fractal dimension will be clarified in the next Section.)

From the engineer's point of view often without mathematical proofs, the following typical behaviour observed during experiments in deterministic dynamical systems is indicating complex or chaotic behaviour:

• *Sensitive dependence on initial conditions* [34], [36], [45]

this means that despite the fact that two trajectories start from initial conditions lying very close to each other (See. Fig.1) they will eventually separate as time goes on and will be totally different (but they remain bounded.). This property is very important from the practical point of view. Usually the initial state of the system cannot be specified with infinite precision. This applies both to measurements taken

Fig. 1. Illustration of the sensitive dependence on initial conditions. Two trajectories starting from inital conditions very close to each other will eventually separate but always remain bounded.

with some error ε and computer experiments affected by finite wordlength, rounding and truncation errors in operations done in the processor, integration errors etc. Below some fixed level, we are not able to distinguish between two different initial conditions. Thus we can understand how two trajectories, starting from apparently identical initial conditions, diverge from each other — it is impossible to predict trajectory behaviour over long periods of time no matter how precisely we fix the initial conditions in experiments — solutions of the deterministic system behave in a random way, they are chaotic.

- *Classification*

Refering to the classification given by Birkhoff, by having some experience it is possible to distinguish between different types of solutions on the basis of their phase-portraits or time evolution (taken e.g. by means of an oscilloscope):
— to the first category belong all trajectories which converge towards a point on the phase portrait or a constant value in the time evolution;
— second type of trajectories correspond to closed curves observed on an oscilloscope;
— phase portraits of the quasiperiodic orbits in a "regular" way fill densly a torus-like object;
— solutions that behave in a highly irregular way in the observation time interval can be considered "practically chaotic". This class of solutions takes into account feasibility of observation and measurements — periodic solutions with periods longer than available observation time, behaving in an erratic way during this period are "practically chaotic" ([31]).

- *Universal "routes" to chaos*

Detection of one of the known universal "routes" to chaos when varying system parameters: i.e. period doubling sequence [1], [2], [17], [26], period adding sequence, intermittency, torus breakdown [16], [20], [34], [47], [48]. Universality refers to the fact that similar quantitative behaviour of systems depend rather on some general system properties and not on detailed physics or paticular model description. We will discuss this problem in more detail for period doubling sequences encountered in Example 1. (See [19] for a collection of papers on universality in nonlinear dynamics.)

- *Fractal basin boundaries*

In nonlinear dynamical systems possessing more than one attractor, uncertainty in initial conditions often leads to uncertainty in the final asymptotic state (it should be stressed that this property differs from the sensitivity to initial conditions in which case the asymptotic state was unique — but chaotic). The sets of points belonging to the boundaries between the domains of attraction of each of the attractors have fractal dimension. In measurements, this means that even though the attractors are simple (asymptotic behaviour is not chaotic), results of experiments appear random due to uncertainty in initial conditions.

- *Fractal structure of the parameter plane*

In experiments we sometimes find extremely complicated patterns in the bifurcation parameter (system parameters controlling changes in dynamic behaviour are called bifurcation parameters) space — existence regions of distinct trajectories are interwound, often forming infinite structures of diminishing sets; there are domains in the parameter space where it is not any more possible to specify the type of behaviour due to uncertainty in system parameters.

3. QUANTIFYING COMPLEX BEHAVIOUR

There are several quantitative ways for the dynamical characterization of systems. The most interesting concepts are the following.

- *Lyapunov exponents* [72]

The concept of Lyapunov exponents is the following : In an n-dimensional system we observe evolution of an infinitesimally small ball of initial conditions in a long time interval — after a time t, the ball deformates into an ellipsoid. i-th Lyapunov exponent λ_i is defined by the length z_i of the i-th principal axis of the ellipsoid :

$$\lambda_i = \lim_{t \to \infty} \frac{1}{t} \log_2 \frac{z_i(t)}{z_i(0)} \qquad (4)$$

if such limit exists. Lyapunov exponents define the time average of squeezing — stretching properties in different directions of the nonlinear system phase space. They are generalizations of eigenvalues in linear systems (for linear systems, Lyapunov exponents equal eigenvalues).
A system is considered chaotic if at least one Lyapunov exponent is positive. This property is often chosen as the definition of a chaotic system. Existence of a positive Lyapunov exponent quantifies the above mentioned sensitive dependence on initial conditions.

- *Dimension of attractor* [24]

Many authors consider the appearance of a so-called strange attractor as the criterion of chaos. A strange attractor is a specific kind of an attracting limit of trajectories characterised by their fractal dimension. The concepts of dimension are used also for characterisation of the basins of attraction and bifurcation parameter sets — their fractal dimension, even in the

case of normal attractors (like points or closed orbits) is considered as a measure of complexity. There are several definitions allowing the calculation of dimension sets characterizing system behaviour (limit sets, basins of attraction or their boundaries, bifurcation parameter spaces etc.):

- *Capacity or "box-counting" dimension*

  This is the most natural and simple concept of a dimension. It was initially introduced by Kolmogorov as follows:

$$d_C = \lim_{\varepsilon \to 0} \frac{\ln N(\varepsilon)}{\ln (1/\varepsilon)} \qquad (5)$$

  where we imagine a covering of the space by n-dimensional cubes with edge length $\varepsilon \cdot N(\varepsilon)$ is the minimum number of such cubes needed to cover the set. The dimension of an attractor defined in this manner has an interesting interpretation. If we are interested to identify the position of the attracting set with the precision ε then it is sufficient to specify the position of N cubes needed to cover this set. From equation (5) we have for small ε : $\ln N(\varepsilon) \approx d_C \ln (1/\varepsilon)$. Thus the dimension specifies the quantity of information needed to localize the attractor with the required accuracy. Capacity can be considered as a simplified version of the *Hausdorff dimension* [24]. To define the Hausdorff dimension of a subset (attractor) in an n-dimensional Euclidean space, we introduce a covering of the space by n-dimensional boxes of variable edge length ε_i. Let us introduce:

$$l_d = \lim_{\varepsilon \to 0} l_d(\varepsilon) \qquad (6)$$

  where $l_d(\varepsilon) = inf \, \Sigma_i \varepsilon_i^d$, and the infimum extends to all possible coverings satisfying $\varepsilon_i \leq \varepsilon$. Hausdorff proved that there exists a critical value $d = d_H$ above which $l_d = 0$ and below which $l_d = \infty$. This critical value d_H is called the Hausdorff dimension.
  Information dimension is again a generalization of capacity. For an attractor, it takes into account the relative probability of a trajectory passing through each box belonging to the covering:

$$d_I = \lim_{\varepsilon \to 0} \frac{I(\varepsilon)}{\ln (1/\varepsilon)} \qquad (7)$$

  where

$$I(\varepsilon) = \sum_{i=1}^{N(\varepsilon)} P_i \ln \frac{1}{P_i} \qquad (8)$$

  and P_i is the probability of a trajectory staying in the i-th box. $I(\varepsilon)$ gives the amount of information which we gain during a measurement (observation) of the system with an accuracy of ε.

- *Entropy* [72]

  In probability theory, entropy is the amount of information gained (or uncertainty removed) in an experiment. Entropy of a dynamical system is a measure of uncertainty of forecasting the future behaviour of the system in its time evolution on the basis of the observation taken during a time interval. For example in systems having simple attractors like points, limit cycles or quasiperiodic orbits, we observe the "loss of memory" in terms of initial conditions. Many trajectories, starting from initial conditions outside the attractor, eventually converge towards the attractor (e.g. for a system having only one attracting point, all trajectories will converge to this point — the entropy of such a system is zero). In a chaotic system, we have a reversed situation: nearby trajectories starting from initial conditions separated by a very small distance lead to totally different asymptotic behaviours. In such a regime, the longer we take the observations the more information we gain about the system's behaviour.
  Thus positive entropy could be considered as a criterion of chaos in the system. (We omitted here the involved mathematical tools needed to introduce the entropy. Interested readers should consult Piesin [60] and Young [72]).

- *Auto-correlation function*

  The auto-correlation function constitutes another way of quantifying the property of sensitive dependance on initial conditions. It is a measure of similarity of the trajectories at time t and $(t + \tau)$. The temporal auto-correlation function is defined as follows:

$$AC(\tau) = \frac{1}{t_2 - t_1} \int_{t_1}^{t_2} x(t) \cdot x(t+\tau) \mathrm{d}t \qquad (9)$$

  Changing τ we can determine the measure of self-similarity for a trajectory during its time evolution. The Wiener-Khinchin theorem gives a direct link between the states of $AC(\tau)$ and the Fourier transform of the power spectra of $x(t)$. For signals which are constant, periodic or quasiperiodic in time, the power spectra is formed of distinct rays, and $AC(\tau) \neq 0$ for $\tau \to \infty$. This means that periodic and quasiperiodic orbits maintain their internal similarity during the time evolution. For a chaotic signal we have broad — band, contiuous power spectra and $AC(\tau) = 0$ for $\tau \to \infty$. The internal similarity of a trajectory diminishes in time and goes to zero for distant time instants. This property of chaotic signals was used by Ünal in his computer verifiable criterion of chaos existence [70].

The above mentioned characterizations, although intuitively simple, are extremly difficult in real applications. Calculation of Lyapunov exponents or attractor dimensions, despite elegant algorithms developed (see e.g. [58]), still causes many problems. Cost of such calculations is high and, on the other hand, interpretation of results is difficult.

Various characterizations of dynamical systems in terms of their asymptotic behaviour are given in the following Table ([59]).

To study complex (chaotic) behaviour and understand underlying mechanisms, three types of analysis are made:

- laboratory experiments in a real circuit (including analysis of experimental data),
- simulation studies (including calculation of bifurcation diagrams, Lyapunov exponents, dimension of attractors etc.),
- mathematical reasoning

Having introduced some concepts useful for identifying complex phenomena from experimental data, let us next briefly review the main mathematical tools used for the analysis of systems that behave in a complex way.

Classification of attractors

Asymptotic behaviour of trajectories	Type of attractor		Lyapunov exponents	Dimension
	Continuous system	Point mapping		
Equilibrium point	point	—	$0 > \lambda_1 \geq \ldots \geq \lambda_n$	0
Periodic orbit	closed	point	$\lambda_1 = 0$	
Subharmonic	curve	set of points	$0 > \lambda_2 \geq \ldots \geq \lambda_n$	1
Quasi-periodic (two-periodic)	torus	closed curve	$\lambda_1 = \lambda_2 = 0$, $0 > \lambda_3 \geq \ldots \geq \lambda_n$	2
Qusai-Periodic (k-periodic)	k-torus	k-1 torus	$\lambda_1 = \ldots = \lambda_k = 0$, $0 > \lambda_{k+1} \geq \ldots \geq \lambda_n$	k
Chaotic	Cantor like set	Cantor like set	$\lambda_1 > 0$, $\Sigma_i \lambda_i < 0$	non integer

4. MATHEMATICAL METHODS

Experiments alone cannot give a convincing evidence of chaotic behaviour. Only when combined with rigorous mathematical reasoning can experimental results be considered as meaningful.

During the last decade, we observed a mass of publications offering mathematical methods for the analysis of chaotic systems. There are a number of works presenting the state-of-the-art in this subject and a unified approach to chaotic systems [6], [36], [45], [51], [53], [59], [65].

Many systems, totally different from the physical point of view, share the same mathematical models. Because of this, qualitative analysis is usually carried out for a whole class of systems, not only for a particular case. An analysis of this kind has been done e.g. by Komuro [42] and other authors ([12], [14] — "double scroll family", [61] — hysteresis based chaos generator family etc.)

Mathematical studies led to the elaboration of a standard set of mathematical "tools" [34], [35], [72] useful in the analysis of chaotic systems. Most of these methods come from qualitative theory of ordinary differential and difference equations and bifurcation theory [34], [40]. An excellent account of these methods can be found e.g. in the monographes of Guckenheimer and Holmes [34], Thompson and Stewart [66], Devaney [20], Bergé et al. [5]. Most popular and widely used are methods connected with the analysis of special types of trajectories — homoclinic ones (i.e. trajectories doubly assymptotic to an equilibrium point) [46]. Shilnikov's method for autonomous systems [28], [29], [46], [64] has been generalized by the researchers from University of Nice (C. Tresser [67]), as well as Glendinning [29] and Gaspard [28]. This method is most widely used for proving the existence of chaotic motion (e.g. for the double scroll circuit [12])

Melnikov's method is widely used for investigating the strange behaviour in forced systems. Different versions of this method are described in Wiggins' book [71] and works of Gruendler [33] and Salam [63].

The point mapping methods (see e.g. Nejmark [50]) allow the reduction of dimensionality and application of results known for low-dimensional discrete systems (for some applications, see e.g. Mira [47]).

Finally let us mention some other methods used in the analysis of chaotic systems:

- symbolic dynamics [39], [49] used for the description and classification of orbits in an invariant set;
- Knot theory [39] used for classifying various types of orbits using so-called templates ("knot holders"), and proving the existence of Smale's horseshoes;
- cell-to-cell mappings [41] for global analysis of invariant sets, basins of attraction, basin boundaries etc.;
- unstable cycle expansions [18] used for the characterisation of attractors through identification of unstable orbits.

In the author's opinion, the evidence of chaotic behaviour should be given by the results of both experiments and mathematical analysis.

Results of laboratory experiments alone are not sufficient as there are always uncontrollable disturbances, external noise etc. Accumulation of errors can strongly affect outcomes of simulation studies. On the other hand, one can always argue that the analyzed mathematical models are always simplified and could not reflect exactly all properties of real physical systems.

5. EXAMPLES

In this Section, we shall describe some results of experiments and analysis for chosen circuits to show how the approaches, briefly reviewed in previous Sections, could be applied in real situations.

5.1 Example 1 — autonomous RC chaos generator

Let us consider the third-order RC ladder network with a nonlinear voltage controlled voltage source in the feedback loop. The circuit diagram is presented in Fig. 2. Its dynamics are described by an ordinary differential equation of the form

$$\frac{\mathrm{d}x(t)}{\mathrm{d}t} = Ax(t) + BF[C^T x(t)] \qquad (10)$$

where:

$$A = \begin{bmatrix} \frac{-1}{R_1 C_1} + \frac{-1}{R_2 C_1} & \frac{1}{R_2 C_1} & 0 \\ \frac{1}{R_2 C_2} & \frac{-1}{R_2 C_2} + \frac{-1}{R_3 C_2} & \frac{1}{R_3 C_2} \\ 0 & \frac{1}{R_3 C_3} & \frac{-1}{R_3 C_3} \end{bmatrix}$$

$$B = \begin{bmatrix} \frac{1}{R_1 C_1} \\ 0 \\ 0 \end{bmatrix} \quad C = \begin{bmatrix} 0 \\ 0 \\ 1 \end{bmatrix}$$

$$F(\sigma)=\begin{cases} m_0\sigma & \text{for } |\sigma| < \sigma_{bp} \\ m_1\sigma & \text{for } |\sigma| \geq \sigma_{bp} \end{cases} \qquad (11)$$

σ_{bp} — coordinate of the break-point of the piecewise-linear characteristic (see Fig. 2).

This system can also be interpreted as a linear system (RC twoport) described by a transfer function of the form

$$G(s)=\frac{G_1G_2G_3}{D(s)} \qquad (12)$$

where

$$D(s)=s^3C_1C_2C_3+s^2(G_1C_2C_3+G_2C_2C_3+G_2C_1C_3+ +G_3C_1C_3+G_3C_1C_2)+s(G_1G_2C_3+G_1G_3C_3+ +G_1G_3C_2+G_2G_3C_3+G_2G_3C_1+G_2G_3C_2)+ +G_1G_2G_3$$

with a nonlinear feedback $F(\sigma)$.

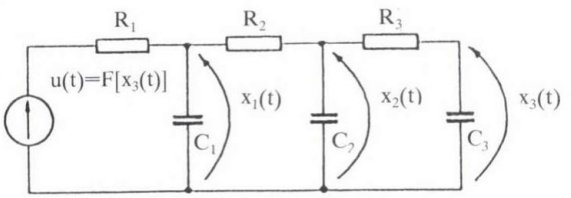

2/a

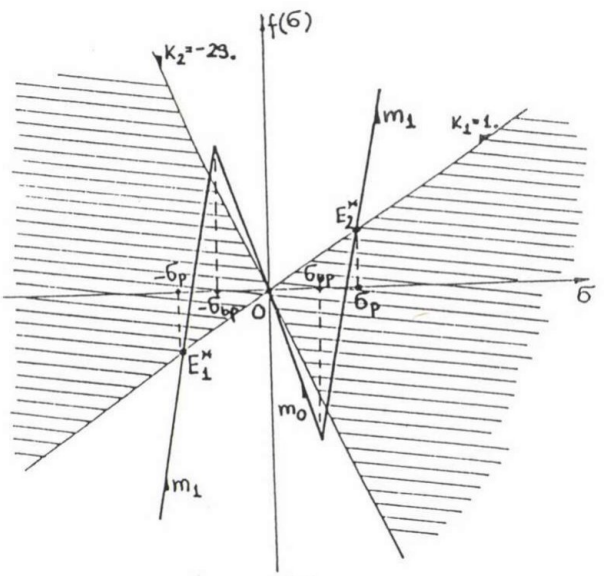

2/b

Fig. 2.a) Circuit diagram of the autonomous RC chaos generator, B) characteristic of the nonlinear element.

The piecewise-linear characteristic has been chosen for simplicity of calculations. Qualitatively similar results are obtained e.g. for a cubic function

$$F(\sigma)=\sigma(a\sigma^2+b\sigma+c).$$

Results of laboratory tests

Using a standard op-amp implementation of the nonlinear characteristic, we made several laboratory experiments in a real physical circuit. When changing circuit parameters along a variety of periodic and seemingly complex aperiodic trajectories, we observed "fuzzy" ones as shown in Fig. 3. All Figures show x_2—x_1 plots taken in our laboratory test circuit. Photograph (c) has been taken in the case of an inversed nonlinear characteristic.

Existence of complicated orbits has been further confirmed by simulation studies, moreover we were able to observe in detail the route leading from periodic behaviour in the circuit to the erratic one when changing para-

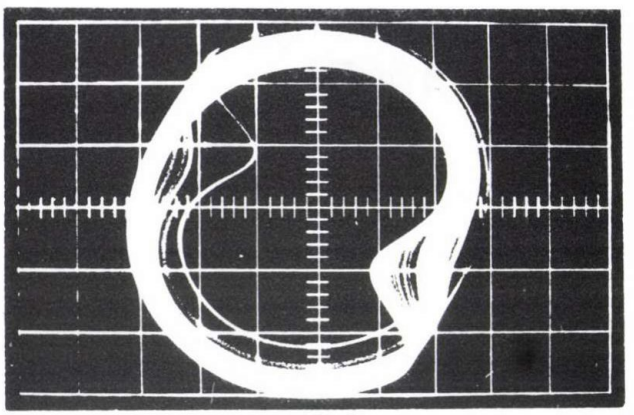

3/a

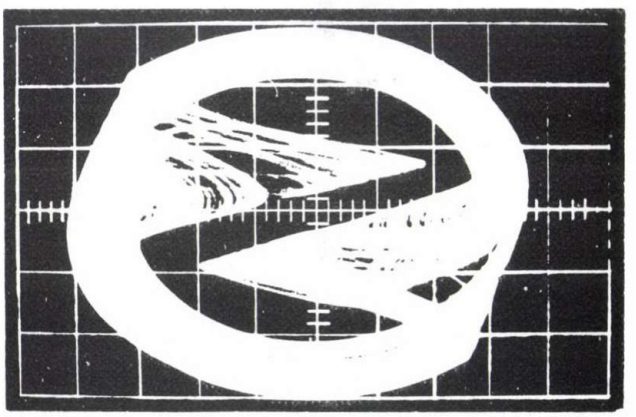

3/b

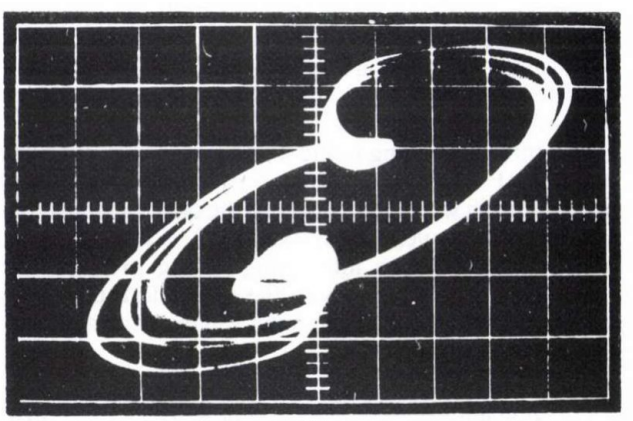

3/c

Fig. 3. Typical complex, aperiodic trajectories observed in a laboratory circuit. All displays show $x_2 - x_1$ plots. Display (c) was observed in the case of an inversed nonlinear characteristic.

(hor. scale x_2 — $\frac{0.2\ V}{div}$, vert. scale x_1 — $\frac{1\ V}{div}$.

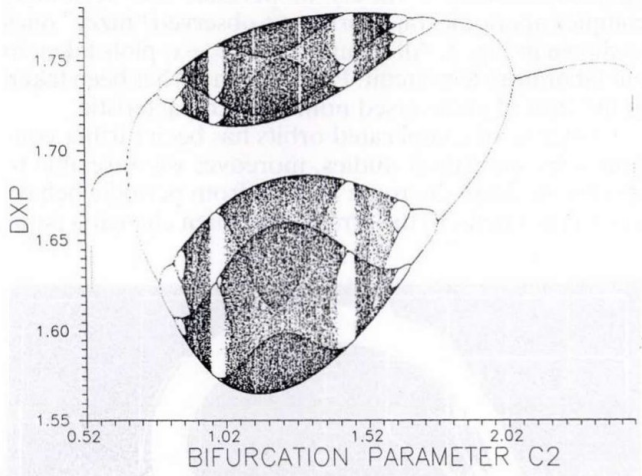

Fig.4. C_2 bifurcation diagram (for fixed $R_1=R_2=R_3=1\Omega$, $C_1=C_3=1F$, $m_0=-33{,}03$; $m_1=330{,}0$; $\sigma_{bp}=0{,}2$).

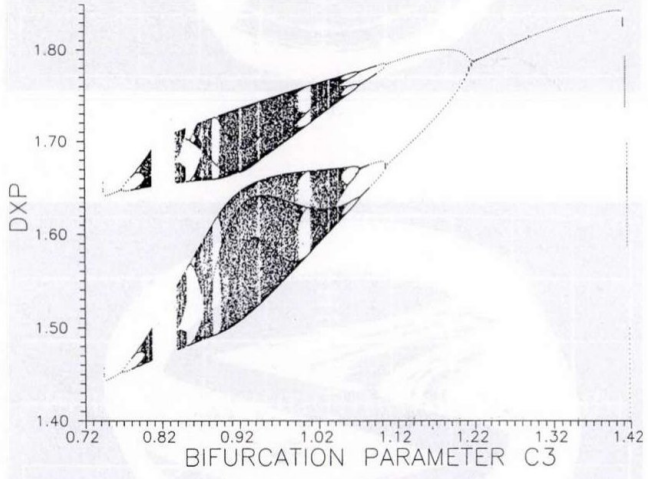

Fig.5. C_3 bifurcation diagram (for fixed $R_1=R_2=R_3=1\Omega$, $C_2=C_3=1F$, $m_0=-33{,}03$; $m_1=330{,}0$; $\sigma_{bp}=0{,}2$).

meters. Typical bifurcation diagrams obtained are shown in Figs. 4 and 5. Following the changes of bifurcation parameter values, we observed very interesting bifurcation phenomena for system orbits. The most common phenomenon is the Hopf bifurcation — birth of a periodic orbit in the system (points HB on the diagram).

The next phenomenon is called pitchfork bifurcation — a periodic orbit splits into two orbits of the same period (poins PB on the diagram).

The most interesting is the so-called period doubling sequence (Feigenbaum [8, 26]) — an infinite sequence of bifurcations in which the period of the orbit doubles (beginning of the sequence is marked PDS on the diagram). Feigenbaum found an interesting scaling property for successive period doublings: if the $i-th$ doubling takes place for the bifurcation parameter value μ_i then a universal constant exists:

$$\delta = \lim_{i \to \infty} \frac{\mu_{i+1} - \mu_i}{\mu_{i+2} - \mu_{i+1}} = 4.6692016\ldots. \qquad (13)$$

For the system under consideration, we estimated the Feigenbaum constant on the basis of the first four-period doubling parameters $\delta'=4.612$ which is very near the universal constant.

Detailed properties of period doubling behaviours can be found in the works of Feigenbaum [26], Alligood and Yorke [1], Crawford and Omohundro [17].

Several other bifurcation phenomena can be found on our diagrams, e.g. periodic windows in the chaos range, crisis [8], [30], remerging sequences [54] etc.

All bifurcation phenomena found in our studies give strong evidence that the circuit is indeed chaotic: it behaves in a typical, universal way experienced in many chaotic systems.

Calculation of Lyapunov exponents and dimensions of the attractor give further evidence of chaotic behaviour — we found for a wide range of parameters (on the basis of time series calculations) one positive exponent, and dimensions of observed attractors between 2.12 and 2.193.

Apart from simulation and laboratory tests, we were able to confirm by a rigorous mathematical proof that our system is chaotic in the sense of Shilnikov (in [52] we discussed the existence of homoclinic orbits in the system and its implications for trajectory behaviour).

As an alternative method of rigorous mathematical analysis, we proposed a one-dimensional model of system dynamics (10) [55], [56]. Analysis of the one — dimensional map [56] gives further confirmation of the chaotic motion — the proposed squeezed spiral map satisfies the fundamental Li-Yorke theorem [44].

5.2 Example 2 — second order digital filter

Our second example is a second-order digital filter realized in direct form as shown in Fig.6. Depending on the actual characteristic chosen for realisation of the overflow operation, this filter can exhibit extremely complex behaviour.

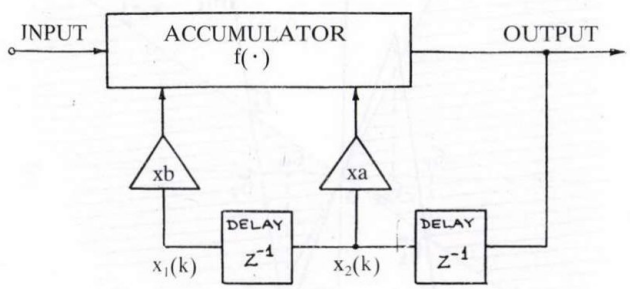

Fig. 6. Second order digital filter

Equations describing its dynamics (with zero-input) are of the form

$$x_1(k+1) = x_2(k) \qquad (14)$$

$$x_2(k+1) = F[bx_1(k) + ax_2(k)] \qquad (15)$$

where $a,b \in R$, $F: R \to R$, $F(\sigma) = \sigma$ for $|\sigma| < 1$,

$F(\sigma) = 1$ for $\sigma \geq 1$, $F(\sigma) = -1$ for $\sigma \leq -1$.

Chua and Lin [13] analysed this system in the case of the 2's complement (modulo) nonlinear characteristic. They discovered that in some parameter ranges, the digital filter with modulo arithmetic can behave in a strange manner generating chaotic oscillations and fractal patterns. One of such fractal trajectories composed of similar ellipses is depicted in Fig. 7.

We found in our earlier studies that possibilities of complex filter behaviour exist in the case of saturation [27].

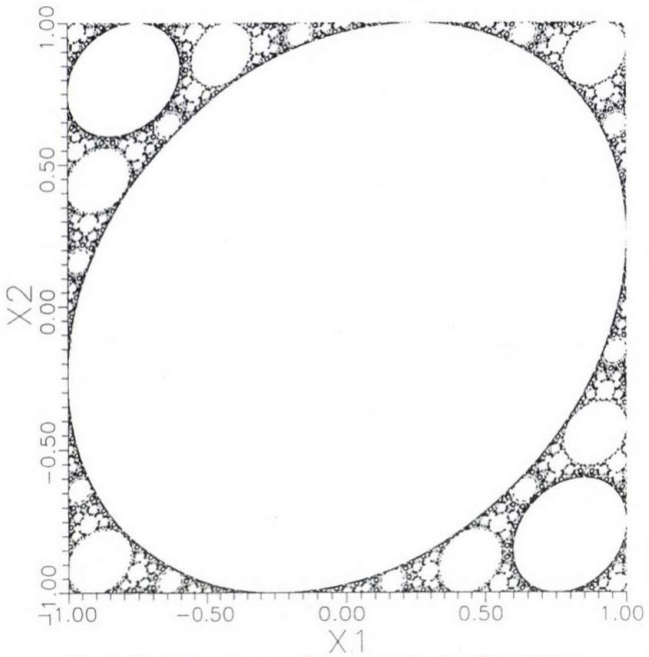

Fig. 7. Typical trajectory of the second order digital filter with 2's complement arithmetic displaying self-similat patterns.

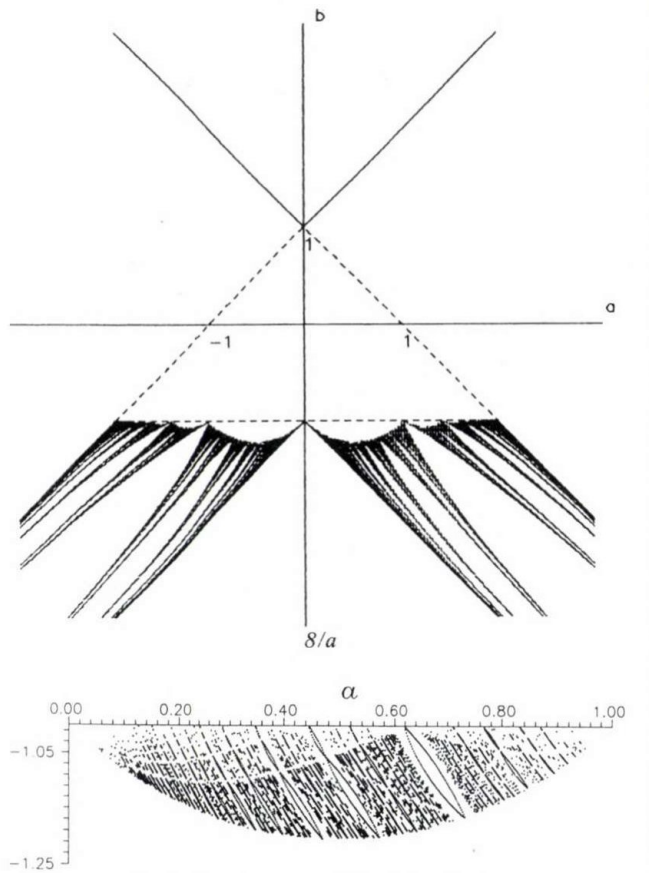

Fig. 8. Two-parameter bifurcation diagram for the digital filter employing saturation.
a) Asymptotic stability triangle and regions of existence of periodic orbits with different rotation numbers (Arnold tongues)
b) further details of the structure of the largest "circular" region.

We carried out a detailed study of filter behaviour for different values of parameters a and b. This study enabled us to draw the diagram shown in Fig.8. The variety of possible periodic orbits is astonishing. Regions of existence of various periodic trajectories form so-called Arnold tongues. It is easily seen that these tongues do not overlap. Even more interesting is the existence of the infinite sequence of "circular" regions of periodic orbits within which one can clearly distinguish smaller similar structures which we call „sausage structures". These regions of existence of periodic orbits with different rotation numbers (rotation number is defined as : $p = \lim_{k\to\infty} \frac{F^k}{k}$, and gives a characterization of orbits of the map F) form in fact a fractal structure — they fill entirely the subregions of the parameter space but when approaching the line $b = -1$, their number tends to infinity — thus by specifying the parameters a and b with finite accuracy, we are unable to specify the type of periodic orbit observed in the filter.

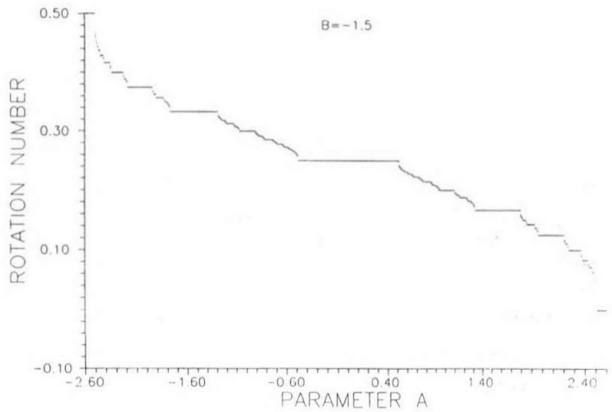

Fig. 9. Rotation number as a function of parameter A, revealing a typical devil's staircase structure.

When we fix one of the filter parameters while changing the other, interesting changes of dynamic behaviour of the filter can be observed. We constructed diagrams to show how the rotation number changes when varying a for a fixed b value. These diagrams reveal the devil's staircase structure as shown in Fig. 9. Zooming-in in this picture shows the repetition of finer structures of this kind. Changes of rotation numbers obey the Farey's rule [47]

$$\frac{p}{q} \to \frac{p+r}{q+s} \to \frac{r}{s} \text{ etc.}$$

Chua and Lin [13] applied symbolic dynamics for the analysis of filter dynamics in the case of 2's complement arithmetic and confirmed its chaotic behaviour.

We should stress here that our experiments in the case of saturation arithmetic so far confirmed existence of periodic orbits of an arbitrarily chosen period, and existence of quasi-periodic orbits but no chaotic ones. The fractal structure of the bifurcation plane indicates complex behaviour. Partial analytical results have been obtained by means of the point mapping method [57] but we were not able to prove chaotic behaviour in this case.

5.3. Example 3 — Digital Phase Locked Loop

As our third example, let us consider a digital phase-locked loop (DPLL) with positive going zero crossing detector. The system diagram is shown in Fig. 10.

Dynamics of this circuit has been analysed in a number of papers [32], [43]. The authors considered in particular a one-dimensional model of dynamics of the system describing correspondence between consecutive instants of sampling the input signal (closing of switch SW) :

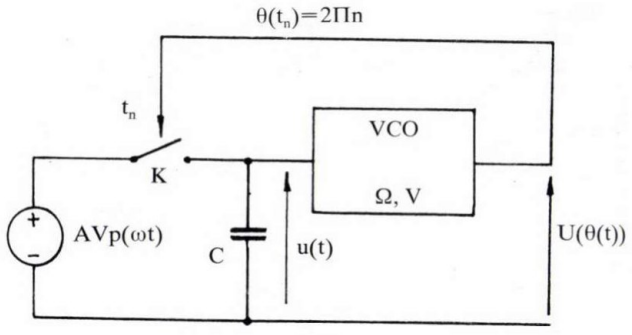

10/a

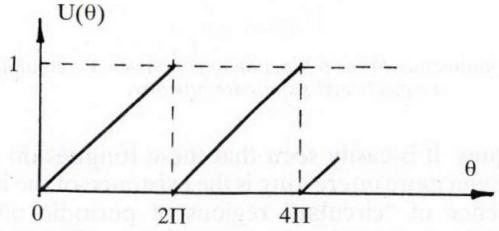

10/b

Fig.10. a) Block diagram of the DPLL, b) characteristic of the VCO.

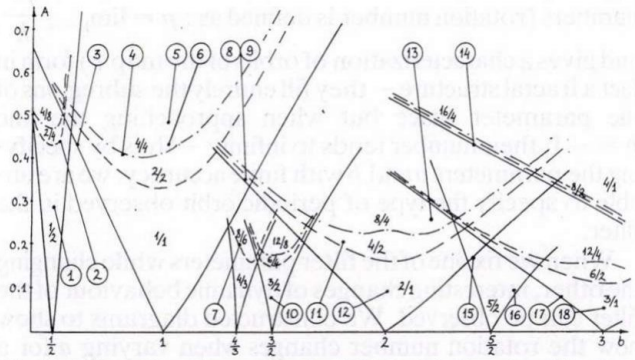

Fig.11. Bifurcation diagram for the DPLL. Principal Arnold tongues are indicated. Labels 1 to 18 show positions of operation points for which phase-plots have been measured.

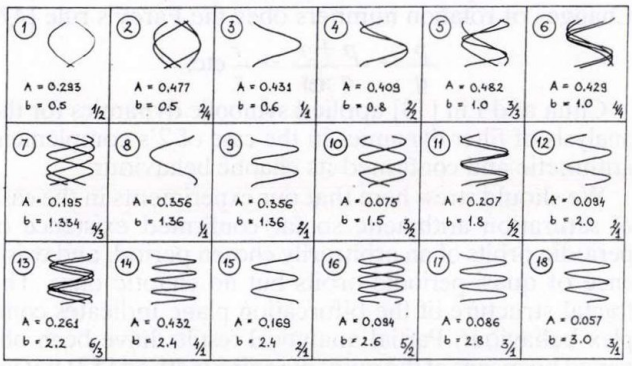

Fig.12. Phase plots (Lissajous figures) observed on the oscilloscope for various DPLL parameter values.

$$T(\tau) = \tau + \frac{b}{1 + Ap(2\pi\tau)} \qquad (16)$$

where : $\tau = \frac{\omega t\, q}{2\pi}$ is the normalized time and $b = \frac{\omega}{\Omega}$ is the normalized frequency of the input signal $AVp(\omega t)$ (where p is periodic with period T: $p(2\pi[\tau+1]) = p(2\pi\tau)$; the output of the VCO is a periodic signal $U[\theta(t)]$ whose frequency depends on the input voltage : $\frac{d\theta}{dt} = \Omega\left[1 + \frac{u(t)}{V}\right]$ and A is the relative amplitude of the input signal).

Figs. 11 and 12 show results obtained via experiments in a real physical DPLL [32]. Fig. 11 shows the bifurcation diagram. Regions of principal periodic oscillations — Arnold tongues of the type 1/1, 2/1, 3/1, 4/1, 1/2, 3/2, 5/2, 4/3 — are depicted. It is worthwhile pointing out that in this case, the Arnold tongues intersect which seems unlikely in the plots presented for the digital filter in the previous Section. Intersection of Arnold tongues means coexistence of various periodic orbits, and gives indication for existence of chaotic behaviour. Labels 1 through 18 indicate points for which phase plots presented in Fig. 12 have been measured by means of an oscilloscope.

In [43], the authors have carried out a detailed analysis of the DPLL proving existence of chaotic oscillations analytically, thus the results of experiments are fully confirmed mathematically.

5.4. Example 4 — single neural cell

Chaotic motion has also been observed in simplest neural networks [3], [62]. Even single neural cells with inertial feedback driven by a periodic input function, can exhibit chaotic behaviour. Let us consider a single neuron with feedback, as shown in Fig. 13 [3].

Dynamics of this simple circuit are described by a second-order differential equation with a periodic driving function :

$$LC\frac{d^2U}{dt_2} + RC\frac{dU}{dt} + U = V = \tan h(\beta U) + \alpha\cos(\omega t) \qquad (17)$$

where: tan $h(\beta U)$ defines the nonlinear characteristic of the neuron and $\alpha\cos(\omega t)$ is a periodic driving current added at the input of the cell.

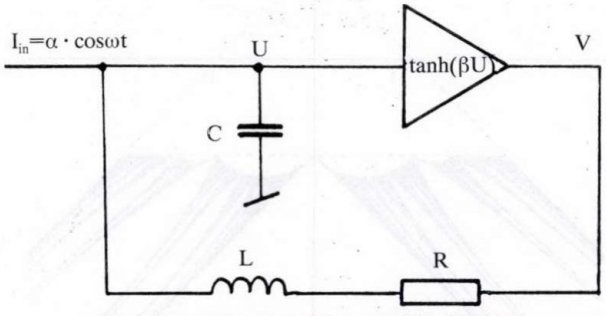

Fig.13. Single neuron with inertial feedback.

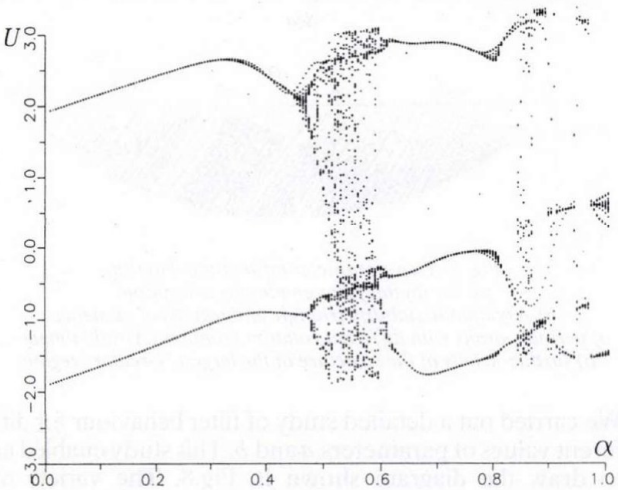

Fig.14. Bifurcation diagram for the single neural cell driven by a sinusoidal input.

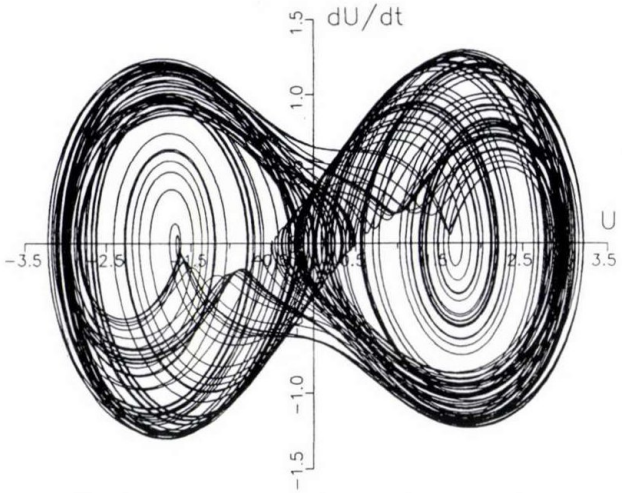

Fig. 15. Chaotic trajectory observed in the neural cell for α=0.55, β=2.0, — R/L=0.2, ω=0.8.

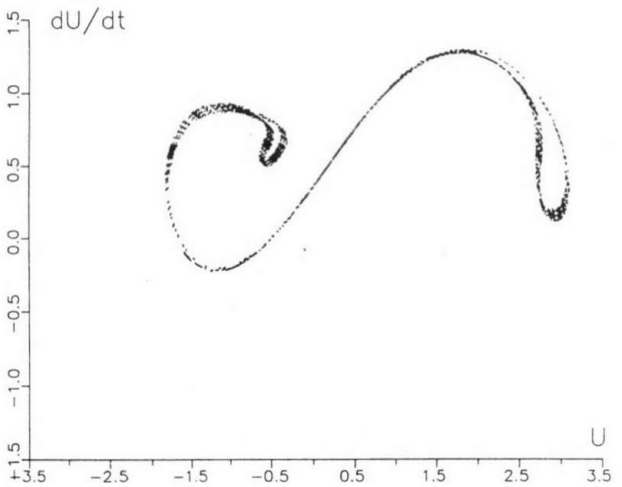

Fig. 16. Poincaré section of the attractor observed for α=0.55, β=2.0,— R/L=0.2, ω=0.8.

When changing the amplitude of the input signal, the circuit undergoes drastic changes of behaviour becoming finally chaotic for $\alpha = 0.511$. Changes of observed dynamic behaviour are reflected in the bifurcation diagram shown in Fig. 14.

Typical chaotic trajectories observed in the circuit for $\alpha = 0.55$ are depicted in Fig. 15. The following figure (16) shows a Poincaré section of the attractor (ie. the points of intersection of system trajectories with consecutive planes separated by 2π in the driving function phase).

It is worthwhile pointing out that the autonomous system ($\alpha = 0$) is completely predictable — it typically possesses two stable stationary points attracting all system trajectories (this corresponds to "on" and "off" states of the neuron) — see [3]. Addition of an external forcing term can produce erratic, pathological behaviour, and extreme sensitivity to changes of initial conditions. The situation becomes even more complex in higher order circuits consisting of interconnections of neural cells containing many feedback loops (see [3] for stability analysis of two coupled neurons).

6. CONCLUSIONS

In addition to different types of analyses described in this paper, we should also mention our first attempts in the area of chaos applications. Let us list the most promising ones :

- random number generators [15], [21],
- applications of chaotic models in short-term forecasting [25],
- pattern and picture analysis and data compression using models generating fractal structures (iterated function systems [4]),
- computer graphics and animation [4].

Finally, let us mention first attempts to chaos-free design methods for electrical and electronic circuits and systems. New topological methods for proving existence and uniqueness of solutions of nonlinear circuits [37] constitute a first step towards avoiding complex behaviour. Ünal [70] proposed a computer verifiable criterion for the existence of chaotic behaviour.

Our review presents only selected aspects and methods of chaotic and complex behaviour in circuits and systems. The number of problems being unsolved is still greater than those that are solved and well understood — this fact gives further stimulus for scientists.

ACKNOWLEDGEMENT

This research has been supported by the Research Funds of the Academy of Mining and Metallurgy. The author wishes to express his gratitude to Prof. Jacek Kudrewicz of the Warsaw Technical University for his encouragement and kind permission to present in this review the results concerning chaos in DPLL.

REFERENCES

[1] Alligood, K.T., E.D. Yorke and J.A. Yorke "Why Period-Doubling Cascades Occur: Periodic Orbit Creation Followed by Stability Shedding." Dept. of Mathematics, University of Maryland, College Park, 1985 (preprint).

[2] Arneodo, A., P.H. Coullet, E.A. Spiegel and C. Tresser, "Asymptotic Chaos." *Physica* 14D. pp. 327-347, 1985.

[3] Babcock, K.L. and R.M. Westervelt, "Stability and Dynamics of Simple Electronic Neural Networks with Added Inertia." *Physica* 23D, pp. 464-469, 1986.

[4] Barnsley, M.F. *Fractals Everywhere.* Academic Press, Orlando 1988.

[5] Bergé, P., Y. Pomeau and C. Vidal, *Order within Chaos. Towards a Deterministic Approach to Turbulence.* John Wiley & Sons (English Translation) 1986, Hermann, Paris 1984.

[6] Bernard, M.-Y. and J.-C. Neau, "Les phénoménes chaotiques nonlinéaires? c'est très simple... au début." *Annales des Telecommunications,* T. 42, No.5—6, pp. 197—209, 1987.

[7] Birkhoff, G.D., "Dynamical systems." *Amer. Math. Soc.* Coll. Publ. USA, Vol.9, 1927.

[8] Bryant, P. and C. Jeffries, "The Dynamics of Phase Locking and Points of Resonance in a Forced Magnetic Oscillator." *Physica* 25D, pp. 196—232, 1987.

[9] Chua, L.O., "Dynamic Nonlinear Networks: State of The Art." *IEEE Trans. Circuits Systems,* Vol. CAS-27, No. 11, pp. 1059—1087, 1980.

[10] Chua, L. O., "Nonlinear Circuits." *IEEE Trans. Circuits and Systems,* Vol. CAS-31, pp. 69—81, 1984.

[11] Chua, L.O., M. Hasler, J. Neirynck and P. Verburgh, "Dynamics of a Piecewise-Linear Resonant Circiut." *IEEE Trans. Circuits Systems,* Vol.CAS-29, No.8, pp. 535—547, 1982.

[12] Chua, L.O., M. Komuro and T. Matsumoto, "The Double Scroll Family." • Part I: Rigorous Proof of Chaos. • Part II: Rigorous Analysis of Bifurcation Phenomena. *IEEE Trans. Circuits Systems.* Vol.CAS-33, No.11, pp. 1073—1118, 1986.

[13] Chua, L.O. and T. Lin, "Chaos in Digital Filters." *IEEE Trans. Circuits and Systems.* Vol.CAS-35, No.6, pp. 648—658, 1988.

[14] Chua, L.O. and G.-N. Lin, "Canonical Realization of Chua's Circuit Family." *IEEE Trans. Circuits and Systems.* Vol.CAS-37, No.7, pp. 885—902, 1990.

[15] Chua, L.Ol., Y. Yao and Q. Yang, "Generating Randomness from Chaos and Constructing Chaos with Desired Randomness." *Int. J. Circuit Theory and Appl.* Vol.18, No.3, pp. 215—240, 1990.

[16] Collet, P., and J.P. Eckmann, *Iterated Maps of the Interval as Dynamical Systems.* Birkhäuser, Basel 1980.

[17] Crawford, J.D., Omohundro P. "On the Global Structure of Period Doubling Flows. *Physica* 13D, pp. 161—180, 1984.

[18] Cvitanović, P., "Invariant Measurement of Strange Sets in Terms of Cycles." *Physical Review Letters,* Vol.61, No.24, pp. 2729—2732, 1988.

[19] Cvitanović P. (Ed.), *Universality in Chaos.* Hilger, Bristol 1984.

[20] Devaney, R.L., *An Introduction to Chaotic Dynamical Systems.* The Benjamin/Cummings Publishing Co. Inc. 1986.

[21] Espejo-Meana P., A. Rodriguez — Vasquez, J.L. Huertas and J.M. Quintana, "Application of Chaotic Switched — Capacitor Circuit for Random Number Generation." *Proc. 1989 European Conference on Circuit Theory and Design,* IEE Publication 308, pp. 440—444, Brighton 1989.

[22] Endo, T. and L.O. Chua, "Chaos from Phase — Locked Loops." *IEEE Trans. Circuits and Systems.* Part I. Vol.CAS-34, No.8, pp.987—1003, 1988; Part. II: High — dissipation case. Vol.CAS-35, No.2, pp. 255—263, 1989.

[23] Endo, T. and T. Saito, "Chaos in Electrical and Electronic Circuits and Systems." *Trans. IEICE Japan,* Vol.E73, No.6, pp. 763—771, 1990.

[24] Farmer, J.D., E. Ott and J.A. Yorke, "The Dimension of Chaotic Attractors." *Physica* 7D, pp. 153—180, 1983.

[25] Farmer, J.D. and J.J. Sidorowich, "Exploiting Chaos to Predict the Future and Reduce Noise." Los Alamos 1988 (preprint).

[26] Feigenbaum, M.J., "Universal Behavior in Nonlinear Systems." *Physica* 7D, pp. 16—39, 1983.

[27] Galias, Z. and M.J. Ogorzałek, "Bifurcation Phenomena is Second Order Digital Filter with Saturation-Type Adder Overflow Characteristic." *IEEE Trans. Circuits and Systems.* Vol.CAS-37, No.8, 1990.

[28] Gaspard, P. and G. Nicolis, "What Can We Learn from Homoclinic Orbits in Chaotic Dynamics?" *J. Stat. Physics.* Vol.31, No.3, pp. 499—518, 1983.

[29] Glendinning, P. and C. Sparrow, "Local and Global Behavior near Homoclinic Orbits." *J. Stat. Physics.* Vol.35, No.5/6, pp. 645—696, 1984.

[30] Grebogi, C., E. Ott and J.A. Yorke, "Crises, Sudden Changes in Chaotic Attractors, and Transient Chaos." *Physica* 7D., pp. 181—200, 1983.

[31] Grabogi, C., E. Ott, Pelikan pp. and J.A. Yorke, "Strange Attractors that Are Not Chaotic." *Physica* 13D, pp. 261—268, 1984.

[32] Grudniewicz, J., J. Kudrewicz and T. Barczyk, "Synchronization and Chaos in a Real Discrete Phase — Locked Loop." *Proc. 1988 IEEE International Symposium on Circuits and Systems,* Vol. 1, pp. 269—272, Helsinki 1988.

[33] Gruendler, J., "The Existence of Homoclinic Orbits and the Method of Melnikov for Systems in R^n." *SIAM J. Math. Anal.* Vol.16, No.5, pp. 907—931, 1985.

[34] Guckenheimer, J. and P. Holmes, *Nonlinear Oscillations, Dynamical Systems and Bifurcations of Vector Fields* Springer Verlag, New York-Berlin-Heidelberg 1986 (2 Ed).

[35] Guckenheimer, J., "Toolkit for Nonlinear Dynamics." *IEEE Trans. Circuits and Systems.* Vol.CAS-30, No.8, pp. 586—590, 1983.

[36] Hasler, M., "Electrical Circuits with Chaotic Behavior." *Proc. IEEE.* Vol.75, No.8, pp. 1009—1021, 19 7.

[37] Hasler, M., "Avoiding complex behavior." *Helvetica Physica Acta.* Vol.62, pp. 552—572, 1989.

[38] Hasler, M. and J. Neirynck, *Circuits non linéaires.* Presse Polytechniques Romandes, Lausanne 1985.

[39] Hockett, K. and P. Holmes, "Nonlinear Oscillations, Iterated Maps, Symbolic Dynamics and Knotted Orbits" *Proc. IEEE* Vol.75, No.8, pp. 1071—1080, 1987.

[40] Holmes, P. and D. Whitley, "Bifurcations of One- and Two-dimensional Maps" *Phil. Trans. Royal Society London,* Vol.311A, pp. 43—102, 1984.

[41] Hsu, C.S., "Cell-to-Cell Mapping" *Applied Mathematical Sciences* Vol. 64, Springer Verlag 1988.

[42] Komuro, M., "Normal Forms of Piecewise Linear Vector Fields and Chaotic Attractors" • Part I-Linear Vector Fields with a Section. • Part II-Chaotic Attractors. *Japan Journal Appl. Math.* Vol.5, No.2, pp. 257—304, 1988 and No.3, pp. 503—549, 1988.

[43] Kudrewicz, J., J. Grudniewicz, B. Świdzińska, "Chaos, Phase Slipping and Cantor -Like Sets in a Discrete Phase-Locked Loop" *Proc. ECCTD'87,* Vol.2, pp. 507—512, Paris 1987.

[44] Li, T. Y. and J.A. Yorke, "Period Three Implies Chaos" *American Math. Monthly,* Vol.82, pp. 985-992, 1975.

[45] Matsumoto, T., "Chaos in Electronic Circuits" *Proc. IEEE.* Vol.75, No.8, pp. 1033—1057, 1987.

[46] Mees, A.I. and C.T. Sparrow, "Some Tools for Analysing Chaos" *IEEE Proc.* Vol.75, No.8, 1987.

[47] Mira, C., "Chaotic Dynamics. From the One-Dimensional Endomorphism to the Two-Dimensional Diffeomorphism" *World Scientific* 1987.

[48] Moon, F., *Chaotic Vibrations.* J. Wiley & Sons, New York 1987.

[49] Morse, E. and G. Hedlund, "Symbolic Dynamics" *Amer. Journ. Math.,* • Part I — Vol.60, pp.815—866, 1938, • Part II — Vol.62, pp. 1—42, 1940.

[50] Nejmark, Ju.I., *Mietod toczecznych otobrażenij w tieorii nieliniejnych kolebanij.* Nauka, Moskwa 1972.

[51] Ogorzałek, M.J., "Some Observations on Chaotic Motion in Single Loop Feedback Systems" *Proc. 1986 IEEE Conference on Decision and Control,* Vol.1, pp. 588—589, Athens, 1986.

[52] Ogorzałek, M.J., "Order and Chaos in a Third Order RC Ladder Network with Nonlinear Feedback" *IEEE Trans. Circuits and Systems.* Vol.CAS.36, No.9, pp. 1221—1230, 1989.

[53] Ogorzałek, M.J., "Towards Unified Analysis of Autonomous Chaotic Electronic Circuits" *Numerical and Applied Mathematics,* Ed.: W.F. Ames, pp.303—309, J.C. Baltzer AG, Basel 1989.

[54] Ogorzałek, M.J., "Remerging Bifurcation Sequences in an Autonomous Electronic Circuit" *Proc. Conference on Circuit Theory and Design,* Brighton, IEE Publication 308, pp. 142—146, 1989.

[55] Ogorzałek, M.J., "The Squeezed Spiral Map" *Proc. 1990 IEEE International Symposium on Circuits and Systems.* Vol.1, pp. 595—598, New Orleans 1990.

[56] Ogorzałek, M.J., "A One-Dimensional Model of Dynamics for a Class of Third Order Systems" *Int. J. Circuit Theory and Appl.,* Vol.18, No.6, pp. 595—624, 1990.

[57] Ogorzałek, M.J. and Z. Galias, "Limit Sets of Trajectories in a Nonlinear Digital System" (accepted for MTNS'91, Kobe June 17—21 1991).

[58] Parker, T.S. and L.O. Chua, *Practical Numerical Algorithms for Chaotic Systems.* Springer Verlag, New York 1989.

[59] Parker, T.S. and L.O. Chua, "Chaos: A Tutorial for Engineers" *Proc. IEEE.* Vol.75, No.8, pp. 982—1008, 1987.

[60] Piesin, J., "Characteristic Lyapunov Exponents and Smooth Ergodic Theory" *Russ. Math. Surveys,* Vol.32, No.4, pp. 55—114, 1977.

[61] Saito, T., "The Hysteresis Chaos Generator Family" *Proc. 1988 IEEE International Symposium on Circuits and Systems.* Vol.1, pp. 15—18, Helsinki 1988.

[62] Saito, T., "Chaos form a Forced Neural- Type Oscillator" *Trans. IEICE Japan,* Vol.E73, No.6, pp. 836—841, 1990.

[63] Salam, F.M.A., "The Melnikov Method for Highly Dissipative Systems" *SIAM J. Appl.* ath. Vol.47, pp. 232—243, 1987.

[64] Shilnikov, L.P., "O suszczestwowanii sczotnogo mnozestwa pieriodiczeskich dwizenii w okriestnosti gomokliniczeskoj kriwoj" *Doklady AN SSSR.* T.172, No.2, pp. 298—301, 1967.

[65] Tang, Y.S., A.I. Mees, L.O. Chua, "Synchronization and Chaos" *IEEE Trans. Circuits and Systems.* Vol. CAS-30, No.9, pp. 620—626, 1983.

[66] Thompson, J.M.T. and H.B. Stewart, *Nonlinear Dynamics and Chaos.* John Wiley & Sons, New York 1986.

[67] Tresser, C., "About Some Theorems by L.P. Šilnikov" *Ann. Inst, Henri Poincaré,* Vol.40, No.4, pp. 441—461, 1984.

[68] Ueda, Y. "Randomly Transitional Phenomena in the System Governed by Duffing's Equation" *J. Stat. Physics.* Vol.20, No.2, pp. 181—196, 1979.

[69] Ueda, Y., C. Hayashi and N. Akamatsu, "Computer Simulation of Nonlinear Ordinary Differential Equations and Nonperiodic Oscillations" *Electronics and Telecommunications in Japan,* Vol.56A, No.4, pp. 27—34, 1973.

[70] Ünal, A., "An Algebraic Criterion for the Onset of Chaos in Nonlinear Dynamical Systems" *Proc. IEEE International Symposium on Circuits and Systems.* Vol.1, pp. 19—22, Helsinki 1988.

[71] Wiggins, P., *Global Bifurcations and Chaos. Analytical Methods.* Springer Verlag, New York 1988.

[72] Young, L.S., "Entropy, Lyapunov exponents and Hausdorff Dimension in Differentiable Dynamical Systems" *IEEE Trans. Circuits and Systems.* Vol.CAS-30, No.8, pp. 599—607, 1983.

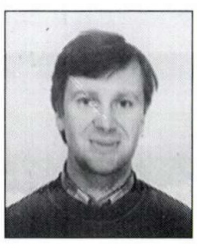

Maciej J. Ogorzalek was born in Kraków, Poland in 1955. He received the MSc degree with an award of excellence from the Academy of Mining and Metallurgy, Kraków in 1979 and the PhD degree in electrical engineering in 1987. Since 1979, he has been with the Department of Electrical Engineering, Academy of Mining and Metallurgy, since 1987 as an assistant professor. He had several visiting appointments — as a visiting scientist with ADM Development Consultants, London (1984 and 1986) and Systems Dynamics Group, MIDIT, The Technical University of Denmark, Lyngby (1988), as visiting professor at the Chaire des Circuits et Systemes, Swiss Federal Institute of Technology (1989) and Systems Dynamics Group, MIDIT, The Technical University of Denmark, Lyngby (1990). He is the author of over fifty technical papers and owns one patent. Dr. Ogorzalek is a member of the Association of Polish Electrical Engineers, the Polish Society of Theoretical and Applied Electrical Sciences and the IEEE. His research interests are in the areas of nonlinear circuits and systems, both analog and digital, nonlinear oscillations and chaos, and dynamics of nonlinear and neural networks.

A NEURAL NETWORK APPROACH TO ALGORITHMICAL PROBLEMS

JÓZSEF SIMOLA

SOFTWARE ENGINEERING STUDENT, FACULTY OF ELECTRICAL ENGINEERING, TECHNICAL UNIVERSITY OF BUDAPEST

In this paper a way of solving difficult algorithmical problems by a highly interconnected network having nonlinear analog amplifiers is described. A circuit construction to solve the NP-complete maximal independent point problem is also presented.

1. INTRODUCTION

Several algorithmical problems belong to the class comprising NP (Nondeterministic Polynomial)-complete problems. For an exact computation solution, these require a computation time which increases as exp(const*N) where N is the size of the problem. This involves a rapidly prohibitive cost as N increases. Problems belonging to this class can be transformed into one another during a time interval which can be expressed as a polynomial of the problem size. The solution cannot be found rapidly in an algorithmical way but if we had a guess we could check that in polynomial time. Therefore, methods capable of forecasting a guess of the solution are of great importance.

In the literature, neural networks have been already used for finding a solution of another NP-complete problem [2].

In this paper, a new problem, the maximal independent point problem is introduced. This is easier to solve by the Hopfield network because the problem configuration and the Hopfield network match each other.

In Section 2, the Hopfield-network is discussed. In Section 3, the problem is introduced and the new method is provided. Conclusions can be found in Section 4.

2. THE HOPFIELD-NETWORK

The analog network, as described in previous papers by Hopfield [1], [2], is shown in Fig. 1.a. The processing elements are nonlinear analog amplifiers having a sigmoid input-output relation $V=g(u)$ as shown in Fig. 1.b. The input current of the j*th* amplifier is provided through the externally supplied input current I_j and the T_{ij} conductances that connect the output of amplifier j with the input of amplifier i. Each amplifier has an inverted output as well in order to obtain negative and positive output currents from the same processor. In this way, the negative T_{ij} conductances can also be realized through resistors. Thus the T_{ij} matrix defines the connections between the amplifiers, and the I vector determines the external input currents.

If the T_{ij} matrix is symmetrical, its diagonal elements (T_{ii}) are 0 and the gain of the amplifiers is high. The stable states of the network comprising N processors then occur at the local minima of the quantity

$$E = -\frac{1}{2}\sum_{i=1}^{N}\sum_{j=1}^{N} T_{ij}V_iv_j - \sum_{i=1}^{N} V_iI_i \qquad (1)$$

which is a Ljapunov-function of the system. The network seeks the minima of this function in the state space which is the interior of an N-dimensional hypercube determined by the output limits V_i=0 and 1 of the amplifiers. It can be shown that with 0 diagonal elements, these minima occur at the corners of the cube. The network thus provides discrete answers and can be applied for solving algorithmical problems by constructing an adequate function corresponding to the problem.

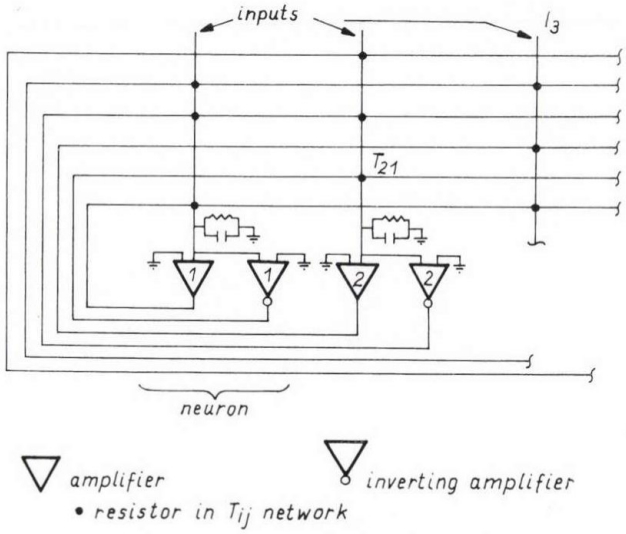

Fig. 1.a. The Hopfield-network. The circles at intersections correspond to resistive connections (T'_{ij}s). Connections between inverted outputs and inputs represent negative (inhibitory) feedback

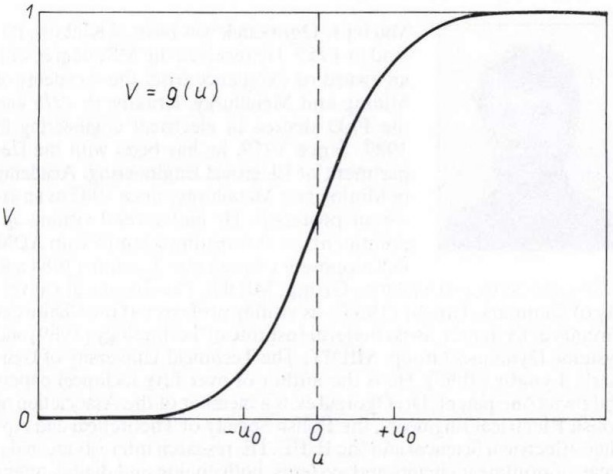

Fig. 1.b. The nonlinear monotonic input-output relation of the amplifiers [2]

3. THE MAXIMAL INDEPENDENT POINT PROBLEM

One member of the NP-complete class is of our special interest. This is the maximal independent point problem: Find in an undirected graph the biggest size point set in which the points are not connected (e.g. there are no edges among these points at all).

The network minimizes only its Ljapunov-function so the problem must be described in terms of this function by choosing the T_{ij} matrix and the I_i vector. The output of the i*th* amplifier can represent the i*th* point of the graph. If the point is within the set then the V_i output should be 1; and 0 otherwise. The graph is characterized by its adjacency matrix A_{ij}; the A_{ij} element of the matrix is 1 if the i and j points are connected, and 0 otherwise. The T_{ij} matrix and the I_i current vector will represent the adequate network for the problem. As seen before, we must fulfill two conditions. First, the point set should be independent, and second, it should be maximal size. Let's select $T_{ij}=K\ A_{ij}$ where $K<0$. So the first term of Eq.(1) will be zero if and only if there are independent points in the selected set. Otherwise the sum is greater and this would violate the minimizing demand. The second term of Eq. (1) should minimize the E function by maximizing the size of the set. This can be achieved by choosing $I_i=L$ where $L>0$. So the more outputs are set to 1 the more negative is the second term. E has a form given by

$$E=-\frac{1}{2}K\sum_{i=1}^{N}\sum_{j=1}^{N}A_{ij}V_iV_j-L\sum_{i=1}^{N}V_i \quad (2)$$

In that way, a Ljapunov-function of the problem has been constructed. Weighting K and L, we can find the trade-off between the two conditions.

A PASCAL program has been written [3] in order to simulate the network. The result has been checked by solving the problem in algorithmical way. Having analyzed the results of the simulations we found that the network works perfectly. Experiments with a ten point graph gave a hit rate of about 99 per cent. The remainder produced a suboptimal solution where the size of the set was not maximal. Networks of up to 100 amplifiers can be simulated in this way.

4. CONCLUSION

A new method for solving the NP-complete maximal independent point problem (defined in section 3) has been given. This problem matches well the Hopfield-network. With a guess given by the neural network and by algorithmical checking, the method can provide a fast solution of the problem. With computer simulation of the network we learnt the basic properties of the new solving method. Several technical problems lead to NP-complete problems, and by solving one of these, a fast solution can be achieved for the whole class.

REFERENCES

[1] Hopfield, J. J., "Neurons with graded response have collective computational properties like those of two-state neurons," *Proc. Natl. Acad. Sci. U. S. A.*, vol. 81, pp. 3088—3092, 1984

[2] Hopfield, J. J. and D. W. Tank, "'Neural' computation of decisions in optimization problems," *Biological Cybern.*, vol. 52, pp. 141—152, 1985

[3] Simola, J., "Analog neural network for solving algorithmical problems," *Scientific Student Conference Study*, Tutor: Dr. Edit Halász, Inst. of Communication Electronics, Technical University of Budapest, 1990, (in Hungarian).

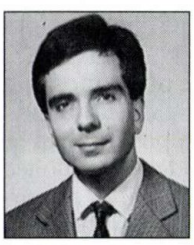

József Simola is a fifth year software engineering student at the Technical University of Budapest. His interests include software emulation, finite element method and neural networks. In 1989 he received a scholarship and spent a term at the Technical University of Munich. He was awarded several prizes at the Scientific Student Conferences at the Technical University of Budapest.

TINA: TOOLKIT FOR INTERACTIVE NETWORK ANALYSIS

MIHÁLY KOLTAI—TIBOR HORVÁTH—PÉTER ILLÉS
ANDRÁS OLÁH—ÁRPÁD ILLÉS

RAIR COMPUTER LTD.
H—1145 BUDAPEST, GYARMAT U. 45/C

New software called TINA has been developed for nonlinear circuit analysis and design. In addition to the usual DC, AC, Transient, Fourier and statistical analysis the program has several unique features. The optimization allows the user to specify a desired quantity, then the program finds the nominal value and sensitivity of a selected component that meets this specification. With the built in measurement interface one can compare the simulation with the reality and then tune, test or troubleshoot the circuits in the same integrated environment. Combining analysis, measurement and optimization parameter extraction and sophisticated automatized measurements can be carried out. User defined models can be added to the program to fulfill special requirements.

INTRODUCTION

Computer programs for design and analysis of electronic circuits are used for several decades and a number of excellent programs are available worldwide [1]—[6]. However, the autors' idea to create an integrated environment for simulation and measurement required the development of a totally new program based on modern circuit theory and software technology. Taking advantage of a new development many special features (word processor and DTP interface, optimization, statistical analysis, harmonic analysis and Fourier transformation, user defined device model facility, etc.) have been implemented which are not all present—especially not in integrated form—in other programs. In this paper we shall mainly concentrate on the new features while giving a description of the whole system.

1. GENERAL FEATURES

In TINA circuit diagrams are designed in an easy-to-handle schematic editor. Once the circuit has been created DC, AC, transient and Fourier analysis can be carried out, the results are graphically presented on the screen. The built in word processor of the system allows the user to add text to the circuit diagrams or to the results in order to create complete documentation or educational/training material. The circuit diagram as well as the results can be directly printed on many printers or saved into disk.

TINA allows stepping of component values, model parameters and of temperatures. The results may be plotted as a family of curves. During the DC analysis component values and model parameters can be swept i.e. altered continously. A special feature of the program is the optimization. Specifying a desired quantity (voltage, current, power, frequency, etc.) in the circuit, prompts the program to find the value (resistance, capatitance, etc.) of a selected component that meets this specification.

Tolerances can be assigned to all circuit components and their parameters. Monte-Carlo and worst case analysis are available to statistically test circuit performance.

If a TINA-Lab measurement card is connected to the system, the user can compare the simulation with the reality. The TINA-Lab cards will provide the same excitation which was used during the simulation and read back the response of the circuit. An IEEE-488 interface is also in development to establish connection with external instruments.

In addition to the standard models built-in for all the semiconductor components, the user can develop and add his own models to the system. A library of procedures is available providing an interface to the system.

The described features of the system are shown in Fig. 1.1.

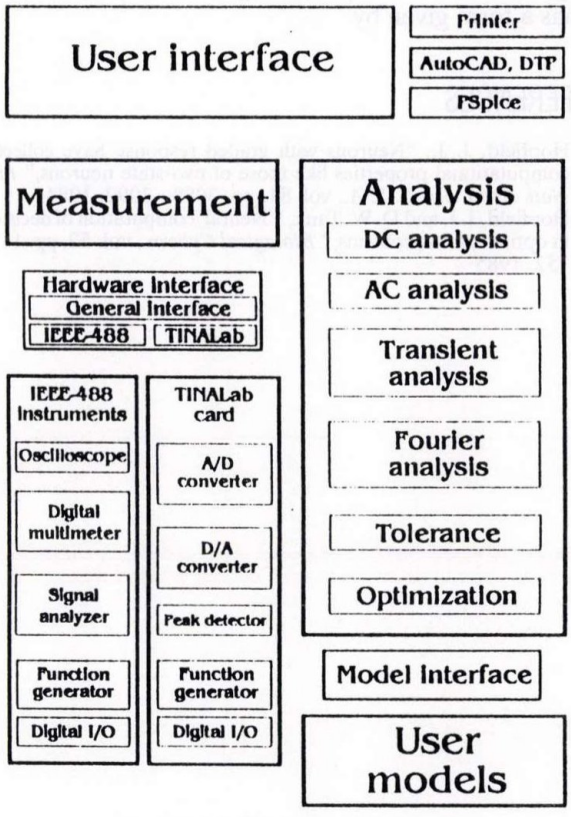

Fig. 1.1. The block diagram of TINA

2. THE SCHEMATIC EDITOR

From the point of view of the user one of the most important part of the system is the graphic circuit editor. With the aid of this editor the circuit components can be choosen from the component catalog and are positioned by the cursor keys or a mouse and rotated and/or mirrored appropriately. The schematic editor can be addi-

tionally used to generate input files for PSpice [1]. Once the circuit scheme is edited the graph of the circuit will be generated, and an internal netlist will be provided showing component types and values between the automatically numbered nodes.

The following standard elements are allowed:

- Passive elements: resistor, capacitor, inductor, coupled inductors
- Independent sources: voltage and current sources, waveform generators
- Controlled cources: All four kind of controlled sources (e.g. current controlled current source, voltage controlled current source, etc.)
- Instruments: voltage-, ampere-, impedance-, and wattmeters
- Ideal operational amplifier
- Operational amplifier
- Semiconductor devices: diode, bipolar transistor, enhancement- and depletion-mode MOSFET, P-channel and N-channel JFET.

The screen format of the schematic editor with a part of the component list is shown in Fig. 2.1.

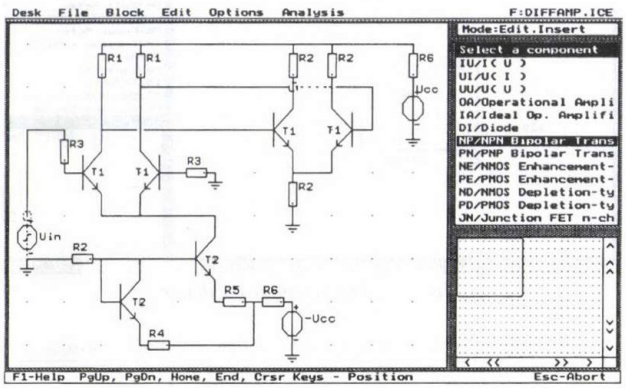

Fig. 2.1. The editor screen with a differential amplifier

3. DC, AC, TRANSIENT AND FOURIER ANALYSIS

The basic algorithm of the program is the modified nodal analysis method, targeting the direct determination of the following quantities:

- Nodal potentials
- The current of those components where the current cannot be expressed directly with the voltage drop. Such components are for example: independent or controlled voltage sources, amper meters, coupled inductors, output of operational amplifiers, etc.

The advantage of this procedure lies in giving correct results even if the above mentioned components are inserted—as opposed to the traditional method of nodal potentials which cannot be applied in such cases or gives only approximations ([7], [8]).

DC Analysis

For linear circuits the automatically generated linear system of equations is solved by Gaussian elimination. In the case of nonlinear circuit components the Newton—Raphson method is applied. First the difference of the right and left sides of the system of nonlinear equations is computed, based on an initial approximation. Next the linearized system of equations is solved giving an estimation for eliminating the error. This procedure is repeated until the error is lower than a predefined threshold. The Newton—Raphson method provides quick convergence in the vicinity of the solution but needs careful handling far from the solution. In TINA a number of analysis parameters can be accessed through a menu and with the appropriate choise of them quicker convergence can be achived.

In addition to the determination of nodal voltages TINA allows the calculation of the transfer characteristic. The transfer characteristic of the previous differential amplifier is shown in Fig. 3.1.

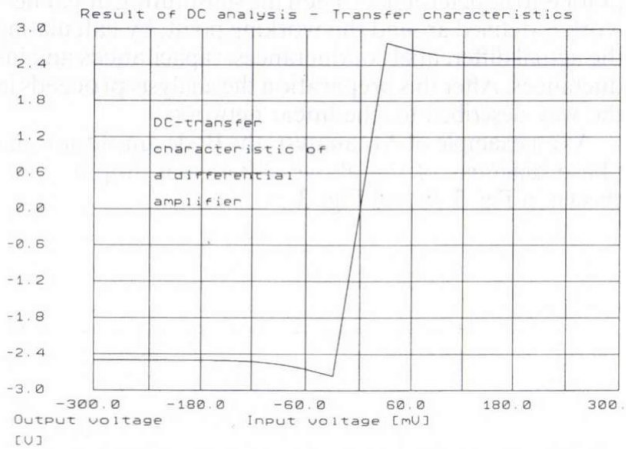

Fig. 3.1. DC transfer characteristic of the differential amplifier in Fig. 2.1.

A special feature of the DC-transfer characteristic calculations that the independent variable can be not only an input voltage or current but also a parameter of any component, while the output can be a quantity displayed by an instrument (e.g. impedance-meter, power-meter, etc.). Fig. 3.2/b shows the output voltage and the power dissipated by the pass transistor in a regulated power supply (Fig. 3.2/a) as function of the load resistance.

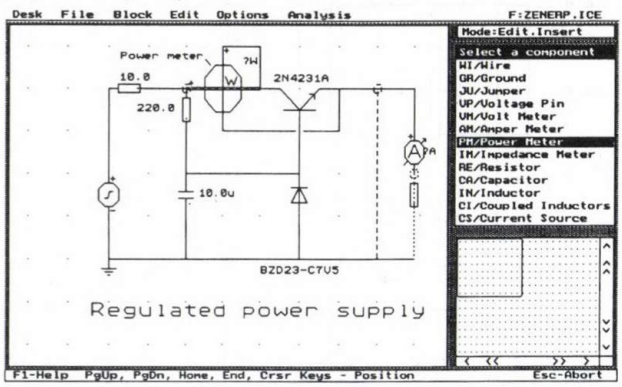

Fig. 3.2a Regulated power supply with the power meter measuring the dissipated power of the pass transistor

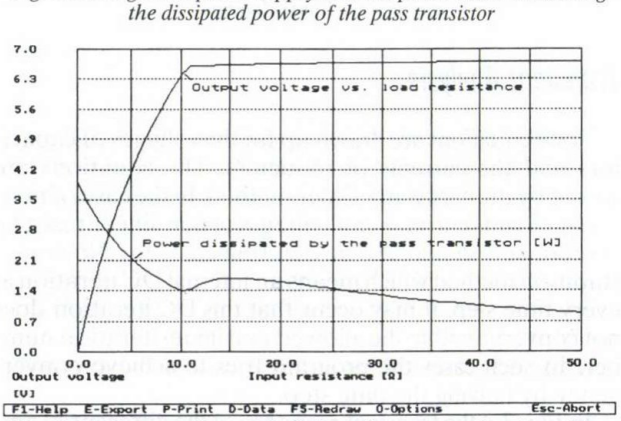

Fig. 3.2b Output voltage and dissipated power as a function of the load resistance

AC Analysis

When analyzing a linear AC network, TINA first computes the impedance of reactive (L and C) components and the complex peak values of exciting voltages and currents, and then solves the resulting system of complex linear equations consecutively at different frequency points resulting the amplitude and phase characteristics.

In case of non-linear networks first the DC working point is to be determined. Then the substituting linear network is defined around the working point, by calculating the actual differential conductances, capacitances and inductances. After this preparation the analysis proceeds in the way described for the linear networks.

As an example of AC analysis the Bode amplitude and phase diagrams of the above differential amplifier are shown in Fig. 3.3a and Fig. 3.3b.

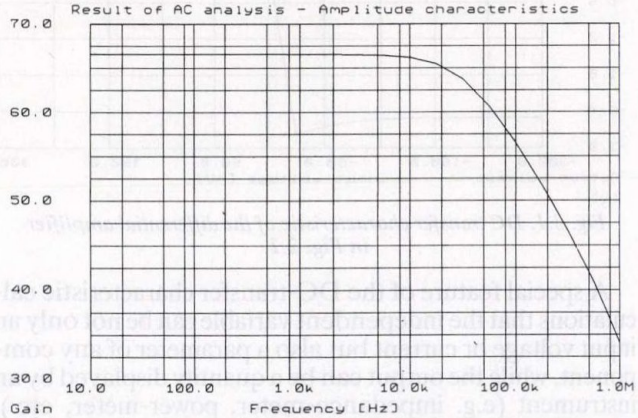

Fig. 3.3a Amplitude diagram

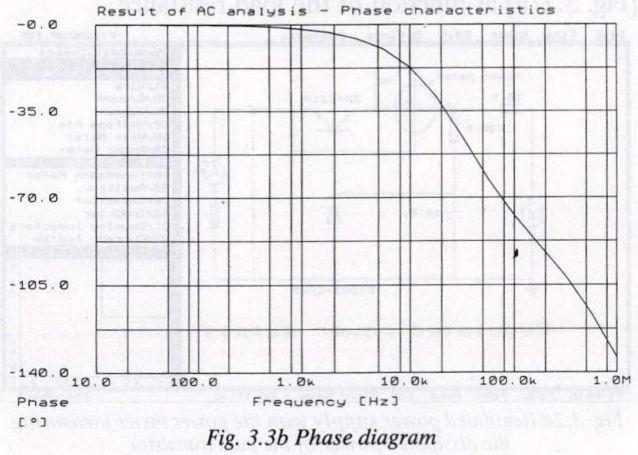

Fig. 3.3b Phase diagram

Transient Analysis

State equations are drawn up for the voltages of capacitors and the currents of inductors. The equations are solved by the backward-Euler method. In the case of non-linear circuits currents and voltages of non-linear resistive components should also be determined by the Newton–Raphson method which means an internal DC iteration at every time step. It may occur that this DC iteration does not converge within the allowed maximum iteration number. In such cases the program tries to achieve convergency by halving the time step.

In Fig. 3.4 the transient response of the differential amplifier is shown with a square wave excitation on the input.

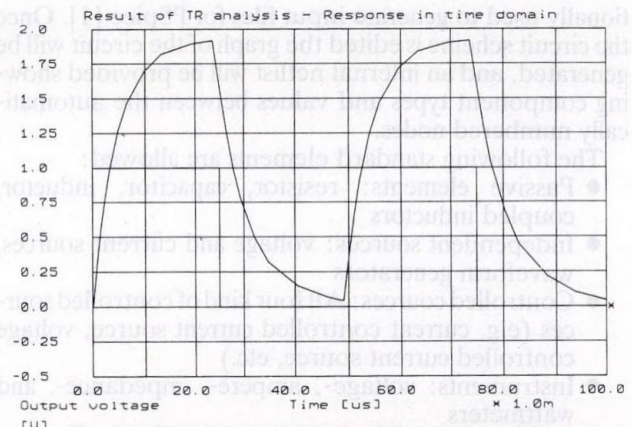

Fig. 3.4. Transient response of a differential amplifier

Another example of the transient analysis is the Tunnel diode oscillator shown in Fig. 3.5.

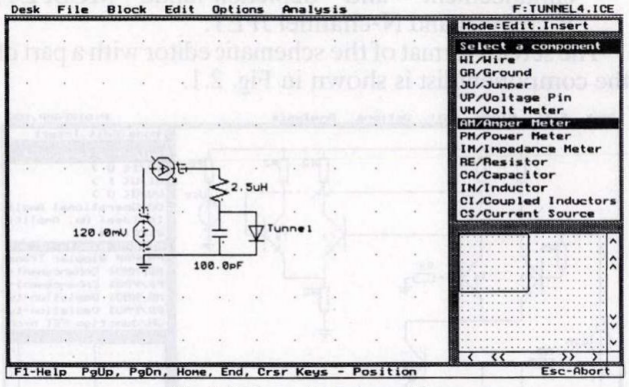

Fig. 3.5. Tunnel diode oscillator

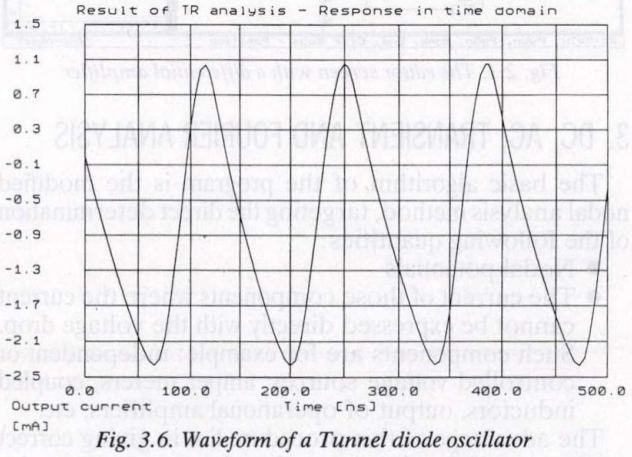

Fig. 3.6. Waveform of a Tunnel diode oscillator

After executing the transient analysis the user can draw and evaluate either the discrete or continuous Fourier spectrum, obtained by using the Fast Fourier Transformation (FFT) method.

Let us examine the above oscillator through Fourier analysis. In Fig. 3.7 the Fourier spectrum of a 2 μs long sample is shown. Running the crosshairs on the spectrum we can read the base frequency at the first $f \neq 0$ maximum. We also see the higher harmonics maximums at integer multiples of the base frequency.

We can read from the picture that the base frequency is at 7.47 MHz. Of course the base frequency could have been computed directly from the waweform as well.

Now knowing the base frequency compute the harmonic distortion of the waweform. The value of the first five harmonics and the harmonic distortion are shown in Fig. 3.8.

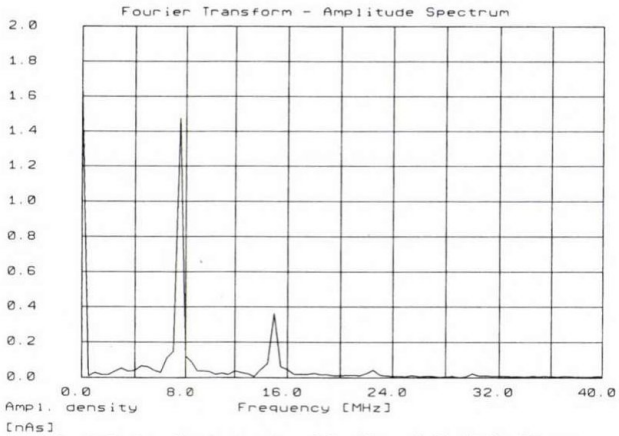

Fig. 3.7. Amplitude density of the Tunnel diode Oscillator

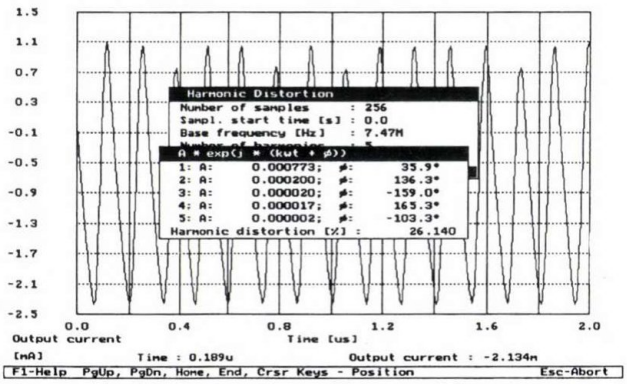

Fig. 3.8. Fourier series coefficients and distortion

4. OPTIMIZATION

In most non-linear circuit analysis programs the analysis can be carried out with given parameter values only. If the result is not suitable the user can try other parameters.

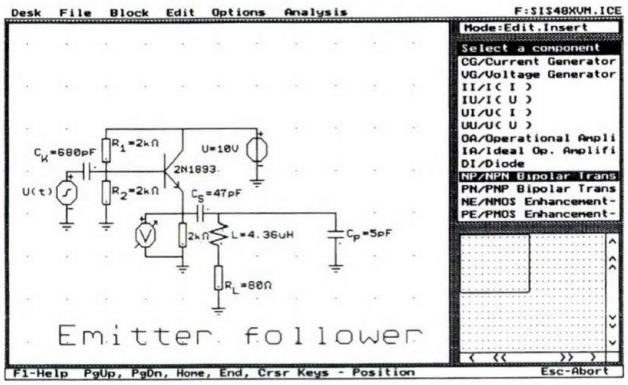

Fig. 4.1. Emitter follower

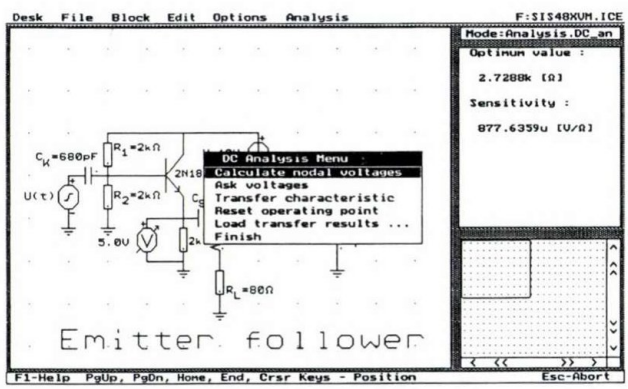

Fig. 4.2. Results of optimization

This cumbersome procedure can be avoided with TINA through its built in optimization feature.

Consider the emitter follower in Fig. 4.1 loaded with a resonant circuit [5]. With the given nominal values the voltage of the emitter is 4.24 V. Suppose that the required value is 5 V and we want to achive this goal by changing the value of R2. In the optimization mode one can select the emitter voltage as a target and the R2 resistor as a goal (Fig. 4.1). The program will provide the a resistor value of R2=2.7 kΩ and the absolute sensitivity: 878 μV/Ω. (Fig. 4.2.)

5. WORST-CASE AND MONTE-CARLO ANALYSIS

These analyses allow to evaluate the effect of component tolerances. Note that sophisticated tolerance schemes are allowed e.g. nonsymmetric distributions, semiconductor components coupled through group tolerance including negative tracking as well.

In the worst-case analysis TINA provides two methods: an analytic and stochastic approach. If the analytic method is chosen the program calculates all the possible component value combinations. For a small number of components this method is fast and accurate, however for a large number of components it slows down. In this case the stohastic method is to be used and the program will choose parameter values randomly at the end of the tolerance band. One can choose between the two methods considering that the number of necessary analyses in the analytic method increases as a power of 2. For example if we study the effect of tolerances on two components it needs four analyses and even study on six elements need 64 analyses only. Above that number of components, we arrive to the usual range of the stohastic calculations where these methods are faster.

The Monte-Carlo analysis calculates component parameters in the tolerance band and in its vicinity using the uniform or Gaussian distribution functions.

As an example take the circuit in Fig. 4.1. and examine by the Monte-Carlo analysis. The emitter voltage is set to 5 V using the result of the above optimization. Suppose that the resitors R1, R2 have 20% tolerances with Gaussian distribution. Calculate the distribution of the emitter voltage for 1000 random cases. The distribution is shown in Fig. 5.1. On the horizontal axis the emitter voltage on the vertical the relative frequency for the different bars of the diagram are shown.

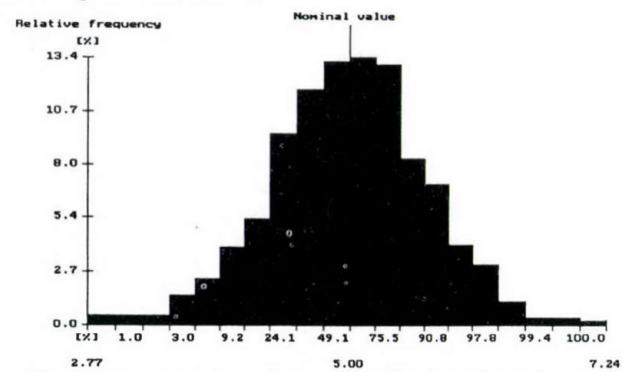

Fig. 5.1. Monte-Carlo analysis with 20% independent tolerance

Evaluating the distribution we consider emitter voltages between 4 V and 6 V are still acceptable. The result of such an evalutation is:
Nominal value: 5.0 V
Mean value: 5.015 V

Standard deviations: 0.683 V
Production yield: 86.1%
Faulty product: 13.9%

Suppose now that due to technological reasons the tolerance of the components consists of a 15% independent and a 5% group tolerance (tracking). In other words 5% of the deviation from the nominal value will change together for the concerned components. The distribution yielded by the Monte-Carlo analysis is shown in Fig. 5.2

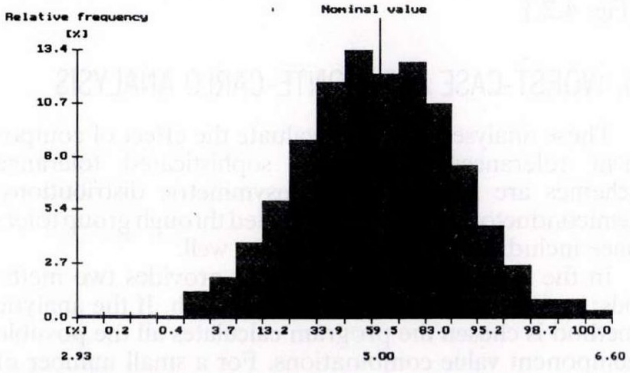

Fig. 5.2. Monte-Carlo analys with 5% group tolerance

The result of the evaluation of this distribution with the same condition:

Nominal value: 5.0 V
Mean value: 4.993 V
Standard deviations: 0.53 V
Production yield: 94.8%
Faulty product: 5.2%

As it could be expected the range of the emitter voltage deviation is less and the production yield is greater since the tracking has a certain compensation effect on the base current.

Finally suppose 5% negativ tracking between the two components. It means the R2 is greater by 5% then R1 is less by the same percentage.

The result of the evaluation is:

Nominal value: 5.0 V
Mean value: 4.992 V
Standard deviations: 0.567 V
Production yield: 92.1%
Faulty product: 7.9%

In this case the tracking enhances the dependance of the base current on resistors, the production yield is less.

6. DEVICE MODELS

TINA has a number of sophisticated models for the different semiconductor components. The user can choose an appropriate model for the application or using the user defined model facility can create and add a new model. The hierarchy of the models will be illustrated through the operational amplifier for which already four different models are available at present.

Ideal operational amplifier

The simplest way of modelling an OPAMP is the ideal operational amplifier. It is defined by infinite amplification, zero voltage and current on the input and there is no restriction for the output. For a number of DC applications it is a good approximation, note however that offset currents and voltages cannot be modelled. It also works well for many AC and transient circuits but it does not work for a number of active filters. It is also not appropriate for oscillators where the saturation effects of the OPAMP play important role. In Fig. 6.1 a integrator circuit is shown and its response to a square wave excitation. For small frequencies all four modells will give similar result.

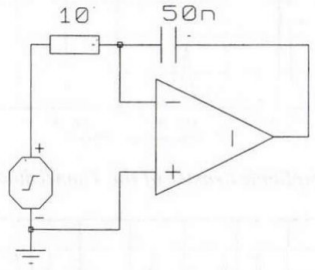

Fig. 6.1. Integrator circuit with ideal OPAMP

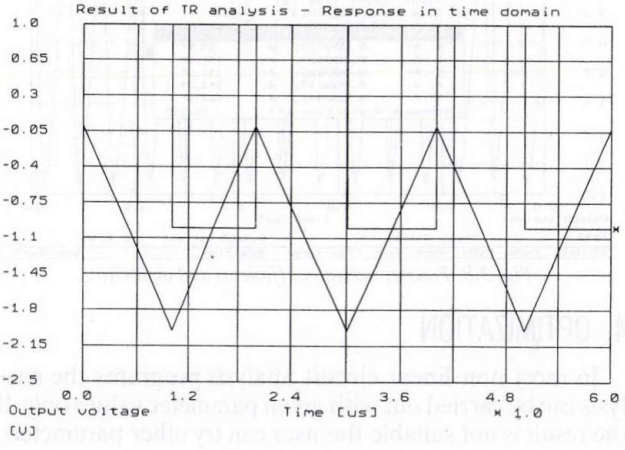

Fig. 6.2. Time response of the integrator

Linear OPAMP model

The linear OPAMP modell of TINA is described through the following parameters:

Open loop gain
Input resistance [Ω]
Output resistance [Ω]
Dominant pole [Hz]

The equivalent circuit of the model is shown in Fig. 6.3.

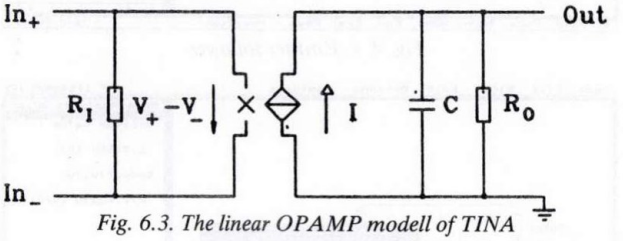

Fig. 6.3. The linear OPAMP modell of TINA

where:

$$I = \frac{A_0}{R_O} \cdot (V_+ - V_-) \quad C = \frac{1}{2\pi \cdot f_1 \cdot R_O}$$

This model gives good results for many active RC applications. As an example consider the circuit in Fig. 6.4. The amplitude characteristic is shown in Fig. 6.5.

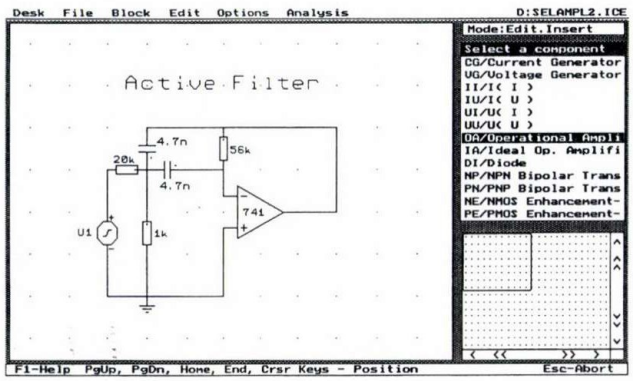

Fig. 6.4. Second order active filter

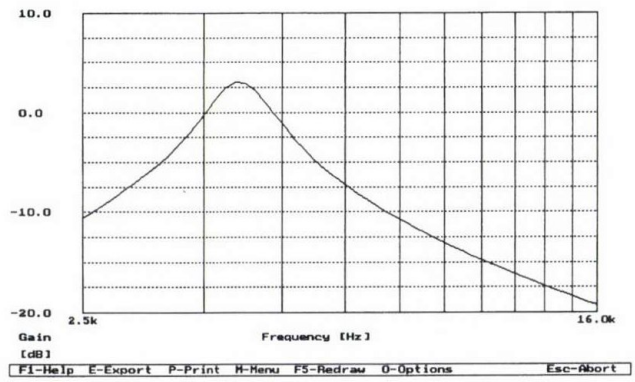

Fig. 6.5. Calculated amplitude characteristic

Standard non-linear OPAMP model

In the standard non-linear model of TINA the following parameters are included [9]:

A_0	open loop gain
R_I	input resistance
R_O	output resistance
V_{peak}	maximum output voltage
S_r	maximum slew rate
f_1	dominant (first) pole
f_2	second pole
V_{IO0}	input offset voltage at 27° C
I_{IB0}	input bias current at 27° C
I_{IO0}	input offset current at 27° C
ϑ_{VIO}	temperature coefficient of the input offset voltage
D	current doubling coefficient

Constants

T_0	input 27° C
R_1	100 kΩ
R_2	100 kΩ
$g_{m1} = g_{m2}$	0.1 mS
c	0.99

The equivalent circuit of the model is shown in Fig. 6.6.

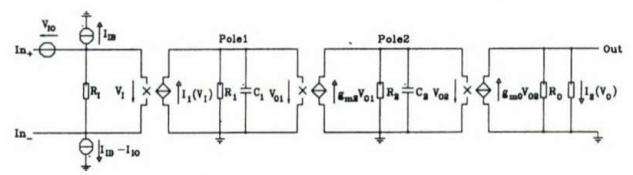

Fig. 6.6. The equivalent circuit of the standard nonlinear OPAMP model of TINA

This model includes saturation effects, it is appropriate for DC, AC analysis and certain transient processes can be also modelled with it. However it is not appropriate for modelling comparators due to the phase shift produced by the RC model of the dominant pole. A more complex model suitable for all cases is the OPAMP macromodel is described in the next section.

The OPAMP macromodel

The macromodel of OPAMPs in TINA is based on [10], [11]. The explanation of the name is that the model is somewhat similar to the original IC but it contains much less PN junctions. This model gives fairly good results for most applications and solves the above mentioned problem too. Using this model is very time consuming and the determination of the parameters is hard. However in addition to the accuracy it is a great advantage that the parameters of this model are often supplied on diskette directly by the manufacturers. The equivalent circuit of this model for NPN inputs used in TINA is shown in Fig. 6.7, for more details we refer to the literature.

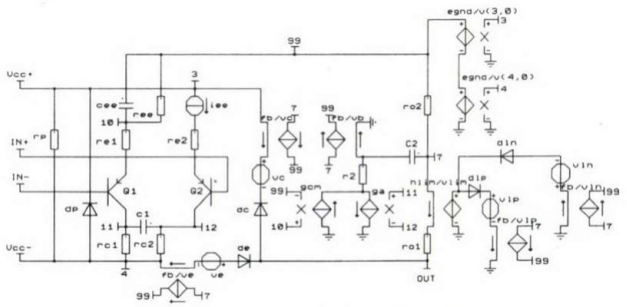

Fig. 6.7. The macromodel of OPAMP

7. USER DEFINED MODELLING

In addition to the available device models in TINA the user can design and add her/his own device models to the system by using a set of procedures and the TURBO PASCAL compiler. One can either add an additional model to an existing device (e.g. add a Tunnel diode model to the existing normal diode model) or define a totally new element including its new graphics symbol (e.g. a triode). The defined new models or components become integral part of the program since the built components and models have been defined with the same tools. As an examples of the user defined modelling consider the definition of the Tunnel diode used in para. 3. which is usually not part of the system.

The equivalent circuit of the diode is given in [12], [13].

The current of the Tunnel diode consists of two parts:

An ideal diode current:

$$I = Is * Exp(U/Ut - 1) \qquad (7.1)$$

An Esaki current [13]:

$$I = \begin{cases} 0 & \text{, if } U > Um \\ K\,(Um-U)^2 * th\,(U/2Ut) & \text{, if } Um > U > 0 \\ (K * Um^2/2Ut) * U & \text{, if } 0 > U \end{cases} \qquad (7.2)$$

Where Ut is the thermic potential, Is, K and Um are parameters, U and I are the voltage and the current of the tunnel-diode respectively.

The main steps of defining the new model:

Define the number of components in the equivalent circuit:

```
SetNoOfElements(3);
```

Define the topology of the equivalent circuit between nodes Pnode and Nnode:

```
CreateConductiveBranch(1, Pnode, Nnode, NonLinear);
CreateConductiveBranch(2, Pnode, Nnode, Linear);
CreateCapacitiveBranch(3, Pnode, Nnode, Linear);
```

Calculate the current of the diode:

```
PROCEDURE Tunnel_Eval;
BEGIN
    U :=GetVoltage(Pnode, NNode);
    Id :=IdDiodeCurrent(U, Vt, Is, gd);
    Ie :=EsakiCurrent(U, Vt, Vv, K, ge);
    I  :=Id+Ie
END;
```

Where the functions IdDiodeCurrent and EsakiCurrent realise the current formulas (7.1) and (7.2) and their derivates.

Connect the new model with the system:

```
SetModelRoutine(Tunnel_Eval);
```

8. MEASUREMENTS FROM TINA

From TINA in addition to the computer simulation the user can directly control the measurement of the circuit under development. TINA provides two tools to do that. One way is on use a TINA-Lab measurement card designed and tailored specially for TINA available as an extension card for IBM PC compatible computers. Another way is to control external instruments through an IEEE-488 interface. In this article we describe the measurement with the TINA-Lab card only. The IEEE-488 measurements will be a topic of a later publication.

The Block Diagram of the TINA-Lab 1 card is shown in Fig. 8.1.

With the TINA-Lab1 card measurement of DC voltages, automatic measurement of DC transfer characteristic, logarithmic amplitude characteristics (Bode diagram) and transient recording can be carried out from TINA. The voltage range is 25 V the maximum frequency is 100 kHz. A family of further cards and external accesories is under development.

To demonstrate combined simulation and measurement from TINA consider first the simple circuit in Fig. 8.2 for wich we carried out a simulation and measurement of transfer characteristic. In Fig. 8.3 a number of simulations are presented with different reverse currents showing that the forward voltage drop on the diode heavily depends on this parameter. Using optimization with the condition to match the calculated and the measured current in one point we could not only get a good agreement between the simulated and measured data but also determine the reverse current of the diode (10 pA) which was not given in the catalog and would have been very hard to measure directly.

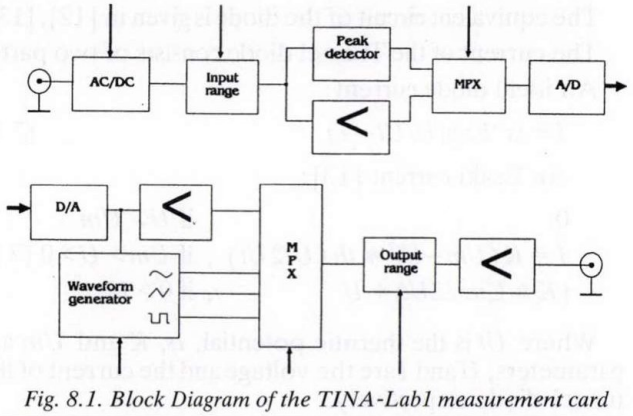

Fig. 8.1. Block Diagram of the TINA-Lab1 measurement card

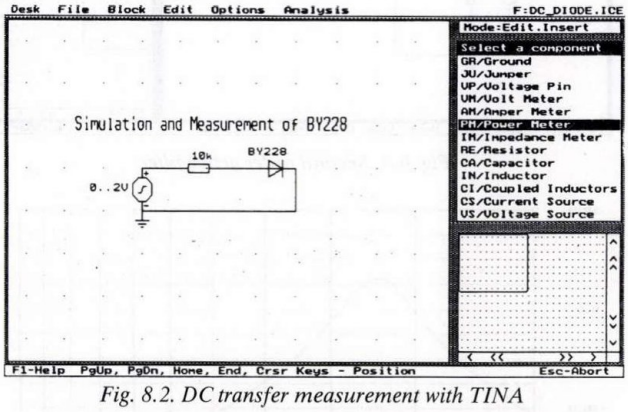

Fig. 8.2. DC transfer measurement with TINA

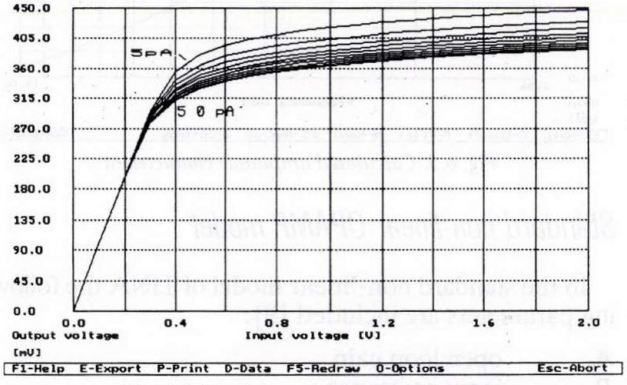

Fig. 8.3. The forward voltage on the diode

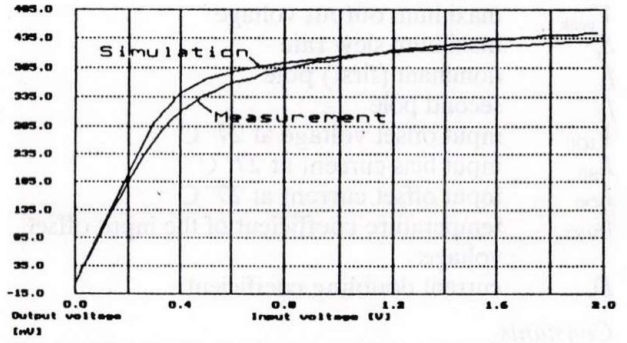

Fig. 8.4. The calculated and measured DC-transfer charachteristic

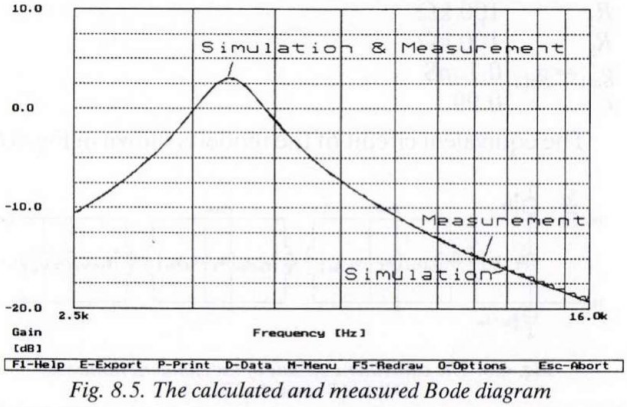

Fig. 8.5. The calculated and measured Bode diagram

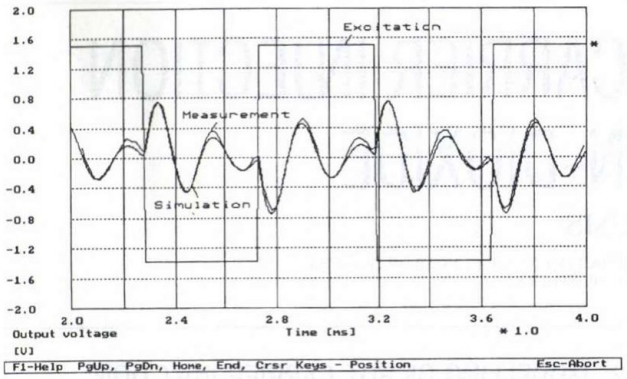

Fig. 8.6. The calculated and measured transient response

The calculated and measured Bode diagram of the active RC circuit (Fig. 6.4) are shown in Fig. 8.5. The agreement between the measured and calculated data is rather good.

Figure 8.6 shows the transient response of the same circuit under a square wave excitation.

9. CONCLUSIONS

Today's computer technology allows very high level of integration. Very different tools can be now integrated into a common frame. Though computer simulation, optimization and computer controlled measurement are used for a long time, TINA is the first system integrating these tools in the same unified environment, providing the first complete toolkit for electronic circuit development. TINA has been developed in Hungary by RAIR Computer Ltd. At present the software is distributed in more then twenty countries in education, training and industry.

REFERENCES

[1] Tuinenga, P. W., *A Guide to Circuit Simulation & Analysis Using PSpice,* Prentice Hall, 1988

[2] *Microcap III.* Instruction Manual, Spectrum Software, 1990

[3] *COMTRAN,* Comtran Integrated Software, 1990

[4] Székely, V. "Accurate Algorithm for Device Heat Dinamics: a Special Feature of the TRANZ-TRAN2 Circuit analysis program." *Electronics Letters* Vol. 9, No.6 pp. 132—134

[5] Spiro, H. *Simulation integrierter Schaltungen* R. Oldenbourg Verlag, 1990

[6] *ANAL-13* Research Institute for Telecommunications, 1980

[7] L. Chua—Pen-Min Lin: *Computer Aided Analysis of Electronic Circuits.* Prentice Hall Inc.

[8] Fodor, Gy. *Nodal Analysis of Electrical Networks* Elsevier, 1989

[9] Vlach, J. *Computer Methods for Circuit Analysis and Design* Van Nostrand Reinhold Company, 1988

[10] Boyle, G. R. et al, *"Macromodelling of Integrated Circuit Operational Amplifiers." IEEE Journal of Solid State Circuits,* Vol. SC-9, No. 6, 1974

[11] *Texas Instruments: Linear Circuits, Operational Amplifier Macromodels,* Texas Instruments, 1990

[12] Gentile, S. P. *Basic theory and application of tunneldiodes* D. Van Nostrand Company, 1962

[13] Tarnay, K., "Approximation of Tunnel-Diode Characteristics" *Proc. of IRE,* 1962 Febr.

Mihály Koltai received his M.S. degree in 1973 from the Technical University of Budapest, Faculty of Electrical Engineering and his Ph.D. degree in electromagnetic field computing, in 1976. Since graduation he was a lecturer at the Department of Electromagnetic Theory, giving lectures on circuit theory, field theory, and computer programming. Since 1989 he is Director of Research & Development at RAIR Computer Ltd. Dr. Koltai is a member of the Scientific Association for Telecommunications and the Von Neumann Society for Computer Science. His fields of interest include circuit theory, electromagnetic field theory, automated measurement and control systems.

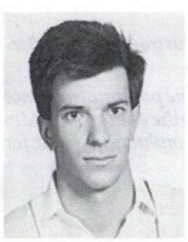

Tibor Horváth received his M.S. degree in 1991 from the Technical University of Budapest, Faculty of Electrical Engineering, in Informatics. He is a Research Associate of RAIR Computer Ltd. His fields of interest include circuit theory, computer aided design and simulation, and educational software. With his collegues, he has won several awards for different software projects. He was granted the "Pro Scientia" Medal in 1989.

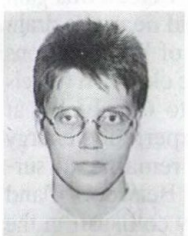

Péter Illés received his M.S. degree in 1991 from the Technical University of Budapest, Faculty of Electrical Engineering, in Informatics. He is a Research Associate of RAIR Computer Ltd. Mr. Illés is a member of the Scientific Association for Telecommunications and the Von Neumann Society for Computer Science, and a founder member of the Youth Section of the Hungarian Branch of the Europe Houses Society. His fields of interest include human machine interaction and graphical user interfaces, software projects management issues, automated measurement and control systems, and educational software. With his collegues, he has won several awards for different software projects. He was granted the "Pro Scientia" Medal in 1989.

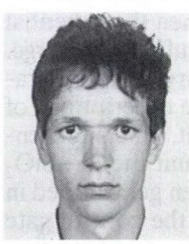

András Oláh is to receive his M.S. degree in 1991 from the Technical University of Budapest, Faculty of Electrical Engineering, in Informatics. At present he prepares his diplomawork at the University of Twente, Holland. He is a Research Associate of RAIR Computer Ltd. His fields of interest include circuit theory, electronic device modelling and computer aided VLSI design. With his collegues, he has won several awards for different software projects.

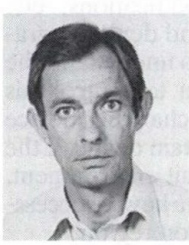

Árpád Illés received his M.S. degree in 1971 from the Technical University of Budapest, Faculty of Electrical Engineering. As a department manager he works at the Central Physics Research Institute of the Hungarian Academy of Sciences. His fields of interest include microcomputer and microprocessor based control systems and data acquisition.

MODELLING OF HOT-CARRIER INJECTION INTO SILICON-DIOXIDE

T. KOCSIS

TECHNICAL UNIVERSITY OF BUDAPEST, DEPARTMENT OF ELECTRON DEVICES
H–1521 BUDAPEST, HUNGARY

Hot-carrier effects leading to long-term instabilities have long been recognized as posing serious limitation on the reduction of feature size pushed forward in n-channel MOSFET VLSI. Channel hot-carrier injection into the gate oxide can result in the degradation of device performance due to the trapping of carriers in the gate oxide and the generation of interface traps which lead to experimentally observed threshold voltage and transconductance changes. The phenomenon of channel hot-electron injection is also widely used as the programming mechanism in EPROM's.

The lucky-electron concept is successfully applied to the modeling of channel hot-electron injection in n-channel MOSFET's, although the result can be interpreted in terms of effective-temperature of hot-carrier as well.

1. INTRODUCTION

Silicon-silicon dioxide is probably one of the most extensively studied solid-state systems, largely because of its importance in the silicon transistor technology. One of the physical phenomena in the silicon transistor structure that is gaining attention in recent years, since advanced fine-line patterning technologies have made it possible for device miniaturization to approach its physical limits, is the emission of hot-electrons and hot-holes from the silicon substrate into the SiO_2 layer. However, the hot carrier induced damage had been known long before the submicron region was entered. Beside being an interesting physical phenomenon in itself the emission of hot-carriers from Si into SiO_2 has found application in Electrically PROgrammable Memory (EPROM) devices. When Insulated-Gate Field-Effect Transistors (IGFET) are used as memory devices, it is important to emit hot-electrons into the oxide layer more effectively.

It is known that in an IGFET, hot-electrons and hot-holes are emitted into the oxide layer when the potential difference between source and drain is sufficiently large. The very high electric fields and the large doping gradients make theoretical and quantitative descriptions of the emission process extremely difficult. The high energetic electrons (and holes) can surmount the Si—SiO_2 potential barrier 3.1 eV (4.8 eV) and then get trapped in the oxide. These charges inferfere with the control gate operation, and produce threshold shifts, transconductance changes, saturation current modifications, etc. which lead to the long-term instability and device degradation. Therefore, it is quite important to understand the hot-carrier emission mechanism in order to control this phenomenon. It is clear that all of the changing device parameters can only be tolerated to a certain degree if the device is to operate properly in its circuit environment. For these reasons, long-term instability is a key to successful design of a MOSFET in the submicron region.

2. MODELLING OF HOT-CARRIER INJECTION

The lucky-electron model of channel hot-electron injection can be described as follows. The scattering events are illustrated in Fig. 1. According to the lucky-electron model, an electron is emitted into SiO_2 by first gaining enough energy from the channel electric field to surmount the Si—SiO_2 potential barrier without suffering an energy stripping collision in the channel and then being redirected toward the Si—SiO_2 interface. For the sake of simplicity, the path of the electron from the bulk to the gate electrode can be split into four parts which are considered separately.

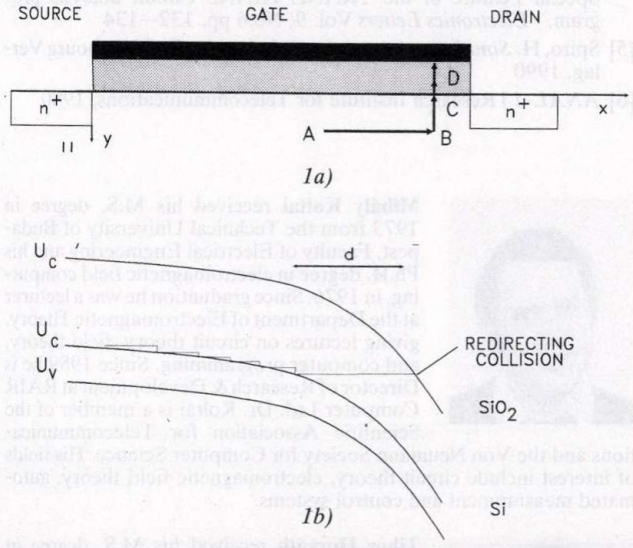

Fig. 1. (a) cross-sectional view of the MOSFET illustrating the scattering probabilities in the model.

(b) Schematic illustration of injected electron into the potential-distance space. The luckyelectron travels a distance d to gain the energy needed to surmount the Si—SiO_2 *potential barrier. The conduction band for* Si *and* SiO_2 *are included.*

(After Tam et al. [2])

From point *A* to point *B*, the channel electrons gain enough energy from the high electric field near the drain to become hot. At point *B*, redirection of hot-electrons takes place by phonon scattering, and the electron travels perpendicularly to the surface. From *B* to *C* (which is at the surface) the hot-electron does not experience energy decreasing collision so enough energy remains to surmount the potential barrier of Si—SiO_2. Between *C* and *D*, the electron does not experience any collision in the oxide image potential as well. *D* marks points in the oxide layer where the potential is maximal. When the electron reaches point *D* it can pass through the oxide toward the gate by the aiding electric field.

Since these processes can be considered to be statistically independent, the total probability of the process is the product of the probabilities for all individual events. The consideration of the models can be split into parts according to the two models. At first, the lucky-electron model will be presented, corresponding to the electric field consideration. This model requires the calculation of the electrical field, strictly speaking the highest field in the channel. This can be done by using analytical field model or 2-D or 3-D device simulations [2]. There is, however, another model, which is based on the effective temperature of the hot-electron.

3. THE PROBABILITY OF ACQUIRING KINETIC ENERGY HIGHER THAN THE SILICON/SILICON-DIOXIDE POTENTIAL BARRIER

3.1. Electric Field Concept

In order for the hot-electron to surmount an Si—SiO_2 potential barrier ϕ_B, its kinetic energy must be greater than ϕ_B [2]. This kinetic energy is gained from the high accelerating electric field of the channel near the drain by covering the distance between points A and B (Fig. 1). For the sake of simplicity, the accelerating electric field E_x is usually assumed to be constant, so the electron has to travel a distance $d$equal to $\phi_B / q \cdot E_x$ to become hot and to acquire this kinetic energy. The probability that an electron can travel this distance or more without suffering any energy robbing collision can be written as:

$$P_{\phi B} = A \cdot \exp(-d/\lambda), \tag{1}$$

where A is a constant of normalization, d is the critical distance and λ is some scattering mean-free-path of the hot-electron which will be discussed later. Hence

$$P_{\phi B} = A \cdot \exp(-\phi_B / q \cdot E_x \cdot \lambda), \tag{2}$$

is the probability of an electron acquiring a kinetic energy greater than ϕ_B. If $P_{\phi B}$ is investigated more rigorously one can see that this probability depends on the direction of the momentum of the electron because the electron must have a sufficiently large momentum perpendicular to the interface. Tam *et al.* [2] made a modification to take into account the effect of the direction of motion. An electron which has exactly the energy ϕ_B will be emitted only if its momentum is directed at an infinitesimally small solid angle perpendicular to the surface. Tam *et al.* assumed isotropic redirection scatterings, and considered only the geometry of the emission process.

According to [2], the modified probability function is given by

$$P_{\Phi B} = 0.25 \cdot \frac{q \cdot E_x \cdot \lambda}{\Phi_B} \exp(-\Phi_B / q \cdot E_x \cdot \lambda), \tag{3}$$

where $P_{\phi B}$ is the probability of an electron acquiring the required kinetic energy from the channel field and retaining the appropriate momentum after the redirection collision. This function differs from (2) which was derived using a simpler assumption, and can be more accurate.

3.1.1. The Potential Barrier Height

The function which describe the potential barrier height ϕ_B between Si—SiO_2 has three terms.

In the first term, the energy difference ϕ_{B0} between the Si and the SiO_2 conductance band is taken into account (Fig. 2.):

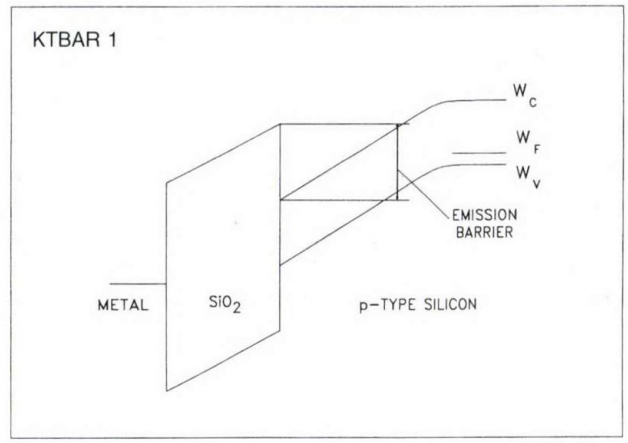

Fig. 2. Schematic energy-band diagram of a MOSFET.

$$\phi_B = \phi_{B0} \tag{4}$$

where ϕ_{B0} is 3.1 eV for electrons, and 3.8 eV for holes in Si [2], [3], [4]. However, the Schottky barrier lowering effect must be included to reach more accuracy. The Schottky effect is the image-force-induced lowering of the potential energy for charge carrier emission when an external electric field is applied [5].

This effect can be taken into account easily by introducing an additional barrier lowering term:

$$\phi_B = \phi_{B0} - \Delta\phi_{B1}, \tag{5}$$

with:

$$\Delta\phi_{B1} = \beta \cdot \sqrt{E_{ox}}, \tag{6}$$

where $\beta = (q^3/4 \cdot \pi \cdot \varepsilon_{ox}\varepsilon_0)^{1/2} = 2.59 \cdot 10^{-4} \mathrm{e(V \cdot cm)}^{1/2}$ for *Si* is a constant [2], [3], [6], E_{ox} denotes the normal component of the oxide-field, and $\Delta\phi_{B1}$ is the amount of the barrier lowering due to the image force which lowers the emission barrier between Si and SiO_2 as illustrated in Fig. 3.

The hot-electrons could be emitted by tunneling as well as by surmounting the Schottky-lowered barrier. However, over-the-barrier emission dominates at large voltages at high emission probabilities, and the tunnel emission becomes appreciable and may even dominate at small voltages at low emission probabilities. Therefore, tunneling must be included in the model.

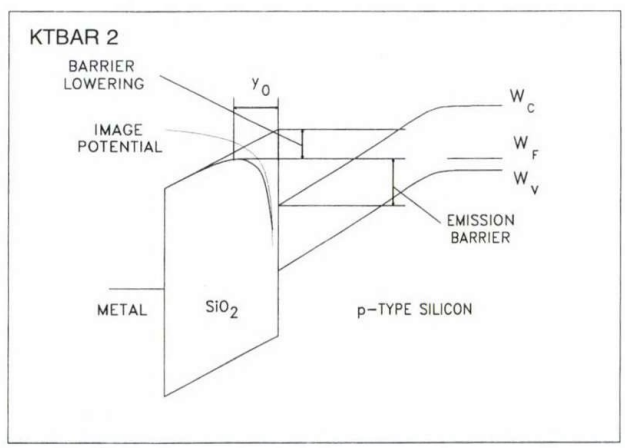

Fig. 3. Schematic energy-band diagram of a MOSFET, illustrating the Schottky barrier-lowering effect.

The proper modelling of the tunnelling would require a detailed knowledge of the hot-electron energy distribution, especially at the top portion of the Scottky-lowered barrier. In the absence of such knowledge, and to keep the model simple within the lucky-electron concept, it shall be assumed that a hot-electron is considered emitted either when its energy allows it to be emitted over the barrier or when it could tunnel into the SiO_2 layer with sufficiently high probability. This assumption is equivalent to introducing an additional barrier lowering term to allow for tunnelling probability (Fig. 4.). This additional barrier

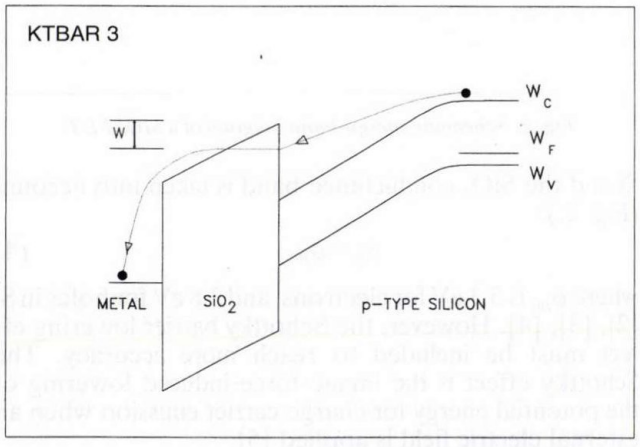

Fig. 4. Schematic energy-band diagram of a MOSFET, illustrating the effect of hot-electrons tunnelling from Si *into* SiO_2.

lowering term should be a function of the oxide field. Its functional form may be obtained from the following consideration:

The probability for a hot-electron, having an energy W below the top of the barrier, of penetrating into the oxide by tunnelling is given by

$$P_T = \exp(-C \cdot W^{3/2} / q \cdot E_{ox}), \tag{7}$$

where $C = 4 \cdot (2 \cdot m^*)^{1/2} / 3 \cdot \hbar$, $\hbar$ denotes the Planck's constant, and m^* is the effective mass of the carrier. For a fixed tunneling probability, after reducing we have

$$W = [-q \cdot E_{ox} / C \cdot \ln(P_T)]^{2/3}. \tag{8}$$

The second additional barrier lowering term needed to correct for tunnelling is proportional to $E_{ox}^{2/3}$:

$$\Delta\phi_{B2} = \alpha \cdot E_{ox}^{2/3}. \tag{9}$$

Unfortunately, there is not enough information about P_T, for this reason α must be determined by comparison with experimental results [6].

($\alpha \cong 1 \cdot 10^{-5} \mathrm{e(V \cdot cm^2)^{1/3}}$ [3], [6]; $4 \cdot 10^{-5} \mathrm{e(V \cdot cm^2)^{1/3}}$ [2])

Including these two additional barrier lowering terms, the final form of ϕ_B is given as

$$\phi_B(E_{ox}) = \phi_{B0} - \beta \cdot E_{ox}^{1/2} - \alpha \cdot E_{ox}^{2/3}. \tag{10}$$

3.1.2. The Mean-Free-Path Parameter

The electrons gain energy from the high field, but inelastic scattering processes limit the number of electrons that attain energies significantly above the conduction band edge. When the electric field exceeds approximately $2 \cdot 10^4$ V/cm, optical phonon emission dominates the scattering effects, and the electron's velocity saturates. When the field strength reaches approximately 10^5 V/cm, the electron gains more energy from the electric field between scattering events than it looses when it scatters. For fields exceeding this value, the electron is no longer in thermal equilibrium with the lattice, and its energy relative to the conduction band edge begins to increase. When this energy reaches a threshold energy W_I, impact ionization becomes a second important energyloss mechanism for the electron. Optical phonon scattering and impact ionization are well described in terms of mean-free-paths, denoted by λ_P and λ_I, respectively, and threshold energy W_I of impact ionization.

When the kinetic energy of the hot-electron is less than W_I, the impact ionization is negligible, and the dominant scattering mechanism for the hot-carrier is due to the optical-phonons. In this case, λ is equal to the optical phonon scattering mean-free-path λ_P:

$$\lambda = \lambda_P. \tag{11}$$

The kinetic energy being greater than W_I, both of these two mechanisms play an important role in the scattering. Therefore, λ can be expressed as

$$\lambda^{-1} = \lambda_P^{-1} + \lambda_I^{-1}, \tag{12}$$

where λ_I is the impact ionization mean-free-path. The published values of λ_I are: 40 nm [7], 70 nm [2], 187 nm [8], and the typical value of W_I is 1.23 eV [2]. Moreover, a modified mean-free-path λ was introduced in the paper of Tam *et al.* [2]: If the hot-electron kinetic energy W is less than W_I, the dominant scattering mechanism is the optical-phonon scattering. When the kinetic energy W becomes higher than W_I (i.e.: $W_I \leq W \leq \phi_B$), both the optical-phonon scattering and the impact ionization are significant. Taking into account this, the probability function can be written as

$$P_{\phi B} \sim \exp(-W_I / q \cdot E_x \cdot \lambda_P) \cdot \exp(-(\phi_B - W_I) / q \cdot E_x \cdot \lambda^*) \tag{13}$$

where λ^* is the mean-free-path defined in (12). By substituting $W_I = \gamma \cdot \phi_B$ into (13),

$$P_{\phi B} \sim \exp(-\phi_B / q \cdot E_x) \cdot (1/\lambda_P + (1-\gamma)/\gamma_I). \tag{14}$$

An average mean-free-path λ can be determined easily from this equation:

$$\frac{1}{\lambda} = \frac{1}{\lambda_P} + \frac{(1-\gamma)}{\lambda_I}. \tag{15}$$

It has to be noted that the influence of impact ionization is weighted by $(1-\gamma)$. The paramter γ can be determined by comparing experimental results.

If the energy loss by impact ionization is assumed to be negligible, then λ is equal to λ_P. Assuming the impact ionization to be temperature independent, the temperature dependence of the emission probability can be described by the temperature dependence of λ_P [8], [9]:

$$\lambda_P(T) = \lambda_0 \cdot \tanh(W_{op} / 2 \cdot k_B \cdot T) \tag{16}$$

where λ_0 is the zero temperature limit of λ_P, W_{op} is the optical-phonon energy, k_B is the Boltzmann's constant and T is the absolute temperature. The typical values for λ_0 are 10.6 nm [2], 10.8 nm [6], and for W_{op} 0.063 eV [5], [6], 0.070 eV [2].

3.2. Carrier Effective-Temperature Concept

The hot-carriers are not in thermal equilibrium with the lattice, in other words, the energy of hot-carriers is higher than the energy in equilibrium. The energy of hot-carriers can be described with the so-called *Carrier Effective-Temperature* T_e. In several papers the following probability function was used to describe the probability $P_{\phi B}$ [2], [10]:

$$P_{\phi B} = A \cdot \exp(-\phi_B / k_B \cdot T_e), \tag{17}$$

which is equivalent to (2) if the energy $k_B \cdot T_e$ is assumed to be equal to $q \cdot E_x \cdot \lambda$. In this equation, the potential barrier height ϕ_B is the same as introduced in Section 3.1.1., k_B is Boltzmann's constant, and T_e is the effective-temperature of hot-electrons, which is discussed in the next Section. However, some authors (i.e. Hofmann *et al.* [4] used the simple thermionic emission formula to describe this probability:

$$P_{\phi B} = A \cdot (k_B \cdot T_e)^{1/2} \cdot \exp(-\phi_B / k_B \cdot T_e), \tag{18}$$

where A is a factor of normalization.

3.2.1. The Relation of Carrier Effective-Temperature Versus Field

The kinetic energy of hot-carriers can also be described by using the effective-temperature T_e of hot-carriers which can be obtained as a function of the electric field E_x. Several $T_e(E)$ functions have been published in the literature. The most simple approach is given by

$$T_e = \frac{q \cdot E_x \cdot \lambda}{k_B}. \tag{19}$$

Thus we have

$$P \sim e^{-\Phi_B / q \cdot E_x \cdot \lambda} = e^{-\Phi_B / k \cdot T_e}. \tag{20}$$

An improved approach for $T(E_x)$ has been given by Bartelnik *et al.* [11]:

$$T_e = \frac{1}{k_B} \cdot \frac{W_0}{1/2 + [1/4 + (W_0 / r \cdot W_r)]^{1/2}}, \tag{21}$$

where:

$$W_0 = \frac{(q \cdot E_x \cdot \lambda_r)}{r \cdot W_r}, \tag{22}$$

where λ_r and W_r are the mean-free-path and the Raman optical phonon energy, respectively, and r is the ratio between the mean-free-paths for ionization scattering λ_I and λ_r. W_r and λ_r are practically the same as W_{op} and λ_P, respectively.

$T_e(E)$ can also be obtained from the well-known energy balance equation (see for example [1], [10]). The balance between the amount of energies can be written as:

$$\frac{\partial < W >}{\partial t} = 0 = q \cdot v \cdot E - \frac{< W > - \frac{3}{2} \cdot k_B \cdot T_L}{\tau_w}, \tag{23}$$

where the first term on the right hand side is the amount of energy that an electron receives from the field in unit time, and the second term is the amount of energy that it looses to the lattice, v is the electron drift velocity which is dependent on the electric field E, T_L is the lattice temperature and τ_w is the energy relaxation time, which is the characteristic time for the energy transfer from the carrier system to the lattice. Its typical value is in the range of 0.05 to 0.2 ps [10].

The average energy of an electron is given by

$$< W > = \frac{3}{2} \cdot k_B \cdot T_e. \tag{24}$$

By substituting (24) into (23) and reducing by k_B, T_e is given by

$$T_e = \frac{2 \cdot q \cdot v \cdot E \cdot \tau_w}{3 \cdot k_B} + T_L. \tag{25}$$

In the paper of Hofmann *et al.* [4], the following equation was used to describe the nonlocal relationship between T_e and the electric field distribution given by Takeda *et al.* [12]:

$$T_e(x) = \frac{2}{5} \cdot \frac{q}{k_B} \int_0^{\infty} E_{\parallel}(x - u) \cdot \cdot \exp\left(-\frac{3}{5} \cdot u \cdot \tau_w \cdot v_s\right) \cdot du, \tag{26}$$

where $E_{\parallel}$ is the electric field component in the direction of local electron current flow, and v_s is the saturation velocity of electrons.

An advanced model, was published by Hänsch *et al.* [13], [14] which is based on a self-consistent treatment of hot-electron transport in submicron devices. The local solution which provided a local mobility and carrier temperature model was derived from the general balance equations for particles and energy.

The local effective-temperature of carriers is:

$$T_e = T_L + \frac{2 \cdot q}{3 \cdot k_B} \cdot \tau_w \cdot v_{sat,n}^2 \cdot \left(\frac{1}{\mu_n} - \frac{1}{\mu_{0,n}}\right), \tag{27}$$

where T_L denotes the temperature in equilibrium, τ_w is the energy relaxation time, v_{sat} *and* μ_0 denote the saturation velocity and low field mobility of electrons. The local mobility is given by

$$\mu_n = \frac{2 \cdot \mu_{0,n}}{1 + [1 + (2 \cdot \mu_{0,n} \cdot Fn / v_{sat,n})^2]^{1/2}} \tag{28}$$

In (28) F represents the driving force for current J:

$$\vec{F}_n = \vec{E} + \frac{1}{n} \cdot \text{grad}\left(\frac{k_B \cdot T_e}{q} \cdot n\right) \tag{29}$$

The driving force F is appropriate to extend the drift-diffusion current relation as:

$$\vec{J} = q \cdot \mu_n \cdot n \cdot \vec{F}_n, \tag{30}$$

These equations can be true in the general situation of an inhomogeneous electric field. With this model, hot-electron effects can be included in submicron device design, and this model allows a simple way to model mobility and electron temperature, which are important for device modeling.

3.3. Probability of Collision-Free Travel to the Barrier Peak

The probability of collision-free travel to the barrier peak can be split into two parts. At first the electrons have to reach the surface with sufficiently high energy to surmount the potential barrier, and after this they have to pass through the insulator.

3.3.1. Probability of Collision-Free Travel to the Interface

After the redirection collision, the hot-electron must travel from point B to interface point C (Fig. 1.) without suffering any collision. The probability of a channel electron travelling to the interface from a depth y without any collision can be described as [2], [4]:

$$P_{TI} = \exp(-y/\lambda)\,, \tag{31}$$

where λ is the above defined mean-free-path of the hot-electrons.

While the place of redirection is unknown, this probability function must be weighted by the electron concentration [2]:

$$P_{TI} = \frac{\int_0^{+\infty} n(y) \cdot \exp(-y/\lambda) \cdot dy}{\int_0^{+\infty} n(y) \cdot dy} \tag{32}$$

where $n(y)$ is the electron concentration at depth y and position x in the inversion layer. The electron concentration can be obtained by numerical device simulation.

3.3.2. Probability of Collision-Free Travel from the Interface to the Potential Maximum

If an electron is emitted into the SiO_2 layer, it travels against a restrain electric field (between the points C and D in Fig. 1.) and must reach the barrier maximum with enough energy to surmount. Hence, scattering inside the potential well reduces the emission probability of hot-electrons [2], [4]. This probability function is expressed as

$$P_{PM} = \exp(-y_0/\lambda_{ox}), \tag{33}$$

where λ_{ox} is the mean-free-path of an electron in the oxide layer, and y_0 is the distance of the potential maximum from the interface (Fig. 3.). The typical value for λ_{ox} is 3.4 nm in SiO_2 [4]. To lower the potential barrier by biasing the gate electrode, the image force also changes and moves the potential barrier maximum (Fig. 3.). For this reason, y_0 is related to the oxide field E_{ox} as:

$$y_0 = (q/16 \cdot \pi \cdot \varepsilon_{ox} \cdot E_{ox})^{1/2}. \tag{34}$$

This assumption is valid for electrons which reach the potential maximum and can reach the gate electrode, or in other words the electrons are not trapped in the insulator.

Now, the probability of collision-free-travel to the barrier peak P_{BP} can be written as the product of P_{TI} and P_{PM}:

$$P_{BP} = P_{TI} \cdot P_{PM}. \tag{35}$$

3.4. The Probability of an Electron Reaches the Gate Electrode

As it was mentioned at the beginning of Section 2, the total probability of the process is the product of the probabilities of individual effects. Thus, the total probability can be written as

$$P = P_{\phi B} \cdot P_{TI} \cdot P_{PM}. \tag{36}$$

This is a very simple approach; however, according to the literature, the gate current can be computed by this with good accuracy. This is usually used in analytical and numerical modelling. The parameters of the probabilities, for example α, β, λ, etc., are determined by comparing the computing data with measurement. By adjusting these fitting parameters, good results can be obtained, but unfortunately, these parameters have to be determined again if the parameters of the device structure (e.g. geometry and doping profile) are changed because to describe the behaviour of the whole system is very difficult. This is very inconvenient when modelling the effects of scaledown or changing process parameters.

4. DISCUSSION

Although intensive progress has been made in the last 15 years, a quantitative model containing all important parameters, such as substrate doping profile, applied voltages, and lattice temperature, is still not available. Theoretical calculations of the hot-carrier emission have been limited to constant-field approximation due to the complexity of the problem. In this approximation, the hot-electron energy distribution is a function of the electric field only. The constant-field approximation should be valid for such samples where the gradient of doping concentration is small. For practical devices and for experimental devices used to study hot-electron emission processes, however, it is not true. It is not clear whether constant-field approximation is applicable to such doping profiles.

It was found that none of these models could be extended from one doping profile to another without readjusting the supposedly constant-value parameters (λ, α, β, etc.). Variation of these parameters with doping profile made it difficult to attach physical meaning to them, and it seriously limited the extendibility of the models to arbitrary doping profiles.

ACKNOWLEDGEMENT

I am grateful to Professor Siegfried Selberherr, Institute for Microelectronics, TU Wien, further to Professor Kálmán Tarnay and dr. Teréz Kormány, Department of Electron Devices, TU Budapest, for their guidence throughout my work and for helpful discussions. Thanks are also due to Predrag Habaš, Karl Wimmer, Peter Dickinger and Péter Verhás, together with the whole staff of the Institute for Microelectronics, TU Wien, for their useful advice in preparing the manuscript.

REFERENCES

[1] Selberherr S., *Analysis and Simulation of Semiconductor Devices* Springer-Verlag, 1984

[2] Tam S., P. K. Ko and C. Hu, "Lucky-Electron Model of Channel Hot-Electron Injection of MOSFET's" *IEEE Transactions on Electron Devices,* Vol. ED-31. No. 9., pp. 1116—1125,1984

[3] Ning T. H., "Hot-Electron Emission from Silicon into Silicon Dioxide" *Solid-State Electronics,* Vol. 21. pp. 273—282, 1978

[4] Hofmann K. R., C. Werner, W. Weber. and D. Dorda, "Hot-Electron and Hole-Emission Effects in Short n-Channel MOSFET's" *IEEE Transactions. on Electron Devices,* Vol. ED-32. No. 3, 1985.

[5] Sze S. M., Physics of Semiconductor Devices, 2nd Edition, JOHN WILEY & SONS, 1981

[6] Ning T. H., C. M. Osburn and H. N. Yu, "Emission Probability of Hot-Electrons from Silicon into Silicon Dioxide" Journal of Applied Physics, Vol. 48, No. 1, 1977

[7] Troutman R. R., "Silicon Surface Emission of Hot-Electrons" Solid-State Electronics, Vol. 21, pp. 283—289, 1987

[8] Verwey J. F., R. P. Kramer and B. J. De Maagt "Mean-Free-Path of Hot-Electrons at the Surface of Boron-Doped Silicon" Journal of Applied Physics, Vol. 46, pp. 2612—2619, 1977

[9] Crowell C. R. and S. M. Sze, "Temperature Dependence of Avalanche Multiplication in Semiconductors" Applied Physics Letter, Vol. 9, No. 6, p. 242, 1966

[10] Schmitt-Landsiedel D. and G. Dorda, "Novel Hot-Electron Effects in the Channel of MOSFET's Observed by Capacitance Measurements" IEEE Transactions on Electron Devices, Vol. ED-32, No. 7, 1985

[11] Bartelnik D. J., J. L. Moll and N. I. Meyer, "Hot-Electron Emission From Shallow p-n Junction in Silicon" Physical Review, 130, pp. 972—985, 1963

[12] Takeda E., H. Kume, T. Toyabe and S. Asai "Submicrometer MOSFET Structure for Minimizing Hot-Carrier Generation" IEEE Transactions Electron Devices, Vol. ED-29, p. 611, 1982

[13] Hänsch W. and M. Miura-Mattausch "The Hot-Electron Problem in Small Semiconductor Devices" Journal of Applied Physics, Vol. 60, No. 2, 1986

[14] Hänsch W., M. Orlowski and W. Weber "The Hot-Electron Problem in Submicron MOSFET" Journale de Physique, C4, No. 9, pp. 597—606, 1988

[15] Narita K. and K. Yamaguchi, "IGFET Hot-Electron Emission Model" Solid-State Electronics, Vol. 23. pp. 721—725, 1980

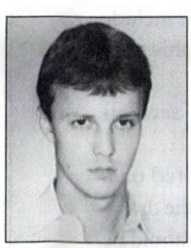

Tamás Kocsis was born in Budapest, Hungary, on November 5, 1965. He was educated at the Technical University of Budapest, Faculty of Electrical Engineering. From September 1987 to December 1989, he was working in the Department of Electron Devices, TU Budapest as a part-time employee. In 1988 he won the 3rd and in 1989 the 1st prize of the Scientific Students Research Conference, TU Budapest. In 1989 he received the award **'For the Hungarian Technology Development'**, founded by the Hungarian Credit Bank. He worked for his Diploma Work at the Institute for Microelectronics, TU Vienna, and received the M. Sc. degree from the TU Budapest, June 1990. From September of 1990, he is working for his Ph.D. degree at the Department of Electron Devices, TU Budapest, as a sponsored student of the Hungarian Academy of Sciences. He is a member of the Hungarian Scientific Associtaion of Telecommunication, and a Student Member of IEEE.

RELECTRONIC '91
8th SYMPOSIUM ON RELIABILITY IN ELECTRONICS
26—30 August, 1991—Budapest, Hungary

Organized by the Scientific Society for Telecommunication and the Optical, Acoustical and Filmtechnical Society

Sponsored by the Department for Technical Science of the Hungarian Academy of Sciences, and the IEEE Hungarian Section.

Chronology: The Symposia on Reliability in Electronics were held in 1964, 1968, 1973, 1977, 1982, 1985 and 1988 in Budapest.
Outstanding experts were attending from abroad and Hungary.

Future: The 8th Symposium on Reliability in Electronics will be held in Budapest from 26—30 August, 1991.

SCOPE: The Symposium is intended as a forum for presenting new results and developments, case studies and experiences,
in the following preferred aspects of **reliability, maintainability and availability:**

- Reliability Theory
- Service Quality
- Network Relability
- Human Factors
- Software Reliability
- Failure Phyisics of Components
- Production Yield

NOTES: The working language of the Symposium is English. A POSTER session will also be organized.
PANEL discussions will be held on topics of special interests.

Registration form and detailed information can be requested from the Secretariat of HTE, Budapest, Kossuth tér 6—8, H—1055

THE ORGANIZING COMMITTEE
of RELECTRONIC '91

Informations for authors

JOURNAL ON COMMUNICATIONS is published monthly, alternately in English and Hungarian. In each issue a significant topic is covered by selected comprehensive papers.

Other contributions may be included in the following sections:

- INDIVIDUAL PAPERS for contributions outside the focus of the issue,
- PRODUCTS-SERVICES for papers on manufactured devices, equipments and software products,
- BUSINESS-RESEARCH-EDUCATION for contributions dealing with economic relations, research and development trends and engineering education,
- NEWS-EVENTS for reports on events related to electronics and communications,
- VIEWS-OPINIONS for comments expressed by readers of the journal.

Manuscripts should be submitted in two copies to the Editor (see inside front cover). Papers should have a length of up to 30 double-spaced typewritten pages (counting each figure as one page). Each paper must include a 100—200 word abstract at the head of the manuscript. Papers should be accompanied by brief biographies and clear, glossy photographs of the authors.

Contributions for the PRODUCTS-SERVICES and BUSINESS-RESEARCH-EDUCATION sections should be limited to 16 doublespaced typewritten pages.

Original illustrations should be submitted along the manuscript. All line drawings should be prepared on a white background in black ink. Lettering on drawings should be large enough to be readily legible when the drawing is reduced to one- or two-column width. On figures capital lettering should be used. Photographs should be used sparingly. All photographs must be glossy prints. Figure captions should be typed on a separate sheet.

For contributions in the PRODUCTS-SERVICES section, a USD 110 page charge will be requested from the author's company or institution.

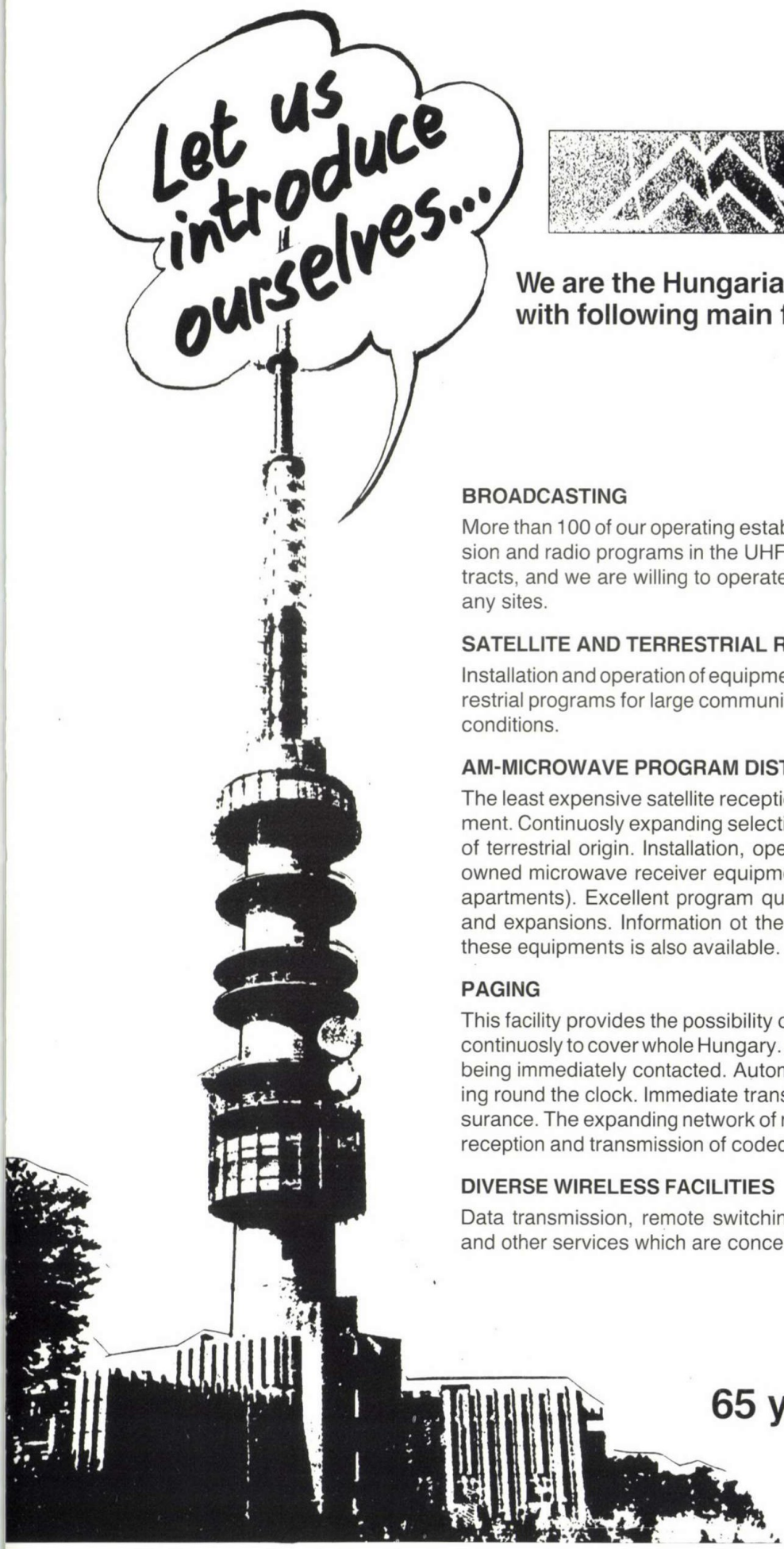

We are the Hungarian Broadcasting Company, with following main fields of activity.

BROADCASTING

More than 100 of our operating establishments serve for transmitting television and radio programs in the UHF, VHF, SW and MW bands under contracts, and we are willing to operate transmitters of other organizations at any sites.

SATELLITE AND TERRESTRIAL RECEPTION

Installation and operation of equipments for the reception of satellite and terrestrial programs for large communities and cable networks, on favourable conditions.

AM-MICROWAVE PROGRAM DISTRIBUTING SYSTEM

The least expensive satellite reception possibility in Budapest and environment. Continuosly expanding selection of up to 20 programs, some of them of terrestrial origin. Installation, operation and maintenance of company-owned microwave receiver equipments for larger communities (over 150 apartments). Excellent program quality even during transmitter changes and expansions. Information ot the necessary authorization of operating these equipments is also available.

PAGING

This facility provides the possibility of selective and group calls, expanding continuosly to cover whole Hungary. A service for those who have interest of being immediately contacted. Automatic and dispatcher message recording round the clock. Immediate transmission of messages with privacy assurance. The expanding network of rural dispatcher centres is ready for the reception and transmission of coded messages comprising up to 12 digits.

DIVERSE WIRELESS FACILITIES

Data transmission, remote switching, advertising, commercial programs and other services which are conceived by you and realized by us.

65 years of Hungarian broadcasting!

Call our Public Relations Department for further information.

Mailing address:		Phone:	Fax:	Telex:
Hungarian Broadcasting Company	Budapest, P.O. Box 8 1440	+361 132 6115 +361 111 7602	+361 111 7602	22 29 05

Christopher Columbus could never learn about discovering an unknown continent in 1492 as he was mistaken in assessing both disctance and time.

You, hower, can discover a new way of establishing contact in 1991.

If you want to overcome distance, and time is an important factor in your life, you should buy a phone card around lake Balaton in any of the post offices, or at news-stands and kiosks.

You may gain several minutes during your vacation! You are awaited in 300 phone booths after buying your phone card comprising 50 or 120 units.

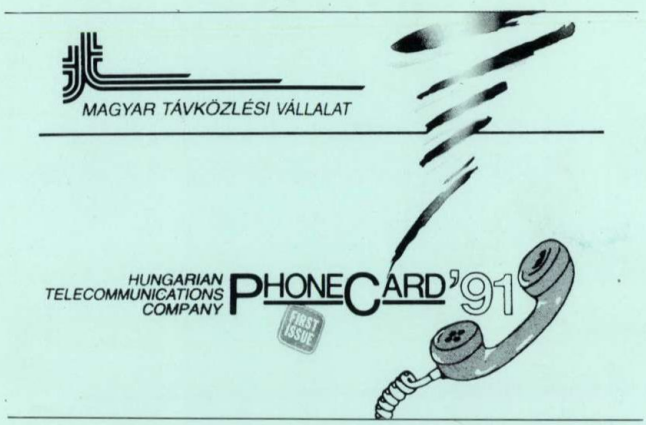

BE THE FASTEST – BY PHONE CARD!

AIRC